UNIVERSITY OF BELGRADE

FACULTY OF TECHNOLOGY AND METALLURGY

Ali R. Elkais

THE INFLUENCE OF THE POLYANILINE COATINGS ON CORROSION PROTECTION OF MILD STEEL IN DIFFERENT ENVIRONMENTS

Doctoral Dissertation

Belgrade, 2013

UNIVERZITET U BEOGRADU

TEHNOLOŠKO-METALURŠKI FAKULTET

Ali R. Elkais

UTICAJ PREVLAKA POLIANILINA NA KOROZIJU MEKOG ČELIKA U RAZLIČITIM SREDINAMA

doktorska disertacija

Beograd, 2013

Ментор:

Др Бранимир Гргур, редовни професор, Универзитет у Београду, Технолошко-металуршки факултет

Чланови комисије:

Др Милица Гвозденовић, доцент, Универзитет у Београду, Технолошко-металуршки факултет

Др Бранимир Југовић, виши научни сарадник, Институт техничких наука – САНУ, Београд

Датум одбране: ___ ___ _____ god.

ACKNOWLEDGEMENT

I would like to express this appreciation to Professor Branimir Grgur, for his supervision, guidance, encouragements, and advice throughout the duration of study and experimental work.

I would also to thanks sincere appreciation to my Mentor Professor Branimir Grgur, Professor Milica Gvozdenović and Dr. Branimir Jugović, for guideless during the work on this doctoral dissertation.

Finally deep thanks to the Libyan Government, and my family, for their patent, and encouragements during my Ph.D study at Belgrade University.

Thank you.

Ali Ramadan Elkais

THE INFLUENCE OF THE POLYANILINE ON CORROSION PROTECTION OF MILD STEEL IN DIFFERENT ENVIRONMENTS

ABSTRACT

Subject and scientific goal of this dissertation was to investigate the corrosion behavior of mild steel as the most widespread and the price very acceptable structural material based on polyaniline coatings in different corrosive environments: corrosion in sea water (3% NaCl), atmospheric corrosion and corrosion in soil (Sahara sand). In the first part was investigated the electrodeposition of polyaniline using galvanostatic technique on mild steel in of sodium benzoate solution in order to determine the corrosion behavior. It was also examined the potential role of polyaniline coating in cathodic protection of mild steel, especially in the case of the failure, and it was found that partial polyaniline coatings provide adequate corrosion protection. It was shown that partial polyaniline films can offer good corrosion protection of mild steel in Sahara sand and against atmospheric corrosion. Based on these studies of a model system, the „switching zone mechanism" has been proposed. For the first time it was discovered that corrosion processes of mild steel covered with polyaniline is affected with light, even the mild illumination was applied (4 mW cm^{-2}).

Since the electrochemical method of of synthesis on mild steel is suitable only for relatively small objects, in the second part of the dissertation has investigated the electrochemical and chemical synthesis polyaniline powder. In this sense, it is determined the yield of the synthesis, the obtained form of polyaniline and its morphology. By the chemical dedoping and doping, polyaniline powder was formed in the form of emeraldine salts or emeraldin base, since there is controversy in the literature which form gives better protection against corrosion of the mild steel. With such obtained and characterized powders the composite coatings with different content of PANI powder (1-10 wt%) was prepared, and applied on the mild steel samples, and the corrosion behavior was investigated using electrochemical impedance technique and the method of moist chamber for samples with artificially induced defects. It was found that chemically synthesized polyaniline in the form of emeraldin salts offers the best protection with the optimal concentration of polyaniline about 5 wt.%. The content of phenazine and azane determined by UV-vis spectroscopy in the investigated samples are connected with corrosion protection ability. The proposed mechanism of corrosion protection of mild steel in a real system was also confirmed.

Keywords: polyaniline, benzoates, mild steel, corrosion, cathodic protection, composite coatings

Scientific field: Chemistry

Specific scientific field: Electrochemistry

UDK number:

УТИЦАЈ ПРЕВЛАКА ПОЛИАНИЛИНА НА КОРОЗИЈУ МЕКОГ ЧЕЛИКА У РАЗЛИЧИТИМ СРЕДИНАМА

РЕЗИМЕ

Предмет и научни циљ рада ове докторске дисертације је било испитивање корозионог понашања меког челика као најраширенијег и по цени веома прихватљивог конструкционог материјала са превлакама на бази полианилина у различитим корозионим срединама: корозија у морској води (3% NaCl), атмосферској корозији и корозији у земљишту (Сахарски песак). У првом делу је испитивано електрохемијско таложење полианилина галваностатском техником на меком челику иу раствора натријум-бензоата у циљу одређивање корозионог понашања. Такође, испитивана је и потенцијална улога превлака полианилина у катодној заштити меког челика, посебно у случајевима њеног отказивања и установљено је да парцијална превлака полианилина пружа адекватну заштиту од корозије. Показано је да делимично нанета превлака полианилина остварује добру заштиту од корозије челика у песку Сахаре и од атмосферске корозије На основу ових испитивања, као модел система, предложен је механизам замене катодних и анодних зона. По први пут је откривено да и релативно блего осветљење (4 mW cm^{-2}) има утицаја на корозију челика прекривеног полианилином.

Са обзиром да је електрохемијски метод синтезе полианилина на меком челику погодан само за релативно мале предмете, у другом делу дисертације је испитивано електрохемијско и хемијско добијање прахова полианилина. У том смислу је одређен принос синтезе, облик добијеног полианилина и његова морфологија. Применом метода хемијског дедоповања и доповања добијени су узорци електрохемијски односно хемијски формираних прахова у облику емералдин соли односно емералдин базе, пошто у литератури постоје контраверзе који облик пружа бољу заштиту од корозије меком челику. Са тако добијеним, окарактерисаним праховима припрмљене су композитна премазна средства са различитим садржајем прах полианилина (1-10 мас%). Оваквим премазним средствима су били заштићени узорци меког челика, а корозионо понашање је испитивано применом електрохемијске импедансне технике и методом влажне коморе за узорке са вештачки изазваним оштећењима. Установљено је да хемијски синтетисани полианилин у облику емералдин соли пружа најбољу заштиту при чему је оптимална концентрација полианилина око 5 мас.%. Применом УВ-вис спектроскопије показано је да садржај феназина и анизина у структури полианилина одређује квалитет антикорозионе заштите. Такође, је потврђен и предложени механизам заштите од корозије меког челика на реалном систему.

Кључне речи: полианилин, бензоати, меки челик, корозија, катодна заштита, композитне превлаке

Научна област: Хемија

Ужа научна област: Електрохемија

УДК број:

CONTENTS

1. INTRODUCTION

Mild steel is undoubtedly the cheapest and the most commonly used construction material. It has been extensively used for centuries in many areas, for water pipes, boats, docks, tanks, vessels, etc. Because of its low nobility and structural defects, mild steel corrodes practically in all environments.

The corrosion of mild steel in water or in the presence of the moisture is mainly connected with dissolved oxygen. Cathodic reaction in near neutral solutions is oxygen reduction under diffusion control:

$$O_2 + 2H_2O + 4e = 4OH^- \tag{1.1}$$

and anodic reaction is dissolution of iron:

$$Fe = Fe^{2+} + 2e \tag{1.2}$$

Depending on pH, Fe^{2+} could react with O_2, OH^- or water molecules, and precipitate in the form of different insoluble oxy-hydroxides (rust).

In the different corrosion environment, mild steel can be protected in many ways: by applying different organic coatings, by using cathodic or anodic inhibitors, cathodic and anodic protection, etc. These protection procedures imply the following problems: organic coatings are to expensive and can ensure protection for limited periods of times, depending on the quality of coatings and their thickens (if scratched,

corrosion progresses with catastrophic consequences); inhibitors cannot be applied under certain conditions (e.g. in the protection of water pipes for human use); cathodic protection combined with organic coatings is very expensive due to high electric power consumption; moreover in the case of cathodic protection failure, steel corrodes if organic coatings are damaged.

The application of electroconducting polymers is a relatively new approach in corrosion protection of mild steel in different environments. Due to the existence of conjugated electron bonds this materials are also called "synthetic metals".

The Nobel Prize in Chemistry 2000 was awarded jointly to Alan J. Heeger, Alan G. MacDiarmid and Hideki Shirakawa "for the discovery and development of conductive polymers".

Most conducting polymers belong to one of the five families: polyacetylenes, polyphenylvinylenes, polypyrrole, polythiophene, and polyaniline.
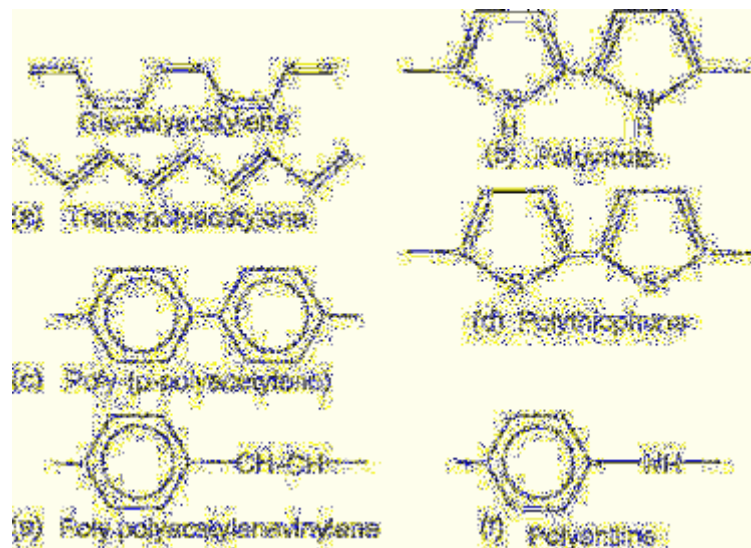

Fig. 1.1. Families of conducting polymers.

Electroconducting polymers have semi metallic or even metallic conductivity, as it can be seen in Fig. 1.2.
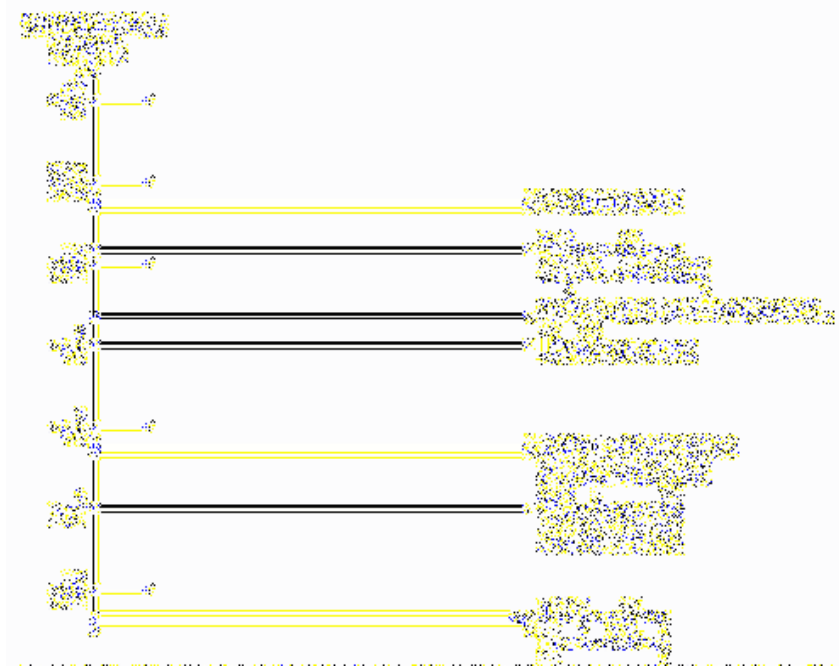
Fig. 1.2. Logaritmic conductivity ladder locating some metals and conducting polymers.

These polymers yield different effects when applied on metals, especially on mild steel. This is abundantly evidenced in literature, indicating a beneficial corrosion protection of many metals and alloys in different corrosion environments in the presence of conducting polymer-based coatings. Since the mid-1980s, numerous studies have shown that polyaniline-, polypyrrole-, or polythiophene-based coatings lower the corrosion rate of mild steel, stainless steel, aluminum, and copper. The conducting polymer can either be applied as a neat coating, undercoat or as dispersion in a polymer binder.

Polyaniline (PANI) is probably the most thoroughly investigated conducting polymer (even it has lowest conductivity) in corrosion protection of mild steel, due to easy synthesis, procesability and low price of the monomere. It has been observed, though it is not well investigated, that, unlike regular organic coatings, PANI can protect metal under a scratched or damaged coating surface. Many different mechanisms explaining the role of PANI in metal protection have been proposed. Unfortunately, the mechanism of corrosion protection is still elusive.

Hence, the idea for this PhD thesis is to investigate the model systems of the corrosion and corrosion protection of mild steel using electroconducting polymers (in tree different environments: see water, sand and atmosphere), and to investigate the influence on cathodic protection on this system and moreover, to investigate the possibility of a practical application of the proposed coating in cathodic protection. Further experiments will be to prepare polyaniline electroconducting powder with different oxidation states which could be incorporated in the regular paint and should be used as electro active undercoat before application of the top coatings.

2. THEORETICAL PART

2.1. SYNTHESIS, PROPERTIES AND APPLICATION OF POLYANILINE

2.1.1. Synthesis of polyanilne

Polyaniline can be synthesized by chemical or electrochemical methods. The most common chemical synthesis of polyaniline is by oxidative polymerization of the aniline monomer with ammonium peroxodisulfate as an oxidant [1, 2]. During polumerization first product is blue protonated perningraniline intermediate, which is further oxidized to green protonated emeraldine.

$$4\,n \quad \text{C}_6\text{H}_5-\text{NH}_2 \quad + \quad 5\,n\,(\text{NH}_4)_2\text{S}_2\text{O}_8$$

Blue protonated pernigraniline intermediate

Green protonated emeraldine

$$+\,3\,n\,\text{H}_2\text{SO}_4 \;+\; 5\,n\,(\text{NH}_4)_2\text{SO}_4$$
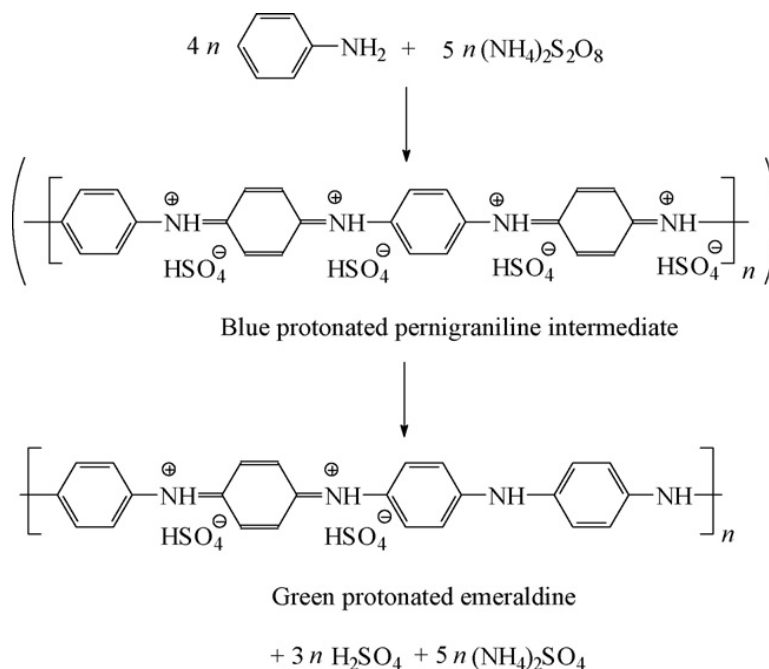
Fig. 2.1. Schematic presentation of the oxidation of aniline with ammonium peroxydisulfate in acidic medium [1, 2].

Depending on reaction conditions polyaniline can be obtained as a powder in the form of nano or micro granules, tubes, fibers, spheres, colloidal particles as shown on Fig. 2.2 [3, 4].
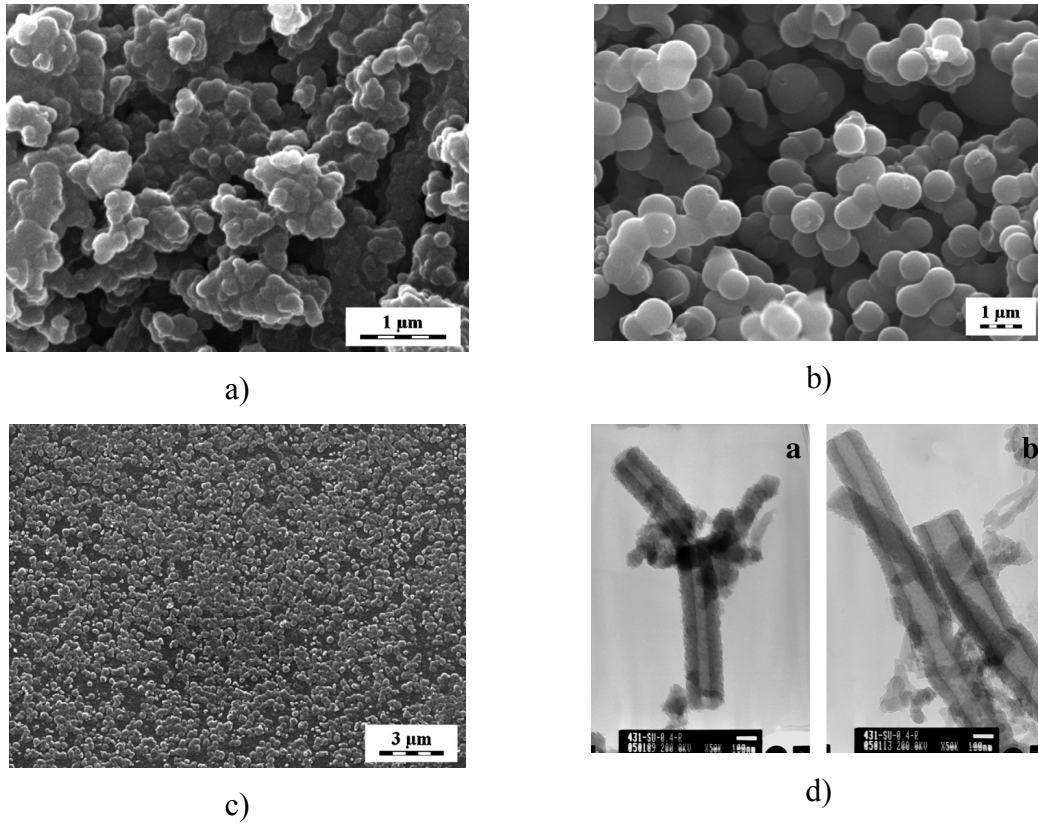

Fig. 2.2. a) Granular morphology of polyaniline powder, b) Sub-micrometer spheres obtained by the oxidation of aniline hydrochloride in ethylene glycol, c) Colloidal polyaniline particles stabilized with poly(N-vinylpyrrolidone), d) Transmission electron microscopy of polyaniline nanotubes. Aniline (0.2M) was oxidized with ammonium peroxydisulfate (0.25M) in aqueous solutions of 0.4M succinic acid [3, 4].

The electrochemical method was discovered in 1862 as a test for the determination of small quantities of aniline [5]. Usual electrochemical methods for polyaniline synthesis are galvanostatic deposition and cyclic voltammetry, as shown in Fig. 2.3 a) and 2.b) [6].
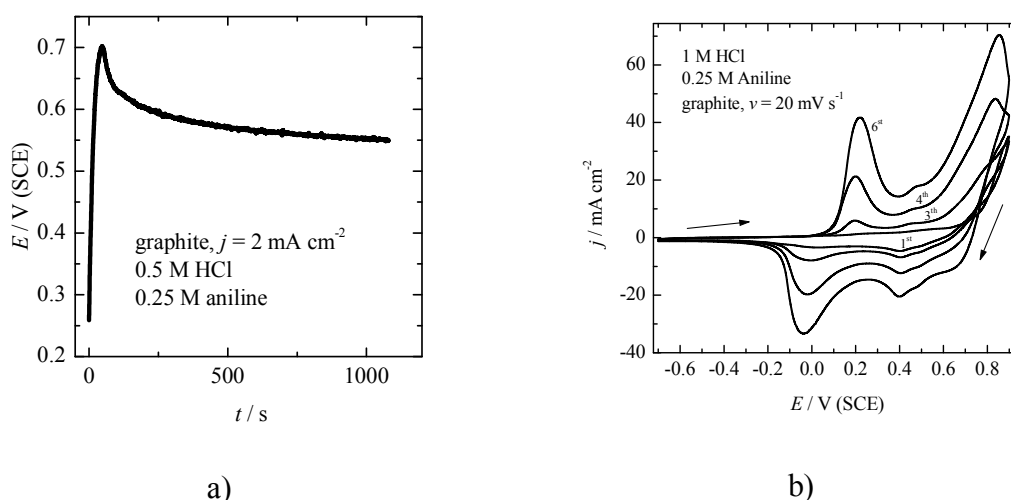
Fig. 2.3. a) Typical galvanostatic transient of polyaniline synthesis on inert graphite substrate, b) Typical cyclic voltammogras of polyaniline synthesis on inert graphite substrate from hydrochloric acid [6].

Due to the simple reaction control by applied current density, galvanostatic electrochemical polymerization could be favorable. For relatively short time of electrochemical polymerization, PANI is obtained as a thin film, while during prolonged electrolysis PANI can be obtained as a relatively adherent powder [7].
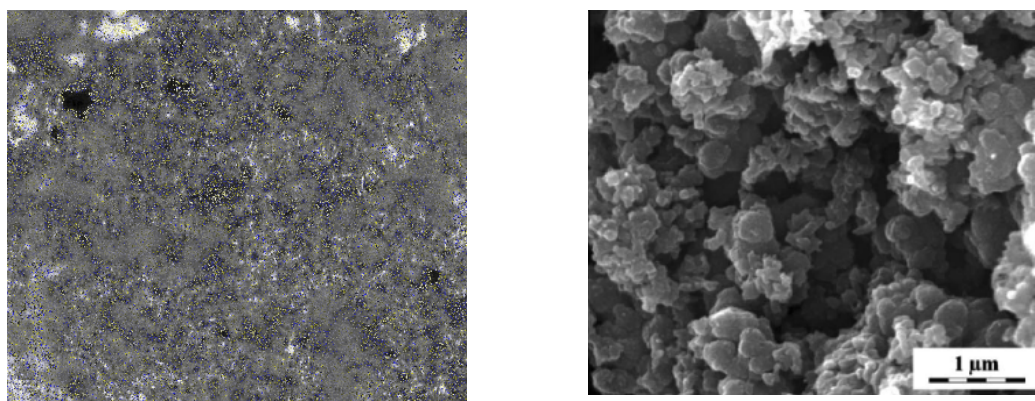

Fig. 2.4. Polyaniline thin film (left) and powder (right) on graphite obtained by galvanostatic method from hydrochlorid acid solution [7].

The most generalized mechanism of aniline polymerization suggested by Wei et al. [8, 9], based mainly on kinetic studies of the electrochemical polymerization of aniline is shown in Fig. 2.5. According to the authors, the slowest step in the

polymerization of aniline is the oxidation of aniline monomer to form dimeric species (i.e. *p*-aminodiphenylamine, PADPA, *N-N*9-diphenylhydrazine and benzidine), because the oxidation potential of aniline is higher than those of dimers, subsequently formed oligomers and polymer. Upon formation, the dimers are immediately oxidized and then react with an aniline monomer via an electrophilic aromatic substitution, followed by further oxidation and deprotonation to afford the trimers. This process is repeated, leading eventually to the formation of PANI.
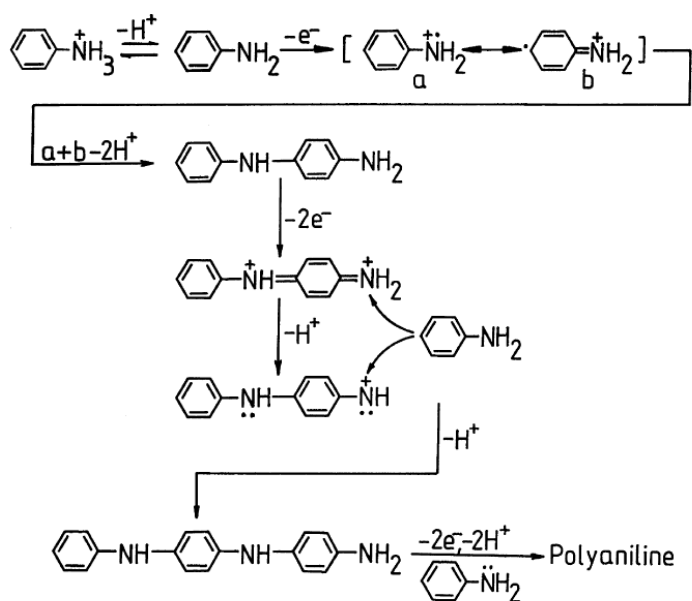
Fig. 2.5. Mechanism of the aniline polymerization, proposed by Wei et al. [8, 9].

2.1.2. Properties of the polyaniline

Polymerized from the aniline monomer, polyaniline can be found in one of three idealized oxidation states:

- **leucoemeraldine** – white/clear or colorless
- **emeraldine** – green for the emeraldine salt, blue for the emeraldine base
- **(per)nigraniline** – blue/violet

Depending on applied potential or oxidation states polyaniline undergoes different redox reaction as shown on Fig. 2.6 [10], characterized by different color as shown in

Fig. 2.7. Redox potentials for leucoemeraldine/emeraldine transition are approximately 0.115 vs. SCE, while for emeraldine/pernigraniline transition is 0.755 vs. SCE [10].
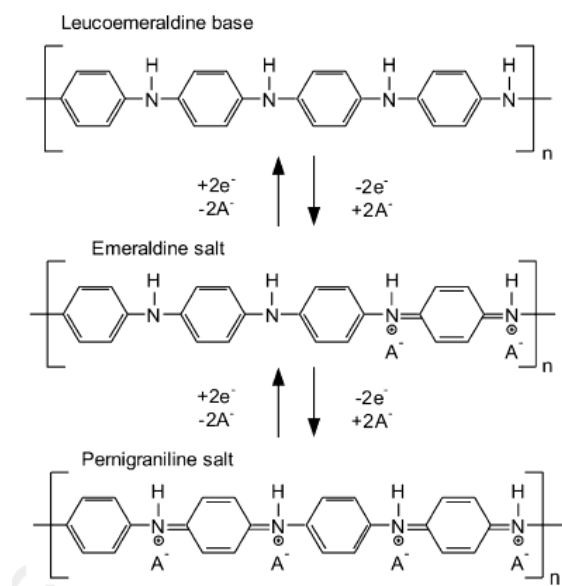
Fig. 2.6. Generalized scheme of the electrochemical reactions for the fundamental PANI oxidation forms [10].
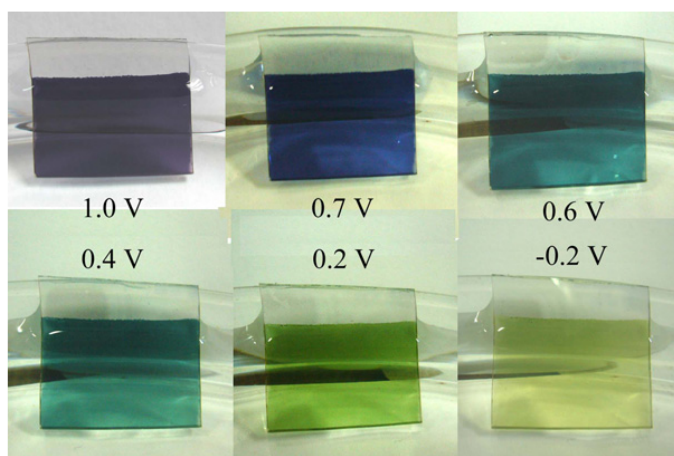
Fig. 2.7. Photographs of the polyaniline samples under different potentials.

The influence of pH leads to formation of different salt-base equilibrium of tree different polyaniline fundamental forms as shown in Fig. 2.8 [11]. In aqueous electrolytes, the extent of protonation depends on the solution pH (increasing left to right). For leucoemeraldine, the pK_a is between 0 and 1: protonation begins at approximately pH 2 and is completed at pH −1. The pH at which the polymer protonates/deprotonates depends on the acid, however. In naphthalene sulfonic acid, for

example, leucoemeraldine is fully protonated even at pH 2. The pK$_a$ of the emeraldine state is approximately 3, while that of pernigraniline is below 0. Fully protonated chains consist only of segments labeled x in Fig. 2.8, but in most acids the chains are mixtures of x and y units, the ratio depending on pH. Only the fully protonated form of emeraldine salt is shown in the left column of Fig. 2.8; this is the lone state of the six that is electrically conducting [11]. The two structures shown for this salt are chemically equivalent resonance structures called polarons.
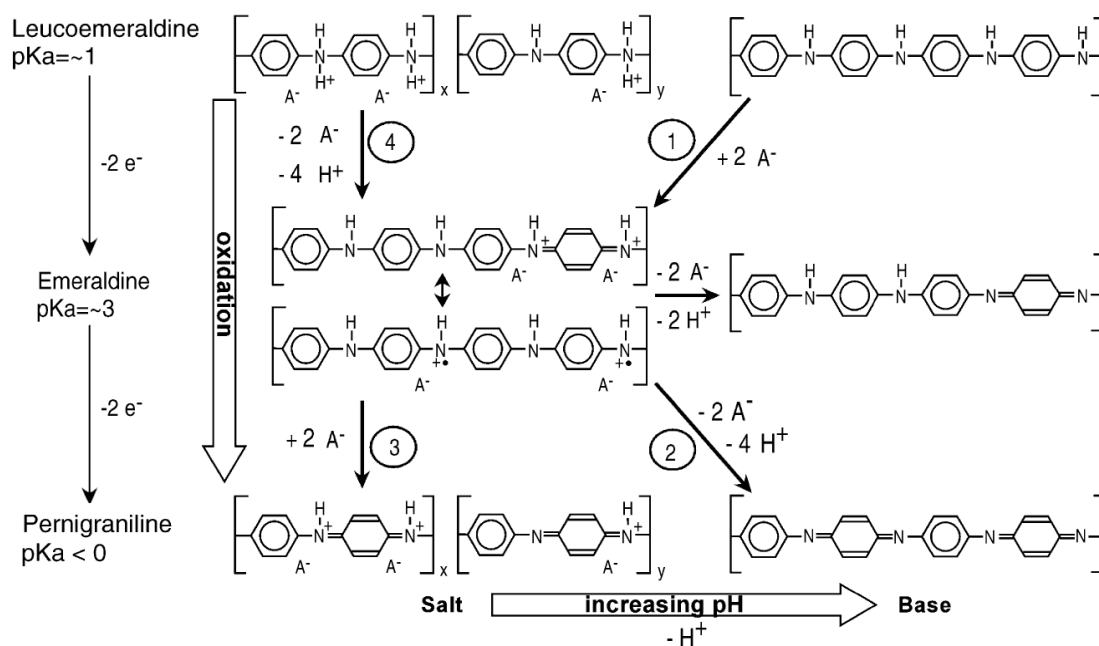
Fig. 2.8. Electrochemical oxidation states of polyaniline. In the fully protonated states (left), the polymer comprises only *x* units, but in most acids the chains are mixtures of *x* and *y* units, the ratio depending on pH. During electrochemicla oxidation in aqueous electrolytes, the gain or loss of anions and protons, and the strain, depends on solution pH [11].

The changes of pH also provoke changes on electrical conductivity of emeraldine as shown in Fig. 2.9 [12]. These changes should be connected with salt-base equilibrium.
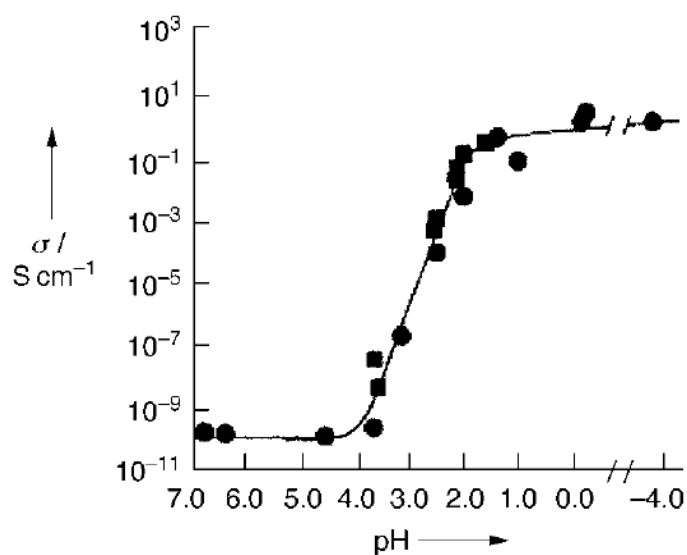
Fig. 2.9. Conductivity of emeraldine base as a function of the pH of the HCl dopant solutions as it undergoes protonic acid doping [12].

2.1.2. Degradation of polyaniline

Degradation of polyaniline is very important issue due to the possible application in corrosion protection of steel under different conditions.

2.1.2.1 Electrochemical degradation

Since the electrochemical application of polyaniline is most important the degradation provoked by electrode potential or oxidation ability is considered first. Above potentials of ~0.4 V or during chemical synthesis or during the electrochemical oxidation the formation of the polyaniline degradation or hydrolysis products occur [10, 13-20]. This can be seen on cyclic voltammograms shown in Fig. 2.10 [21].
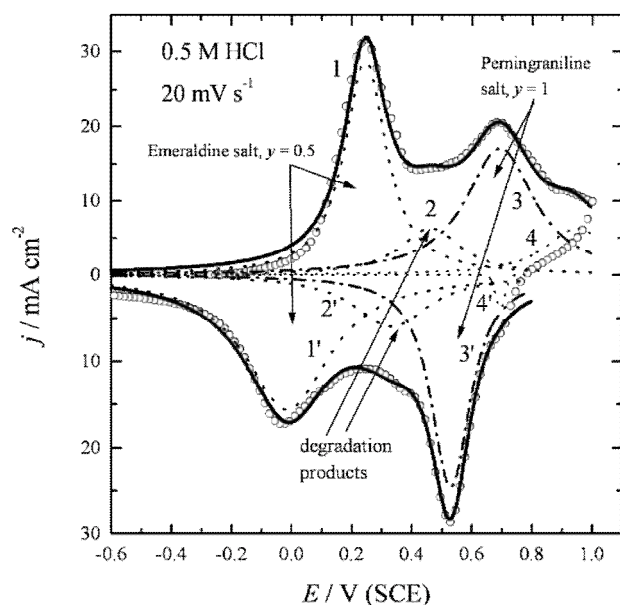
Fig. 2.10. Cyclic voltammogram of polyaniline in 0.5 M HCl with deconvolytion of main peaks [21].

The main degradation product appears to be soluble **benzoquinone** with the redox of the **benzoquinone/hydroquinone** couple, as shown on Fig. 2.11 [22]. Other inactive insoluble degradation products have been suggested to remain on the electrode surface, including PANI strands containing quinoneimine end groups, and *ortho and para*-coupled oligomers [13-20].
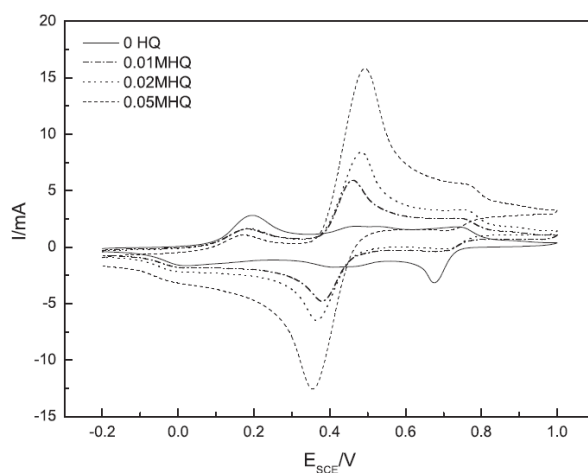
Fig. 2.11. Cyclic voltammograms of Pt-PANI electrode in 0.5 M H_2SO_4 containing different HQ (hydroquinone) concentrations. Scan rate: 50 mVs^{-1} [22].

12

Orto-coupled units may undergo intramolecular cyclization to produce phenazine structures as shown in Fig. 2.12 [2, 4, 23].
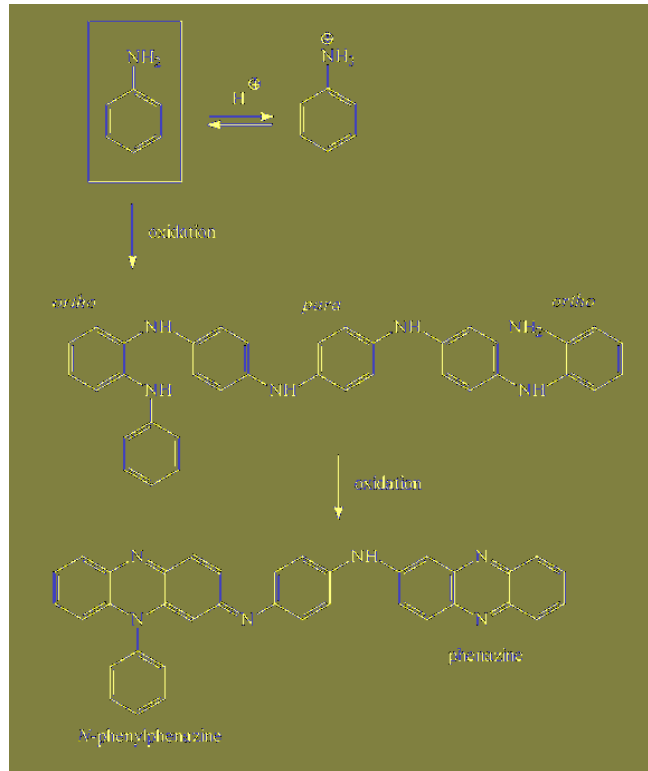
Fig. 2.12. Neutral aniline molecules are oxidized to oligomers having mixed *orto-* and *para*-coupled aniline constitutionl units. *Orto*-coupled units may undergo intramolecular cyclization to produce phenazine structure [23].

The problems which arise from electrochemical degradation are loss of available capacity for reversible exchange of anions, dissolution of polymer via formation of soluble benzoquinone, and formation of inactive insoluble phenazine structures in the polymer matrix.

As an example is loss of the capacity during cyclic anodic polarization of PANI electrode in 0.5 M NaCl due to the formation of degradation products at ~0.5 V, as is shown in Fig. 2.13.
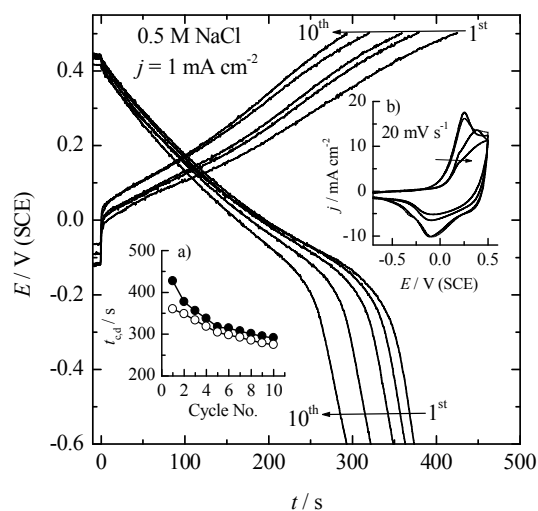
Fig. 2.13. Doping/dedoping curve of PANI electrode in 0.5 M NaCl. Inserts: a) dependance of charge (●) and discharge (○) times on number of cycles; b) cyclic voltammograms before, and after fifth and tenth doping/dedoping cycles.

2.1.2.2. Thermal degradation of polyaniline

Figure 2.14 shows TGD curves of doped and dedoped for granular and nano-road PANI [24].
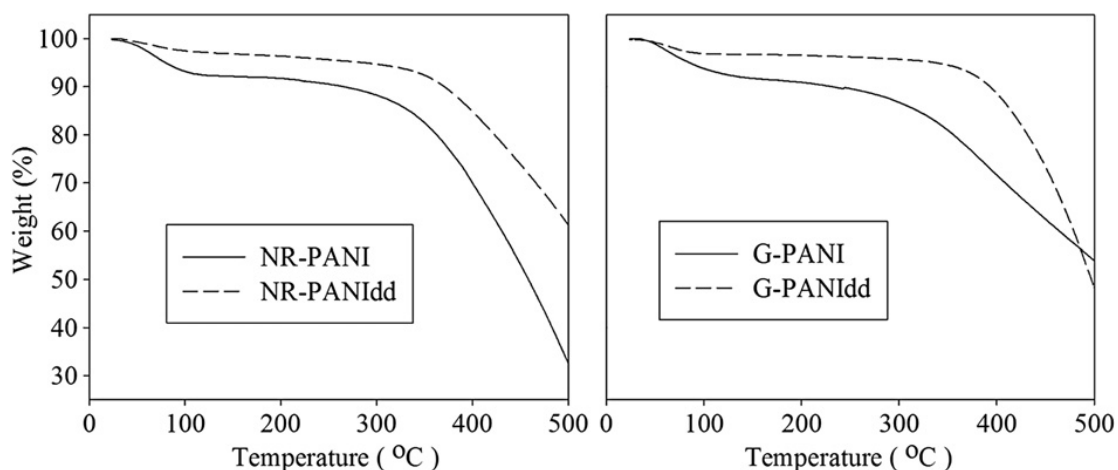
Fig. 2.14. TGA curves of PANI samples having granular (G-PANI and G-PANIdd) and "nanorod" like (NR-PANI and NR-PANIdd) morphologies prepared by oxidizing aniline with ammonium persulfate in the presence and absence of HCl, respectively (dd - dedoped) [24].

The first weight loss in all samples can be attributed to the loss of occluded moisture, out gassing of small molecules and removal of dopants. The first weight losses of NR-PANI and G-PANI, 7.8 and 7.3% respectively, were relatively higher than the first weight losses of NR-PANIdd and G-PANIdd, 2.7 and 3.1% respectively. The loss of dopants from NR-PANI and G-PANI could have contributed to their higher weight losses as NR-PANIdd and G-PANIdd, being the dedoped forms, were deficient in dopants. The modest second weight loss in all samples could be due to chemical changes including **cross-linking and oxidation** by means of deprotonation of the polymer chains. The third weight loss in all samples was of much higher magnitude compared to the first and second weight losses. This weight loss is attributed to significant degradation of polymer backbone. It. have been defined degradation as >10% weight loss excluding the contribution from moisture. Therefore, it can be inferred from the TGA results that NR-PANI, NR-PANIdd, G-PANI and G-PANIdd are thermally stable, to the point of commencement of the third weight loss, up to 300, 340, 250 and 350^0C respectively. NR-PANI and G-PANI had a lower thermal stability compared to their dedoped forms. It has been previously reported that in HCl doped PANI, dedoping predominates other changes at 250^0C, resulting in the loss of bound water and bound HCl. While G-PANI was synthesized in presence of HCl, the protons released from the persulfate oxidant would have created an acidified environment for NR-PANI. It is likely that NR-PANI and G-PANI begin to lose their bound acids from deep inside the bulk of the polymer clusters at 300 and 250^0C respectively, followed by degradation of the polymer chains at higher temperatures. Therefore, the third weight loss for NR-PANI and G-PANI was observed at lower temperatures compared to NR-PANIdd and G-PANIdd.

It is envisioned that cross-linking is established through a link of the imine nitrogen with its neighboring quinonoid ring, and shown in Fig. 2.15. The cross-linking reaction produces cyclized phenazine-like segments containing ternary nitrogen.
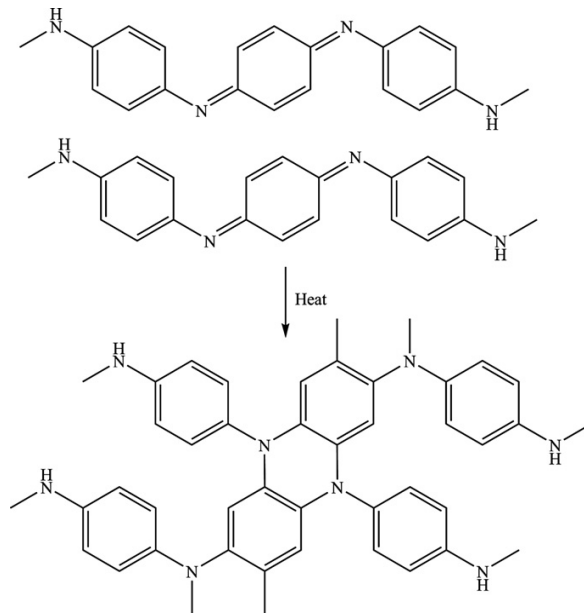
Fig. 2.15. Cross-linking scheme for PANI upon heating [24].

Due to the cross-linking conductivity of PANI decrease with increasing heating temperature, as shown in Table 2.1.

Table 2.1. Effect of heat treatment temperature on the DC conductivity of PANI [25].

Sample	σ_V^{DC} (S/cm)
Untreated PAni	2.6×10^{-3}
Heat treated at 150 °C	0.8×10^{-3}
Heat treated at 200 °C	3.0×10^{-5}
Heat treated at 250 °C	1.0×10^{-8}

Conductivity decrease with increasing aging times at the same temperature, as shown in Fig. 2.16 [26], and with nature of the aging atmosphere, as shown in Fig. 2.17 [27].
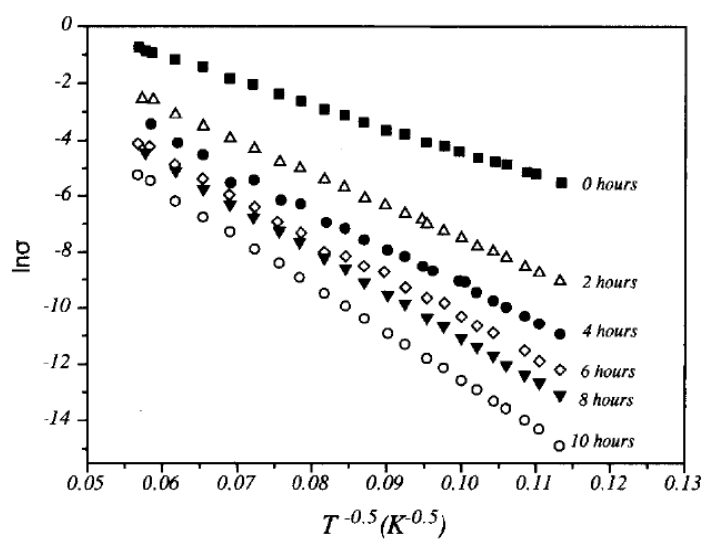
Fig. 2.16. The lnσ =*f*(T$^{-1/2}$) lines for a polyaniline sample with various aging times at 120°C [26].
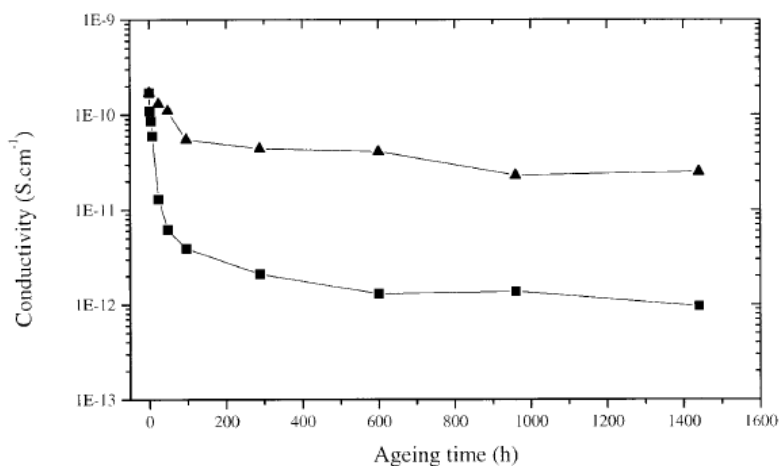
Fig. 2.17. Conductivity for pressed EB (emeraldin base) pellets vs. aging time for (▲) powder aged under vacuum at 140°C and (■) powder aged in air at 140°C [27].

This difference can be explained by influence of oxygen from air, as shown in Fig. 2.18 [28]
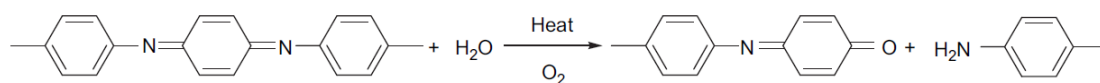
Fig. 2.18. Scheme for the mechanism of oxygen incorporation and chain scission [28].

The influence of thermal treatment leads to spontaneous dedoping of inserted anions, cross-linking of the polyaniline producing phenazine-like structures, crystallizations and losses in electrical conductivity. From this it could be concluded that polyaniline should not to be heated over $\sim 100^0$C.

2.1.2.3. UV degradation of polyaniline

The polyaniline can be applied as materials for solar cell application and electrochromic windows. Under this conditions UV radiation in different gas ambient plays a dominate rolls [29]. Exposure to UV radiation in the range of 380 to 400 nm was seen to increase film transmittance by 4% through photo bleaching, as shown in Fig. 2.19. Different gases ambient were employed for this experiment and progressively more photobleaching was observed for nitrogen, air and oxygen atmospheres, Fig. 2.20. This effect arises due to the destruction of quinoid and benzenoid chromophores on the polymer backbone.
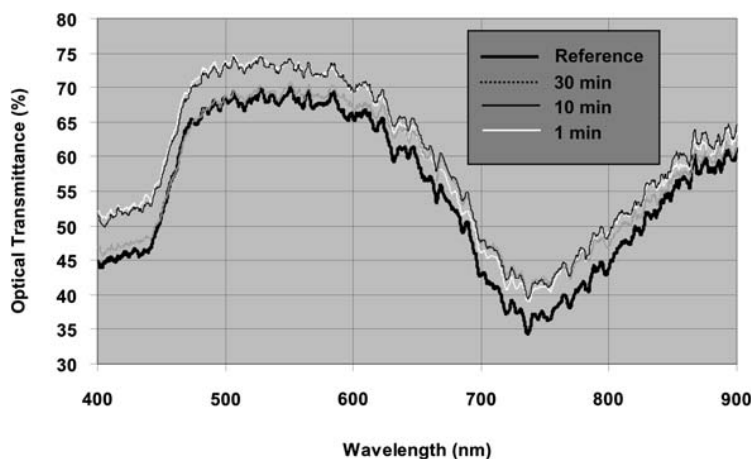
Fig. 2.19. Optical transmittance spectra of polyaniline thin films on glass substrates with various durations of UV exposure: 1, 10 and 30 min [29].
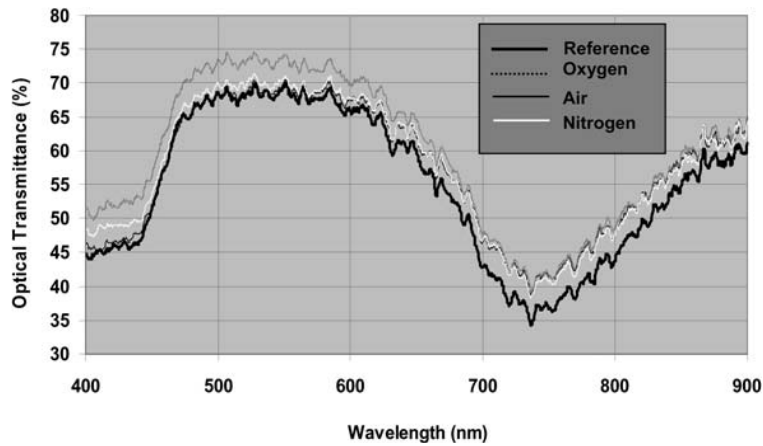
Fig 2.20. Optical transmittance spectra of polyaniline thin films on glass substrates after 30 min UV exposure each under nitrogen, air and oxygen ambient [29].

Concomitantly, a decrease in film resistivity was also observed and this can be attributed to increase oxidative doping of the film material, as it can be seen from Table 2.2.

Table 2.2. Surface resistance of polyaniline films measured between gold contacts 2 mm apart; before and after 30 min of UV exposure under air, nitrogen and oxygen [29].

	Before UV exposure	After 30 minutes UV exposure
Nitrogen	3783 Ω	3592 Ω
Air	3783 Ω	3287 Ω
Oxygen	3783 Ω	3585 Ω

The observations presented above show unambiguously that exposure to UV radiation leads to degradations in polyaniline that adversely affect its electrical characteristics. Other conjugated organic conductors are also susceptible to similar structural modifications under UV irradiation that adversely affect their electronic properties. It is, therefore, important to find ways to prevent these functional polymers from degrading under UV exposure, especially as there will be increasing use of organic photovoltaic devices in the future which will be directly exposed to substantial flux of

UV radiation during their useful lifetime. Towards this end it have been investigated the addition of UV-protecting materials to polyaniline in order to gauge their effectiveness in mitigating the harmful effects of UV radiation. Most organic photostabilizers are characterised by short lifetimes or low populations of the triplet state of molecules and our chosen additive was not an exception to this. While a number of UV absorbers, such as benzophenone and its derivatives, have been long known we explored the use of a more modern especially-designed UV photon absorber that is itself highly stable against UV irradiation in the 280 to 400 nm range. One of such additives is commercially known as Tinuvin 213. This is a hydroxyphenyl benzotriazole-based UV absorber, manufactured by BASF, that competes for UV photons with the base polymer to which it is added. It comes as a rather viscous light yellow liquid that is miscible with many organic solvents. This material is in fact one of an entire class of efficient UV absorbers that possess the ability to convert the energy absorbed from UV light into heat via a mechanism called keto-enol tautomerism. This heat can then dissipate through the substrate. As Fig. 2.21 shows, such light absorbers harvest photons through a cyclic mechanism that keeps regenerating the active absorber species. The intramolecular hydrogen bond (IAHB) present in this absorber is widely believed to be responsible for its outstanding photochemical properties. This efficient photochemistry has made benzotriazoles into widely used functional chemicals in industry for many types of UV protection applications. Tinuvin 213 can be added to polyaniline by first dissolving it in toluene and then adding a small amount of this solution to polyaniline colloidal solution to obtain a concentration of 3% Tinuvin 213 in polyaniline.
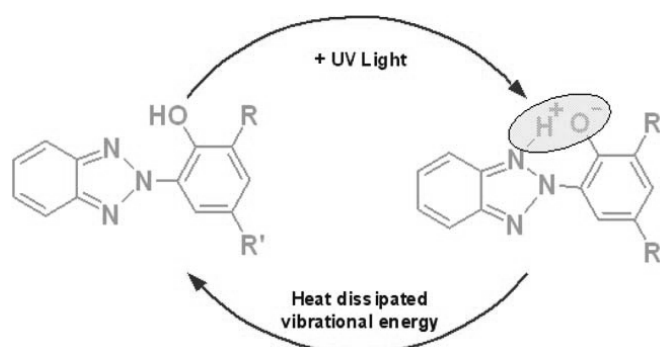

Fig. 2.21. Cyclic keto-enol tautomerism mechanism involved in UV protection through benzotriazole-based UV light absorbers (UVAs) [29].

2.1.3. Application of the polyaniline

Due to the physico-chemical property of polyaniline many applications have been proposed [30-34].

- Their ability to store charge reversibly, suggests they might be used in rechargeable batteries like Zn|PANI, PANI|PbO_2.
- The fact that their color depends upon their redox state has led to the development of 'electrochromic' devices.
- Application in the solar cell materials,
- Application as antistatic materials,
- 'Smart' coatings for military vehicles, the color of which can be switched electrically if the vehicle is re-deployed from, for instance, a forested area to a desert,
- Radar-absorbable coatings for 'stealth' aircraft and ships,
- Gas-sensing devices based on the fact that the conductivity of the polymer film varies on exposure to reducing gases like H_2S or NH_3,
- **Active protection of metal corrosion.**

Efforts are presently underway to develop methods of corrosion protection of different metals that are more effective and also more environmentally friendly than the present techniques. Recently, there has been an upsurge of interest in the prevention of metallic corrosion using coating strategies based on intrinsically conducting polymers (ICPs), thus, creating, an important research field mainly due to restrictions on the use of heavy metals, which have been considered environmentally unacceptable and toxic. Polyaniline (PANI) and its derivatives are among the most frequently studied ICPs used for corrosion protection.

2.2. CORROSION PROTECTION OF THE MILD STEEL WITH POLYANILINE

Classical organic coatings are used to protect metals against corrosion and harsh environments for many years [35]. In recent years, there has been a great interest in using electrically conductive polymers to protect steels, and other metals and alloys [36-39]. Polyaniline is the oldest known synthetic electrically conductive polymer [12]. PANI is readily synthesized and it readily participates in redox reactions. It is thermally stable with high corrosion resistance.

The application of PANI as an inhibitive coating for corrosion protection of active/passive alloys was first reported in 1985 by DeBerry [40]. He electro polymerized polyaniline on the stainless steel from 1 M aniline in 0.1 M $HClO_4$, and observed completely different behavior in 0.2 M H_2SO_4 than for the bare stainless steel, as shown in Fig. 2.22.
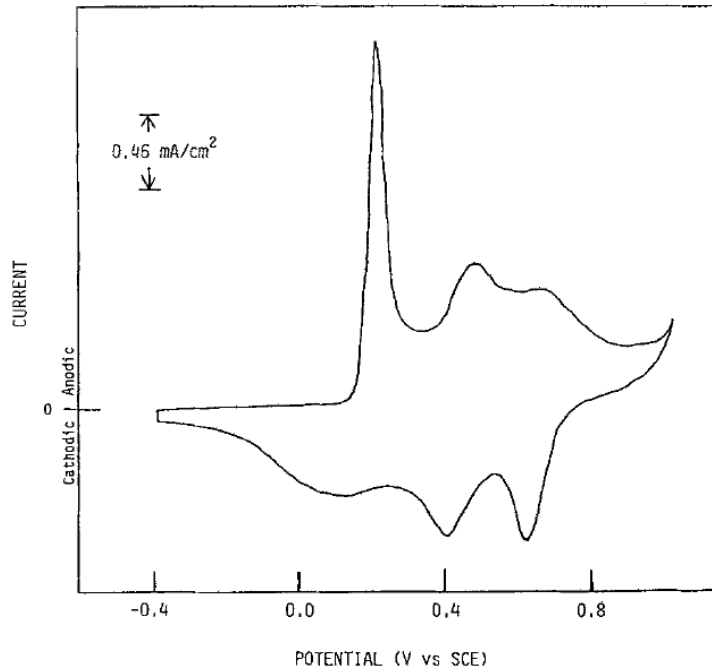

Fig. 2.22. Cyclic voltammogram at 20 mV/s for polyaniline-coated type 410 SS in 0.2 M H_2SO_4 after 19 h exposure [40].

As mentioned earlier, PANI can be synthesized by chemical oxidative polymerization and then be used as corrosion inhibitive pigment in paint coatings to protect sensitive metals or alloys, or it can be deposited on the metallic parts through the electro polymerization of aniline from a suitable medium to limit the dissolution of the substrate. Both electro-polymerized coating [41-43] and polymer-pigmented paint coating method [44-48] have been found to offer corrosion protection.

2.2.1. Electrochemical synthesis of polyaniline on mild steel

The basic problem related to electrochemical synthesis of all conducting polymers on mild steel are relatively high potential of polymerization that lies in the region of intense iron dissolution. Therefore, solutions to be used in the electrochemical synthesis of conducting polymers should be able to passivate iron, with limitation, that the formed passive layer must not exhibit insulator properties [49-51].

As an example these behavior is polymerization of polypyrrole on mild steel [52]. In Fig. 23a the anodic stationary polarization curve of mild steel in 0.1 mol dm^{-3} oxalic acid solution was shown. Corrosion potential of mild steel (E_{corr}) of -0.517 V (SCE) indicate that the steel is in active state without formation of passive layer. Active dissolution occurs up to the potential of -0.42 V with the maximum current density of ~ 3.5 mA cm^{-2}. At the potential more positive then -0.4 V passivation of the electrode with monolayer formation of closely packed $FeC_2O_4 \times 2H_2O$ precipitate occurs with the passivation current density between 10 and 30 μA cm^{-2}. In the potential range between 0.15 and 0.65 V the decomposition of $FeC_2O_4 \times 2H_2O$ precipitate with formation of soluble products occur, followed by steel repasivation. Transpasive region and oxygen evolution reaction at the potential more positive then 1.1 V is observed. In Fig. 23b galvanostatic (1 mA cm^{-2}) response of mild steel and glassy carbon electrodes are shown.
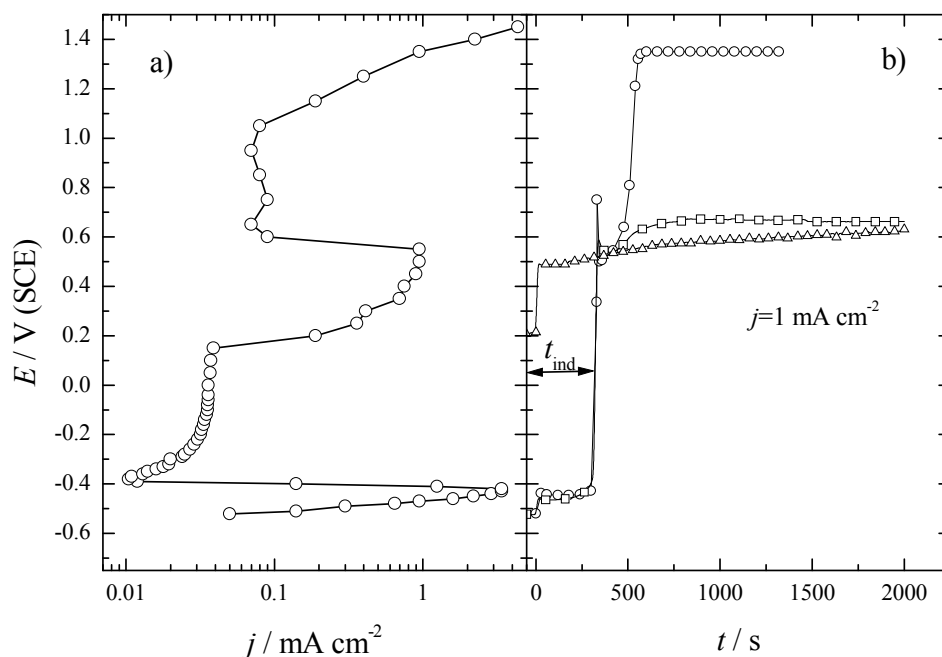
Fig. 2.23. a) Steady state anodic polarization curve of the mild steel in 0.1 mol dm^{-3} oxalic acid, b) galvanostatic (j=1 mAcm^{-2}) responses of (o) mild steel in 0.1 mol dm^{-3} oxalic acid (□) mild steel and (△) GC in 0.1 mol dm^{-3} oxalic acid + 0.1 mol dm^{-3} pyrrole [52].

Without pyrrole monomer in the solution steel electrode dissolves at the potential of –0.44 V for ~ 300 s, with formation of $FeC_2O_4 \times 2H_2O$ precipitate during the so called induction period (t_{ind}). After this period decomposition of $FeC_2O_4 \times 2H_2O$ interlayer starts, followed by pronounced potential peak which proceeds potential plateau at ~1.35 V in transpasive region. When pyrrole monomer was introduced in the solution, after decomposition of $FeC_2O_4 \times 2H_2O$, electrode potential was less positive and had a value of ~0.66 V which corresponds to the polymerization of pyrrole on the passive mild steel surface. Polymerization of pyrrole on the glassy carbon electrode was characterized by the absence of induction period, and polymerization occurs almost at the same potential as for the steel electrode. Based on this result it was concluded that substrate does not have influence on the pyrrole polymerization potential.

Among the large number of electroconducting polymers polypyrrole and polyaniline (PANI) are the most promising conducting polymers for the purpose of the corrosion protection. Nevertheless, the lower price of aniline monomer comparing to pyrrole makes PANI more challengeable. Unfortunately, due to the high polymerization potentials of +0.4 up to 1.0 V [49], only few electrolytes suitable for PANI deposition on mild steel were reported.

Camalet et al., in the series of papers, investigated different electrolytes for electropolymerization of PANI on mild steel [53-57].

From the electrolytes based on 0.3 M oxalic acid with 0.1 M aniline [53, 54] adherent PANI films were obtained. The galvanostatic experiments with different current densities showed iron dissolution, Figs 2.24 and 2.25, in the beginning of electropolymerisation, during so-called induction period. Such films exhibited very good protection against corrosion in an acidic solution (0.4 M NaCl+0.1 M H_2SO_4).

Fig. 2.24. Chronopotentiometric curves of a mild steel electrode polarized at various current densities in 0.3 M aqueous oxalic acid solution [53].

Fig. 2.25. Chrono-potentiometric curves of a mild steel electrode polarized at various current densities in an aqueous solution of 0.3 M oxalic acid + 0.1 M aniline [54].

They also investigated electrochemical behavior of mild steel, and synthesis of PANI films on mild steel from aqueous solution of 1 and 2 M tosylic acid [55, 56]. Galvanostatic experiments on mild steel in this solution with various current densities, showed the improvement regarding the amount of dissolved iron during induction period that can be diminished by increasing current density, as shown in Figs. 2.26 and 2.27.
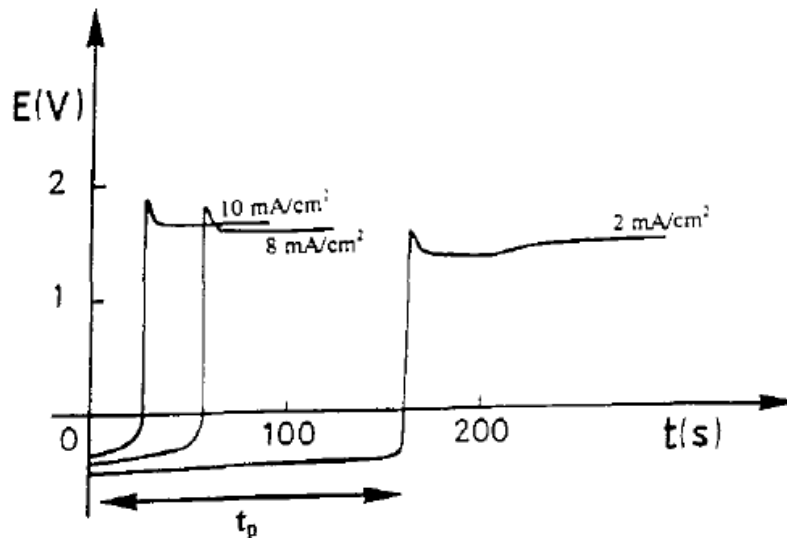

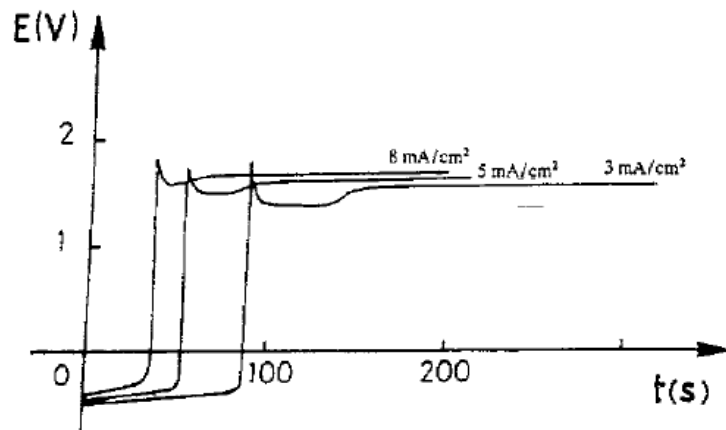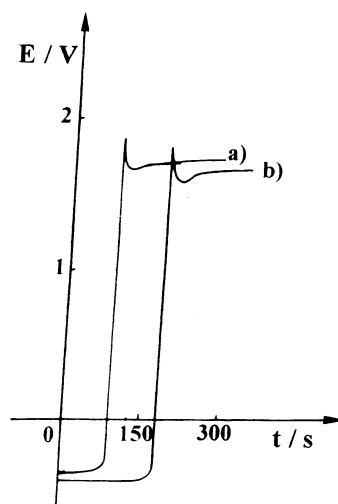**Fig. 2.26.** Chronopotentiometric curves of mild steel electrode polarized at various current densities in 1 M aqueous tosylic acid solution. (a) $j = 20$ mA cm^{-2}, (b) $j = 7$ mA cm^{-2}. [55]

26

Electropolymerization of PANI occurred in the potential range between 1.6 and 1.9 V, Fig 2.27. They showed that PANI film on mild steel could be used as an anticorrosion coating, but the general performance of the deposit should be improved by the formulation of the baths [55].
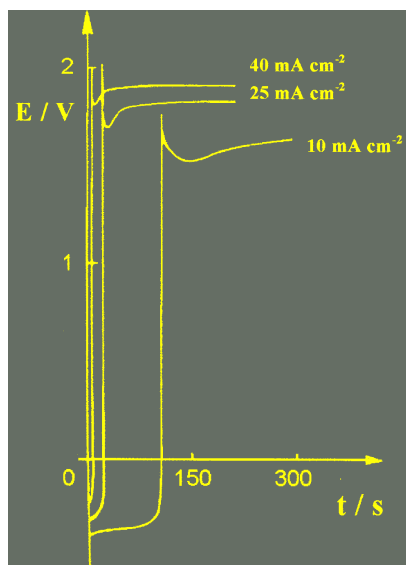
Fig. 2.27. PANI electrosynthesis in 0.4 M aniline+2 M tosylic acid solution for various current densities on mild steel [56].

From neutral solution of 2 M $LiClO_4$ with 0.2 M aniline, the adherent PANI films were obtained galvanostatically without induction period, applying the current density of 0.5, 1 and 5 mA cm^{-2} respectively, as shown in Fig. 2.28 [57].
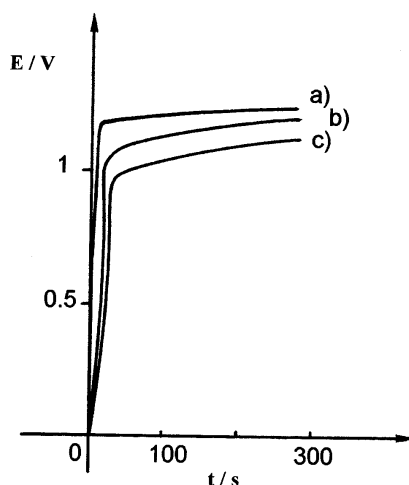
Fig. 2.28. Galvanostatic response of a mild steel electrode in a 2 M $LiClO_4$ + 0.2 M aniline solution at various current densities: (a) 5 mA cm^{-2}; (b) 1 mA cm^{-2}; (c) 0.5 mA cm^{-2} [57].

Popović et al. [58] investigated anodic behavior of mild steel in different organic and inorganic electrolytes, as shown in Table 2.3.

Table 2.3. Electrolyte composition [58].

Compounds	formula	c mol dm^{-3}
Oxalic acid	$C_2H_2O_4$	0.10
Sodium molybdate	Na_2MoO_4	0.10
Ammonium heptamolybdate	$(NH_4)_6Mo_7O_{24}$	0.025
Sodium benzoate	C_6H_5COONa	0.10
Citric acid	$C(CH_2)_2(COOH)_4$	0.10
Sodium nitrite	$NaNO_2$	0.10
Sodium salicilate	OHC_6H_4COONa	0.10

As it can bee seen in Figs. 2.29 and 2.30 mild steel in practically all electrolytes shows passive or pseudo passive behaviors.
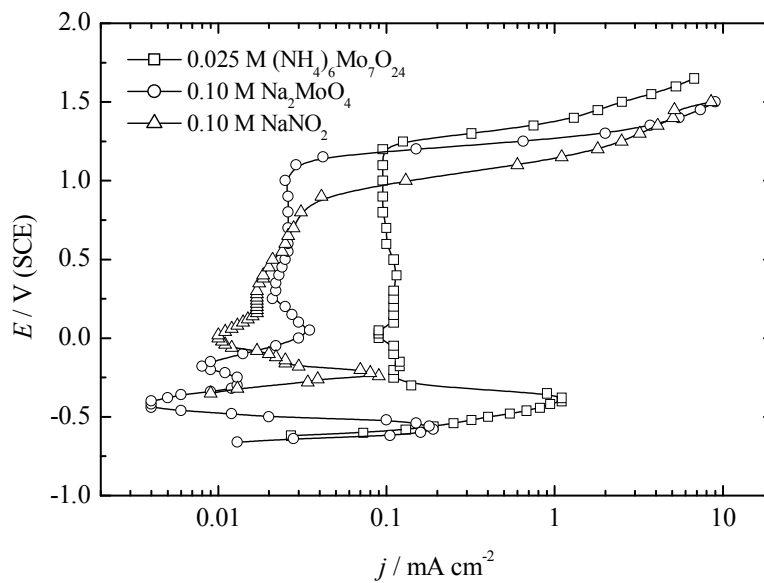
Fig. 2.29. Anodic polarization curves of the mild steel
in different inorganic electrolytes [58].
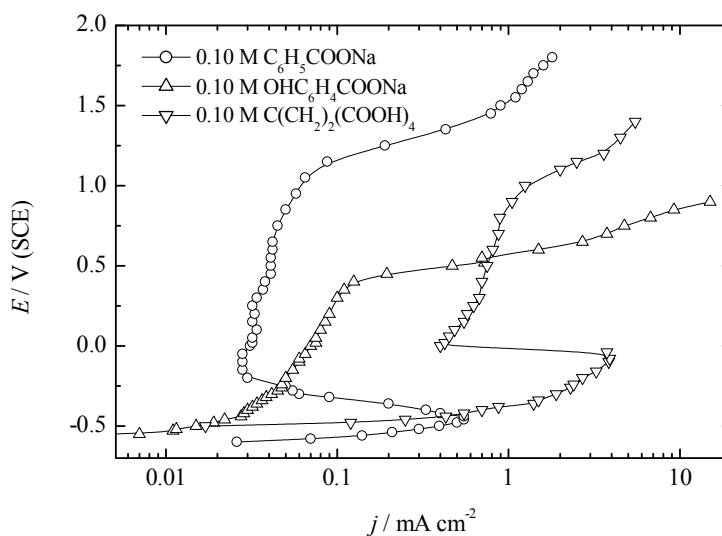
Fig. 2.30. Anodic polarization curves of the mild steel
in different organic electrolytes [58].

In the same solutions, authors investigated galvanostatic responses of the mild
steel and only in the oxalic acid solution observed existence of the induction period as it
can be seen from Fig. 2.31 [58].
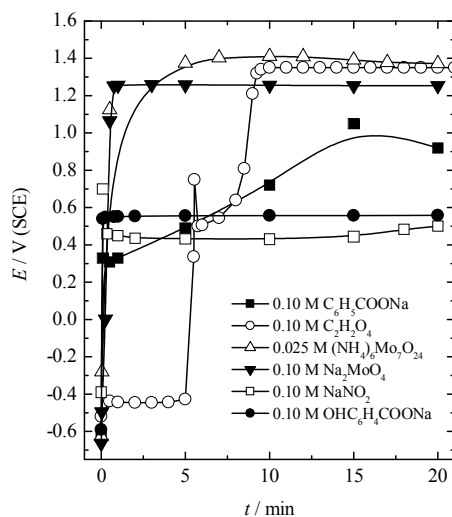
Fig. 2.31. Galvanostatic responses (j=1 mA cm^{-2})
of the mild steel in different electrolytes [58].

Unfortunately, after adding 0.1 M of aniline they found the only electrolyte which was suitable for aniline polymerization was based on sodium benzoate [42].

They found, Fig. 2.32, that without aniline in solution, except for the current density of 1.5 mA cm^{-2}, potential–time curves have relatively stable potential plateau, and induction period was not observed [42]. Applying higher current densities, e.g. 1.5mA cm^{-2}, potential increased from 1.3 to 2.25V for 700 s. After that period, sharp increase of the potential could indicate formation of non-conducting precipitate (e.g. iron-benzoate) on to the electrode surfaces. With aniline in solution, increase of the potential could be connected with polymerization of aniline. It was observed that in the moment when overall steel surface is covered with black film, potential sharply increased, and polymerization stopped. Quality of the film varied with applied current density. For the current density below 0.75mA cm^{-2}, film was partially brown, and no uniform. Above 0.75 mA cm^{-2} film was black. In all cases adhesion, determined by cracking, was good.
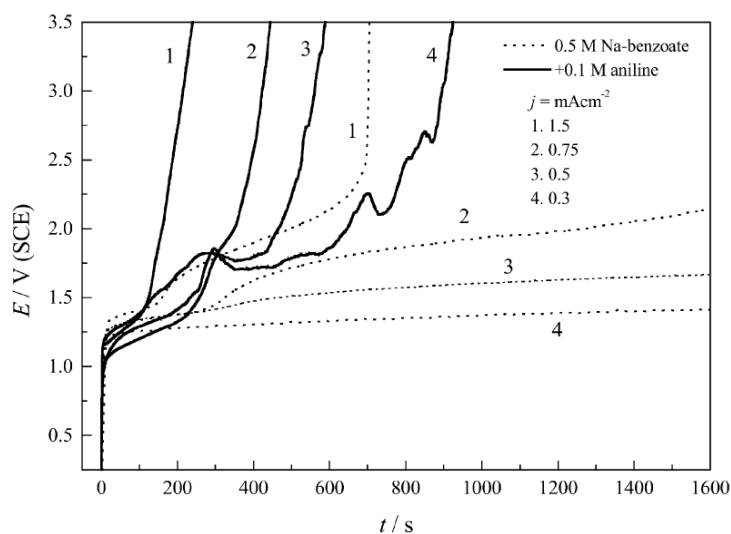
Fig. 2.32. Galvanostatic responses (current densities are marked in the figure) of mild steel in 0.5M Na-benzoate and with 0.1 M aniline [42].

2.2.2. Corrosion of the mild steel with polyaniline coatings

There is considerable evidence indicating that conducting polymers provide beneficial protection to many metals in a corrosive environment [49,50, 59-61]. Many studies since the mid-1980s have shown that a coating of PANI itself can inhibit the corrosion rate of mild steel [49,50, 59].

One of the first corrosion investigations of mild steel - polyaniline coatings was conducted by Wessling et al. [62-64]. Based on their studies clearly indication was shown that polyaniline coatings, made from dispersion, can provide significant corrosion protection to mild steel exposed to the severe corrosion environments of dilute HCI and NaCI. Further, this corrosion protection extends to exposed areas of bare steel that are galvanically coupled to the polyaniline coated steel. This corrosion protection appears to be electrochemically driven, being derived from both anodic and cathodic polarization. This behavior appears to unique among the usual mechanisms of corrosion protection provided by other types of corrosion inhibitors. The level of corrosion protection provided by doped polyaniline to mild steel exposed to dilute HCI was surprising. That this protection extends to bare steel areas was significant and of potential commercial importance. In fact, it appears that the level of protection provided by doped polyaniline is more significant for dilute acid conditions that for neutral saline conditions. It is also evident that the levels of protection provided by polyaniline to steel depend on the form of the polyaniline and the nature of the corrosion environment. Their results to date were obtained with coatings of polyaniline that exhibited rather poor adhesion to steel substrates. They anticipate even better corrosion protection behavior will be observed with good quality, adherent primer coatings for steel containing polyaniline.

Mirmohseni et al. [65] conducted a series of electrochemical measurements, including corrosion potential and corrosion current has been made on polyaniline-coated iron samples in various corrosive environments such as NaCl 3.5%, tap water and acids. Polyaniline was synthesized chemically and dissolved in 1-methyl-2-pyrrolidone (NMP) solution [66]. This solution was cast drop-wise onto pretreated iron samples. A level has

to be obtained before casting. The emeraldine base-coated samples were dried in an oven at 60^0C for about 12 h. It was found that corrosion potential of the polyaniline-coated samples was shifted toward noble potentials indicating better performance of polyaniline coating. A significant decrease in corrosion current was also observed. It was also found that polyaniline coating in many cases can be preferred over a conventional polymer such as PVC. This has been confirmed by electrochemical measurements in corrosive environments such as NaCl 3.5%

Pawar et al. [67] investigated electrochemical synthesis and corrosion protection of polyaniline coatings on mild steel from aqueous salicylate medium. Polarization curves of uncoated and polyaniline coated mild steel is shown in Fig. 2.34 The corrosion rate of polyaniline-coated mild steel was found to be 0.0005 mm/year which was 400 times lower than that observed for uncoated mild steel.
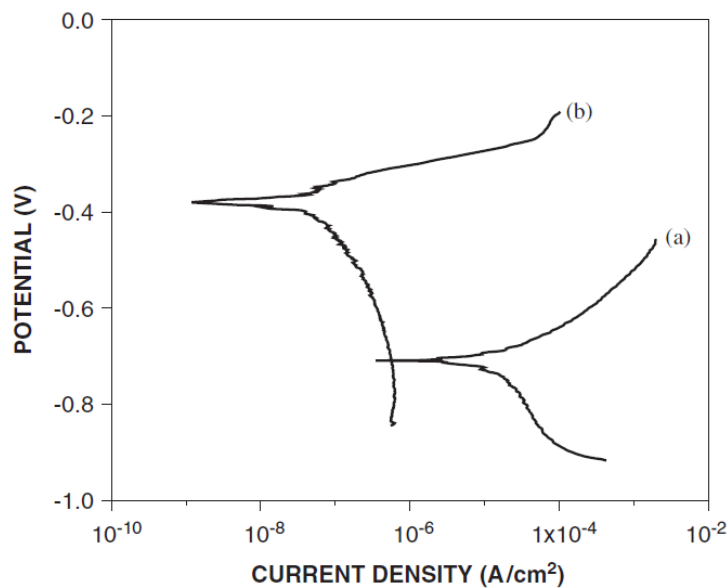
Fig. 2.34. Potentiodynamic polarization curves for (a) uncoated mild steel and (b) polyaniline coated (~6 mm thick) on mild steel in aqueous 3% NaCl solution [67].

Popović and Grgur [42] investigated corrosion behavior of the mild steel and 1.5 μm thick PANI-benzoate coated mild steel in 0.1 M H_2SO_4 using electrochemical

impedance technique. Analyzing the data, Fig. 2.33, they observed that corrosion with PANI coating was an order of magnitude smaller than for bare mild steel.
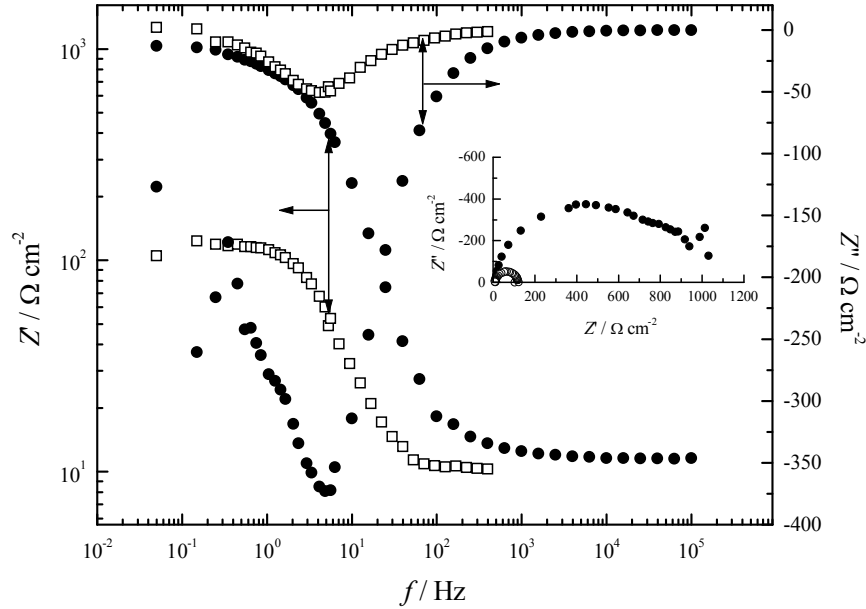
Fig. 2.33. The frequency dependencies of real (Z') and imaginary (Z'') impedance parts for bare mild steel (□) and mild steel covered with 1.5 μm PANI film (●) in 0.1 M H_2SO_4. Insert: Nyquist plot for same systems [42].

The conducting polymer can either be applied as a neat coating as discussed above, or as a dispersion in another polymer binder. In most studies, a barrier topcoat with classical organic coating is also applied over the top of the conducting polymer "primer."

2.2.3. Corrosion of the mild steel with polyaniline undercoat

Fahlman et al. [68] investigated undercoats of emeraldine base polyaniline and found that provide excellent corrosion protection for iron and cold rolled steel. The iron oxide of the steel and iron surfaces, before and after corrosion, were studied and found to have a thin top layer of Fe_2O_3, estimated thickness of 0.15 nm, followed by a thicker layer of Fe_3O_4. The removal of the thicker, preexisting oxide layers were found to

substantially increase the corrosion resistance of the cold rolled steel itself, and further increased the corrosion protecting capabilities of the EB undercoats. It was suggest that the EB undercoats offer anodic protection of both steel and iron. Large values of throwing power, at least 1.5 cm, were demonstrated for EB protected cold rolled steel.

Schauer et al. [69] investigated corrosion of pure iron coated with a commercial polyaniline primer (Ormecon Chemie, Ahrensburg, Germany) and three different epoxy clear topcoats: a solvent-based epoxy (EP), a water-based epoxy (EP1) and a water-based epoxy with wetting additives (EP2) in 0.5 M NaCl. The coatings were applied with a doctor blade in layers of 30 ± 5 µm for PAni-P and 70 ± 5 µm for top coats.
It was possible to distinguish between three separate phases, as shown in Fig. 2.34, in the corrosion protective action of low polyaniline content primers: conversion of original, primary iron oxides and formation of Fe_3O_4 and $g\text{-}Fe_2O_3$ as precursors of a passive layer, surface Fe-polyaniline complexes can also be produced at this stage; active corrosion protection with participation of conductive EB, based on a spatial separation of cathodic and anodic partial reactions as well as passivation of the metal substrate; barrier protection after ES -> EB transition due to the high resistance and sealing effect of EB. The efficiency of the corrosion protection in all three phases was dependent on many factors.
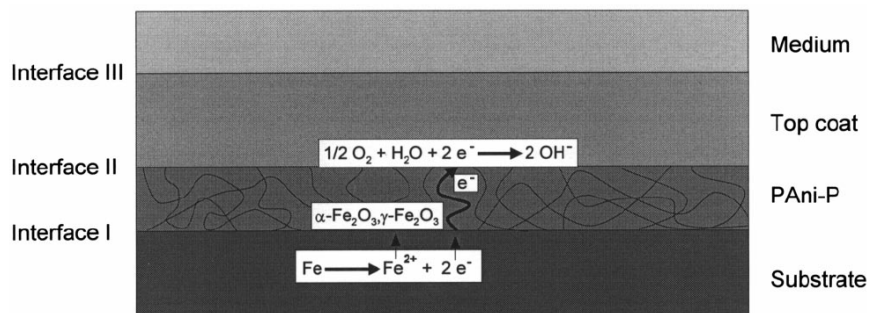
Fig. 2.34. Schematic representation of the protective mechanism of polyaniline in the phase of active corrosion protection [69].

The oxidation state of the iron surface plays an important role in the first phase. The durability of the active corrosion protection depends mainly on barrier properties of both the top coat and PAni-P as well as on the resistance of ES against alkaline media. This kind of protection can take place only by a limited diffusion of water and ions

through the coating and moderate electrochemical activities at the metal substrate. A good resistance of the primer/top coat interface towards elevated pH should be also ensured. In the third phase, only the barrier properties of the PAni-P/top coat system are crucially important. No reversible ES to EB or EB to leucoemeraldine transitions were found. Therefore, it is believed that these processes do not contribute essentially to the corrosion protection by polyaniline. The accompanied irreversible color change from green to blue signifies the change from active protection to barrier protection.

Grgur et al [70,71] investigated corrosion behavior of electrochemically synthesized PANI as undercoat with cataphoretically electrodeposited epoxy topcoat on mild steel in 0.1 M H_2SO_4 and 0.5 M NaCl. It was observed that thin PANI film in 0.1 M H_2SO_4, if used as modification of mild steel prior to epoxy coating deposition had provided better corrosion protection. Enhance of the protective properties of PANI/epoxy coated mild steel was observed in 70× and 20× higher values of the overall impedance, higher values of R_p and R_{ct} and lower values of calculated j_{corr} for two and one order of magnitude comparing to PANI coated and epoxy coated mild steel, respectively, as shown in Fig 2.35.

Fig. 2.35. Time dependences of corrosion current density for PANI coated mild steel, epoxy coated mild steel and PANI/epoxy coated mild steel in 0.1M H_2SO_4 [70].
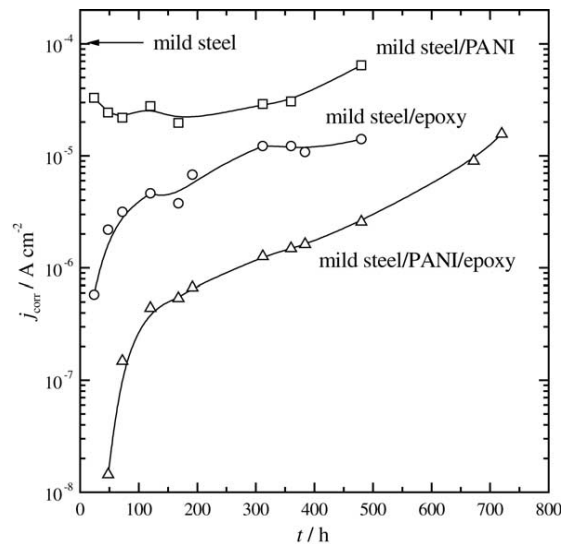
It was concluded, that during cathodic deposition of epoxy coatings on PANI coated mild steel, dedoping of anions occurs rapidly, therefore during exposure to

corrosion agent, the pores of the epoxy coating was not directly in contact with the bare metal, but with low conducting porous PANI film. So, PANI provides additional protection by its barrier effect.

Investigating the same system in 0.5 M (3%) NaCl by electrochemical impedance spectroscopy and thermogravimetric analysis it was shown that during initial time of exposure to 3% NaCl, PANI/epoxy coating system on mild steel has lower values of pore resistance (obtained from EIS), greater amount of absorbed water and lower thermal stability (obtained from TGA) which indicate more porous structure comparing to epoxy coating on mild steel [71]. It has been concluded that during the prolonged exposure to 3% NaCl, PANI/epoxy coating system exhibited increased corrosion protection of mild steel comparing to epoxy coating due to the additional barrier effect of PANI film and periodical doping/dedoping reaction with molecular oxygen. It was suggested that differences between corrosion behavior of PANI/epoxy coated mild steel in acid and neutral solution, as shown in Fig 2.36 are mainly connected with PANI film. After immersion in corrosion media, in 0.1M H_2SO_4 the protonization of leucoemeraldine PANI form can occur, which decreases the concentration of H^+ in the bottom of epoxy coating pores, decreasing the corrosion rate of mild steel. In contrary, in 0.5MNaCl oxygen reduction reaction on mild steel in the bottom of the overlapped epoxy/PANI pores occurs. Dissolved oxygen oxidizes dedoped (leucoemeraldine) PANI form (doping with chlorine anions), which produces the increase in local corrosion potential and faster dissolution of mild steel substrate.
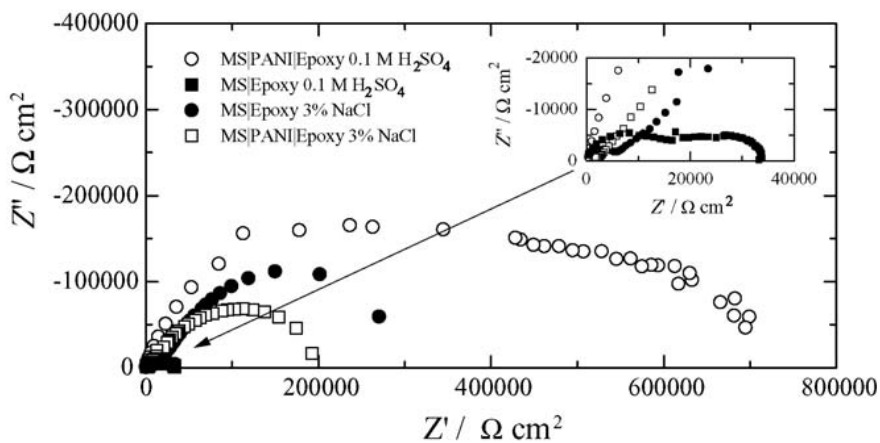

Fig 2.36. Comparison of EIS for epoxy coated mild steel and PANI/epoxy coated mild steel in 0.1M H_2SO_4 and in 0.5M (3%) NaCl after 24 h of immersion [71].

2.2.4. Corrosion of the mild steel with polyaniline blend

Polyaniline blend is usually treated as the best choice for the application in corrosion protection of mild steel. Namely, in such blends, polyaniline is highly dispersed in some classical polymer [72]. Such system can provide many advantages in the application as anticorrosion coatings on steel.

Talo et al. [73] studied emeraldin base polyaniline/epoxy blend coatings on steel in 0.1M HCl, 0.6M NaCl and 0.1M NaOH solutions, and found efficient protection in the latter two media even when a hole was drilled in the coating. These findings indicate that EB offered more than simple barrier protection. X-ray photoelectron spectroscopy (XPS) revealed a passive film of Fe_2O_3/Fe_3O_4 formed on the metal surfaces, suggesting the protection was anodic.

Corrosion protection of mild steel by PANI-HCl containing paint (0.1-20 wt.%) was also studied by Samui et al. [74]. Corrosion protection studies were conducted under both atmospheric and underwater conditions. The paints have shown appreciable corrosion protection properties at relatively low thickness (80 ± 5 μm). In accelerated weathering test painted MS panels did not undergo any corrosion after 1200 h of exposure. Humidity cabinet, salt spray and underwater exposure study has revealed that lower PANI-HCl containing paint protected MS better compared to that containing higher PANI-HCl. Potentiodynamic measurement in 3.5% sodium chloride solution has also shown more noble characteristics of lower PANI-HCl loaded paint. Water vapor permeability of lower PANI-HCl containing paint was very low which indicates its superior barrier properties. The barrier property contributes appreciably towards corrosion resistance of the PANI-HCl containing paint films. The paint system has shown appreciable corrosion resistance without any top barrier coat. Adhesion strength of paint on MS surface was found to be fairly good during the exposure and remains unaffected even after onset of corrosion compared to that containing higher PANI-HCl. Potentiodynamic measurement in 3.5% sodium chloride solution has also shown more noble characteristics of lower PANI-HCl loaded paint. Water vapor permeability of

lower PANI-HCl containing paint is very low which indicates its superior barrier properties. The barrier property contributes appreciably towards corrosion resistance of the PANI-HCl containing paint films. The paint system has shown appreciable corrosion resistance without any top barrier coat. Adhesion strength of paint on MS surface was found to be fairly good during the exposure and remains unaffected even after onset of corrosion.

Anticorrosion performances of polyaniline emeraldine base/epoxy resin (EB/ER) coating on mild steel in 3.5% NaCl solutions of various pH values were investigated by electrochemical impedance spectroscopy (EIS) for 150 days by Chen et al. [75]. They found that in neutral solution (pH 6.1), EB/ER coating of 20 μm offered very efficient corrosion protection with respect to pure ER coating, especially when EB content was 5–10%. The impedance at 0.1 Hz of the coating increased in the first 1–40 immersion days and then remained constant above 10^9 Ω cm^2 until 150 days, Fig 2.37, which in combination with the observation of a Fe_2O_3/Fe_3O_4 passive film formed on steel confirmed that the protection of EB was mainly anodic. In acidic or basic solution (pH 1 or 13), EB/ER coating also performed much better than pure ER coating. However, these media weakened the corrosion resistance due to breakdown of the passive film or deterioration of the ER binder.
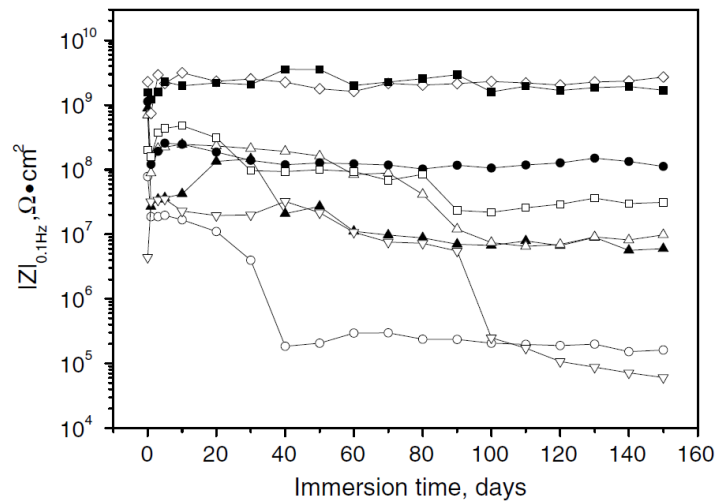
Fig. 2.37. Evolution of $|Z|_{0.1\,Hz}$ with immersion time in 3.5% NaCl solution for steel coated with ER coating (○), EB/ER coatings with EB contents of 1% (▲), 3% (Δ), 5% (●), 7% (◊), 10% (■), 13% (□) and 15% (∇) [75].

Incorporation of polyaniline (PANI) in epoxy type powder coating formulations was investigated by Radhakrishnan et al. [76]. Using specific grade of PANI with low doping degree, it can be incorporated in epoxy powder coating formulations by twin screw extrusion process. The powder formulations were deposited on steel substrates by electrostatic spray coating at −60 kV and baked at 140∘C for 20 min. These samples were extensively tested for corrosion resistance by exposure to hot saline conditions, Fig. 2.38, followed by electrochemical impedance spectroscopy and also salt spray testing.
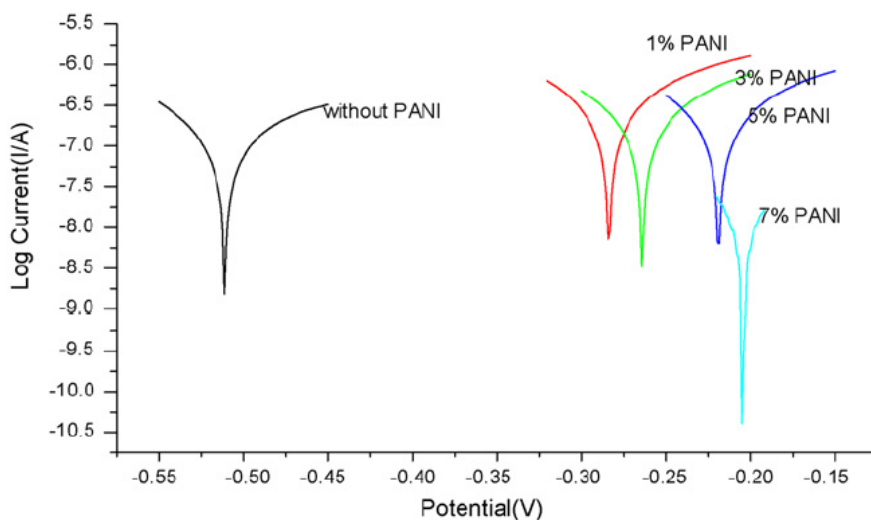
Fig. 2.38. Tafel plots for intentionally scratched epoxy powder coating
and exposed to hot saline conditions [76].

PANI incorporated coatings showed no deterioration even after 1400 h of hot (65∘C) saline treatment. The coatings intentionally scratched also exhibited self healing property and there was no rust formation even after prolonged exposure to hot saline conditions, Fig. 2.39. These results could be explained on the basis of additional crosslinking due to PANI, as confirmed by DSC results, which gave rise to improved barrier property and self healing was associated with the scavenging of ions by PANI which prevented corrosion of the underlying substrate.
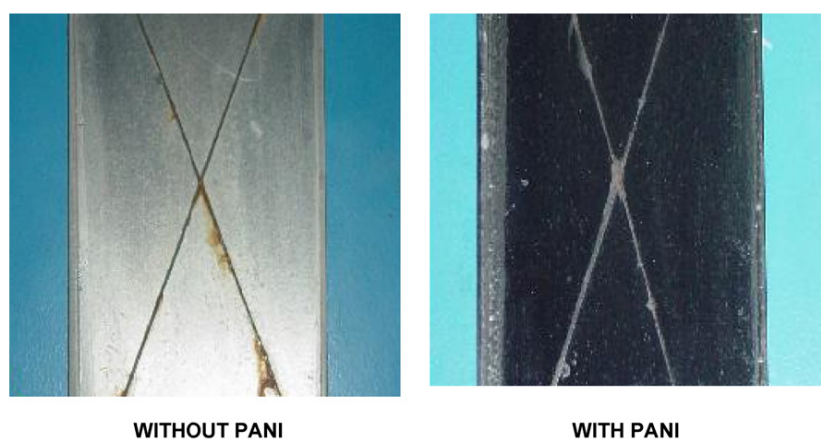
Fig. 2.39. Photographs of surface of epoxy coatings (left) and PANI modified epoxy coating subjected to salt spray tests after 700 h [76].

The epoxy coating with the phosphate doped polyaniline (1%) was able to offer protection in saline and acid media [77]. Phosphate doped polyaniline has been prepared by chemical oxidative method using ammonium persulphate as oxidant. FTIR study has shown that phosphate dopant is present as H_2PO_4- ion in polyaniline. Conductivity measurements indicated that the polymer has got good conductivity. The coating on steel has been found to be more protective in 3% NaCl and 0.1M H_3PO_4 than in 0.1M HCl.

2.2.5. The influence of polyaniline oxidation states on corrosion of the mild steel

Due to the different oxidation states of polyaniline, see Figs. 2.6 and 2.8 corrosion behavior should be considered from that point of views.

There are two forms of emeraldine PANI, doped-salt (conductive) and undoped-base (non-conductive). There are much fewer studies devoted to the corrosion protection properties of PANI in undoped emeraldine base form. Furthermore, there is some controversy on whether the conducting or non-conductive form of PANI exhibits the best corrosion protection properties [78]. For example, Araujo et al. [79] found that undoped PANI does not present required properties needed to be proposed as anti-

corrosive coating, while Spinks et al. [80] by comparison between the emeraldine salt and emeraldine base coatings concluded that the corrosion protection of a steel substrate by emeraldine base coating was superior. Tale et al. [73] and Dominis et al. [81] found that emeraldine base coatings provided a better corrosion protection than the coatings based on a conductive PAni. Meanwhile, Gasparac and Martin [82] found that the corrosion protection properties of PANI were independent of the doping level, and totally undoped emeraldine base coating was equally capable of maintaining the potential of the stainless steel substrate in the passive region. Also Dominis et al. [81] reported that the corrosion protection provided by emeraldine salt primers was strongly influenced by the type of dopant used.

As an example of such investigations are two papers of Armelin et al [83,84]. In 2008 they reported that "The coating constituted by the epoxy paint A modified with Pani-ES dispersed in xylene provided the best corrosion protection, even under very low conducting polymer concentration (0.3 wt%)" Fig. 2.40 [83].

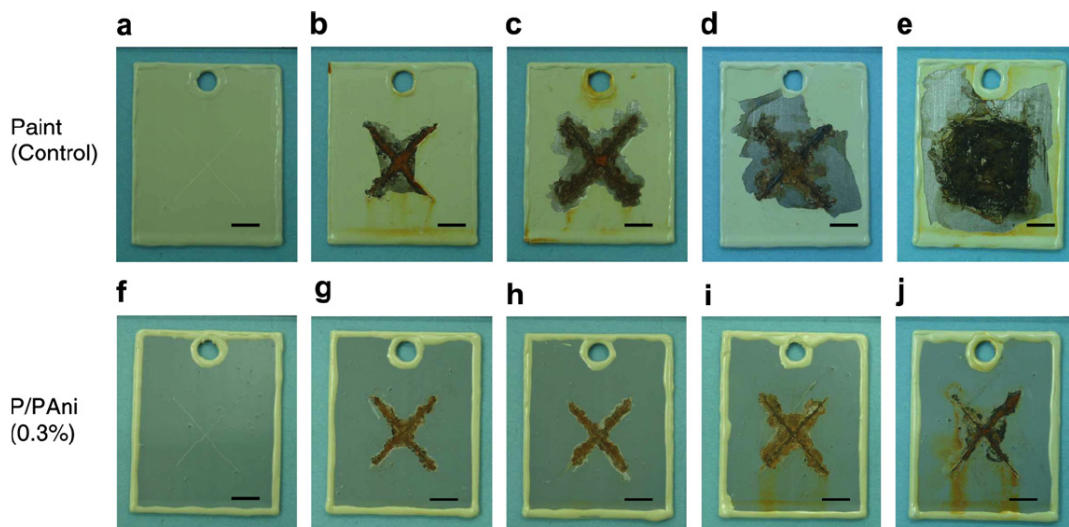**Fig. 2.40.** Test panels of epoxy paint A without conducting polymer (control) and paint modified with PAni-ES (0.3%) before (a,f) and after 120 h (b,g), 240 h (c,h), 480 h (d,i), and 720 h (e,j) of exposure in 3.5% NaCl solution. Scale bar: 9 mm [83].

After one year the same authors [84] concluded the following "Accelerated assays using an aggressive saline solution reveals that the panels coated with the epoxy

+ PAni-EB formulation are significantly more resistant against corrosion than those protected with the unmodified epoxy paint. Thus, results evidence that PAni-EB is very effective in inhibiting corrosion. Furthermore, the epoxy + PAni-EB formulation provides more protection than the epoxy + PAni-ES and the epoxy + $Zn_3(PO_4)_2$, Figs. 2.41 and 2.42. These results combined with those obtained for other epoxy coatings containing conducting and electroactive polymers as anticorrosive additives indicate that the protection mechanism of PAni-EB is based on the ability of this polymer to store charge (molecular condenser). Moreover, as the highest protectionwas imparted by epoxy + PAni-EB paint,we concluded that the mechanism based on the electroactivity of partially oxidized polymers is more effective than that based on the interception and transport of electrons. Finally, comparison between the performance of the epoxy + PAni-EB and epoxy + $Zn_3(PO_4)_2$ suggests the replacement of the conventional inorganic corrosion inhibitors by a small concentration of PAni-EB".
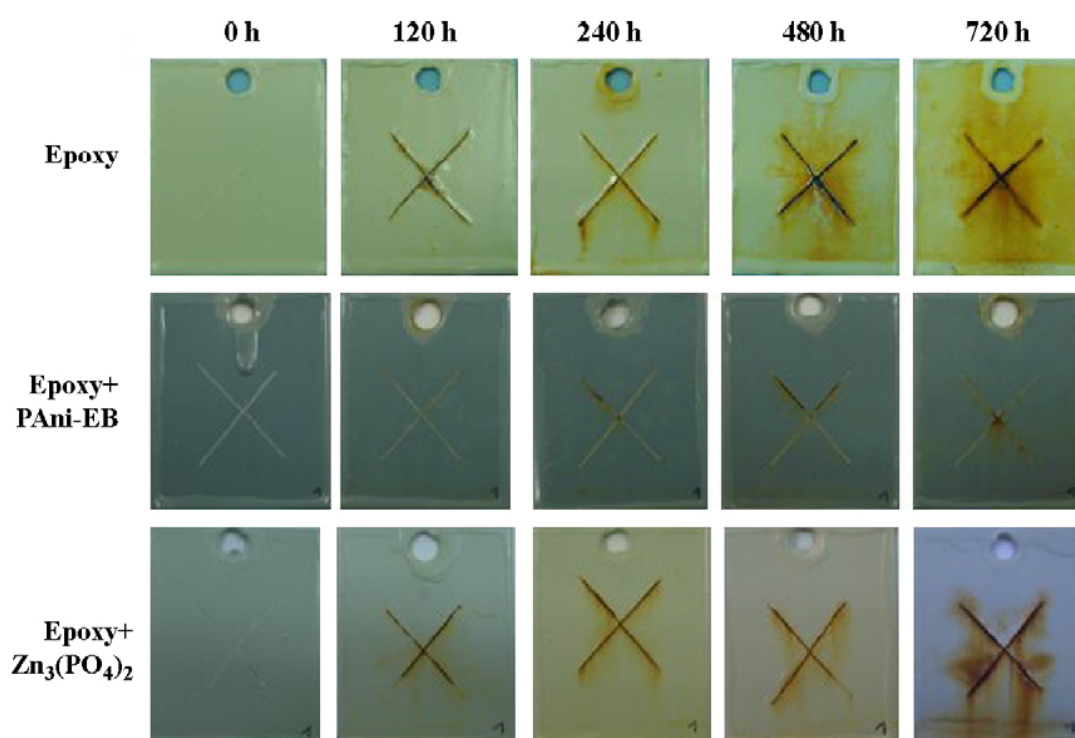
Fig. 2.41. Test panels of epoxy, epoxy + PAni-EB and epoxy + $Zn_3(PO_4)_2$ before and after 120, 240, 480 and 720 corrosion cycles [84].
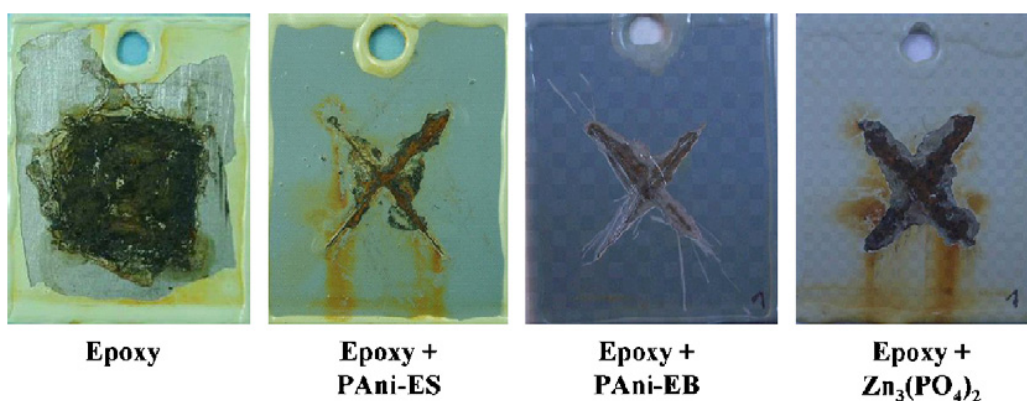
Fig. 2.42. Scrapped test panels of epoxy, epoxy + PAni-ES, epoxy + PAni-EB and epoxy + Zn$_3$(PO$_4$)$_2$ after 720 corrosion cycles [84].

2.3. EXISTING MECHANISMS OF MILD STEEL CORROSION PROTECTION WITH POLYANILINE

Since the uncertainty about the electroactive forms of polyaniline in corrosion protection, different mechanism has been proposed [59-61].

The problem arises due to the fact that many studies have been carried out using a wide variation of experimental procedures, causing difficulties in trying to compare the results. In particular, the surface preparation, the coating deposition method, the corrosion environment and the test method, can be very different from one study to another study. However, an effort has been made in this study to classify the corrosion protection mechanism. The possible mechanisms of corrosion protection of PANI on steel are essentially of following types [61]:

- Barrier properties (involving a *physical action*)
- Corrosion inhibition (involving a *chemical action*)
- Anodic protection (involving an *electrochemical action*)

Barrier properties

Organic coatings in general (including coatings with ICP as PANI) can protect metal substrates against corrosion following a general mechanism [49,71]. It is well established that most of the organic coatings with barrier effect permits the oxygen and water diffusion in quantities higher than the necessary amount for the corrosion rate measured on bare metal. It means that the reduction of oxygen and water availability at the metal surface, due to the presence of the coatings, is not sufficient to reduce remarkably the corrosion rate. The cathodic and anodic reactions are only half of the total corrosion reaction and a balance of the two electrochemical reactions is necessary. In particular it is necessary to have locally an electrical equilibrium balancing the electrical charge: electron and ions. In general it is not a problem for electrons to move, through the conductive metal, from one site to another, but several mobility problems can arise for ion diffusion. In the cathodic area there is an anion production (negative charge), and in the anodic site there is a cation production (positive charge). If the coating has a good adhesion (no lack of continuity at the metal-coating interface), the only possibility for balancing the charge is to move through the coating (from inside to outside or the opposite, or the lateral diffusion inside the coating, which is generally less probable because it involves a longer path) and this process is strongly hindered by the organic coatings. In this way the barrier organic coatings can reduce the corrosion rate of the metal substrate. Applying this mechanism to PANI containing coatings, we can note several problems. Water permeability is, in general, not different from typical values of commercial organic coatings (as epoxy coatings); it means about 3-5% w/w of water uptake maximum. Moreover, oxygen permeability is not very different from traditional organic coatings. Actually, evaluation of oxygen transport is complicated by the problem that the oxygen diffusion rate is dependent on the oxidation state of PANI. The same is true for ions diffusion (the dominating barrier effect for normal coatings). The ion diffusion process is not reduced in PANI, actually it could be higher when PANI is in the salty state. These facts suggest that the barrier effect is not the predominant corrosion protection mechanism for polymer coatings with PANI. A further clear evidence to support this statement is the lower corrosion rate of coatings

with PANI when scratched (defective coatings) in comparison with scratched traditional organic coatings. Even when the barrier effect is vanished, the presence of PANI can modify the corrosion process. In conclusion, **barrier effect cannot be the dominant corrosion protection mechanism**.

Corrosion inhibition

The presence of organic compounds close to the metal surface in principle could affect both anodic and cathodic corrosion reactions [49]. In this case the organic compound is called inhibitor. Organic inhibitors are usually designated to act as film forming, protect the metal by forming hydrophobic film on the metal surface. In this way the corrosion rate is influenced. Their effectiveness depends on the chemical composition, their molecular structures, and their affinities to the metal surface. Because film formation is an adsorption process, the temperature and pressure in the system are the important factors. Adsorption of organic inhibitors on a metal surface is strongly influenced by the ionic charge of inhibitors and the charge of the surface. The strength of adsorption bond is the dominant factor for soluble organic inhibitors. In this way organic inhibitors build up a protective film of adsorbed molecules on the metal surface, which provides a barrier against the dissolution of the metal in the electrolyte. Because the coverage of metal surface is proportional to the inhibitors' concentration, the concentration of inhibitor in the medium is critical. For any specific inhibitor in any given medium there is an optimal concentration. The inhibition effect of an organic compound is also significantly influenced by the mobility of the inhibitors, since it has to migrate to and adsorb on the metal surface. Monomeric aniline (before polymerization) has been proven to act as an organic inhibitor in several environments (acid environments and chlorides) on different substrates. The mechanism is a strong adsorption of aniline forming a hydrophobic surface layer, as in general for inhibitors. However, this behavior is not expected for PANI, because after polymerization the mobility of the molecular chains is strongly reduced. The only important consequence of polymerization, is that the adsorption could promote, in the case of PANI a good adhesion with the steel surface, influencing the long time durability of the coatings. However, in conclusion, **any direct corrosion inhibition effect (chemical action) of**

PANI itself should be excluded. The only possible inhibition effect is indirect and it is related to the released counter ions in doped PANI.

Anodic protection

Anodic protection is a corrosion protection strategy based on an anodic polarization by controlling the potential in a zone where the metal tends to be passive. In other words it is an approach favoring passivity and stabilization. For this reason it can be used only for materials having passivation possibility. Iron (steel) can passivate, as shown in Fig 2.43 [81].
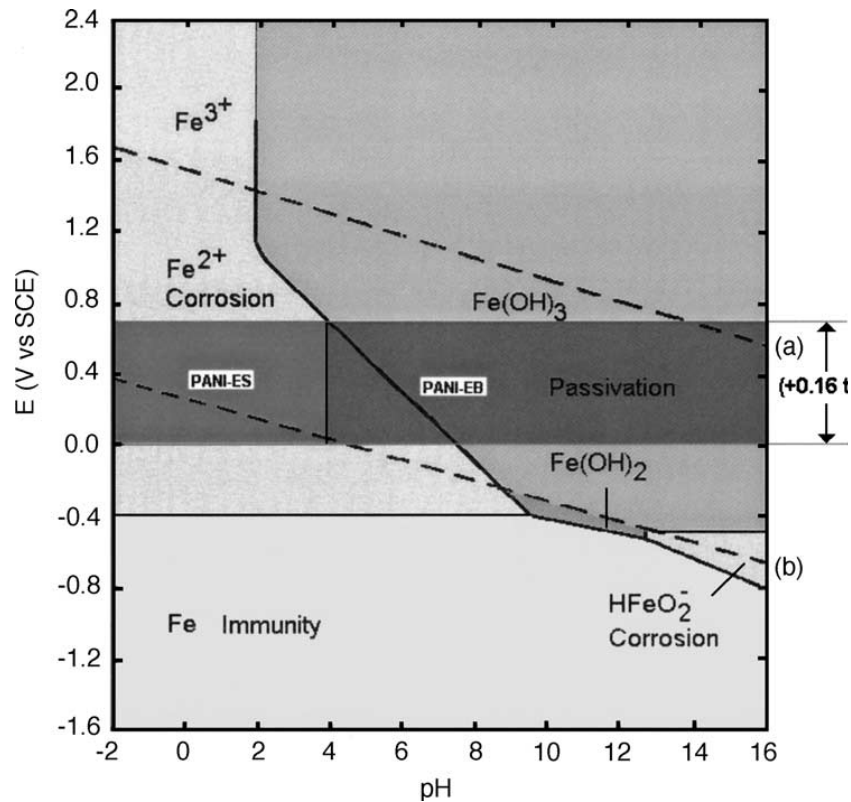
Fig. 2.43. Pourbaix diagram for steel in water. The stable regions for PANi–ES and EB are superimposed on the stable regions for iron. Dashed lines (a) and (b) represent the reduction potential for oxygen (in water) and hydrogen ions, respectively [81].

From Fig. 2.43 it can be deduced that alkaline pH is necessary to promote passivation. This aspect must be considered carefully because it can be in conflict with PANI's pH stability. In other terms, to have an anodic protection action it is necessary

to have a system in which both the passivation layer and the ICP based coating (PANI) are stable. The general anodic protection mechanism of ICP is the following:

$$1/n\ M + 1/m\ CP^{m+} + y/n\ H_2O \rightarrow 1/n\ M(OH)_y^{(n-y)+} + 1/m\ CP^0 + y/n\ H^+$$
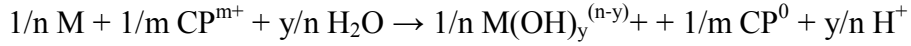
(where M is the metal (steel) and CP any electroactive conductive polymer), and

$$m/4\ O_2 + m/2\ H_2O + CP^0 \rightarrow CP^{m+} + mOH^-$$
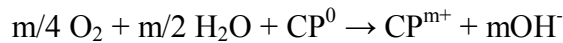
Many authors have tried to prove this mechanism by using different experimental approaches: open circuit potential measurements, metal surface analysis to identify the oxide layer, and surface analysis of CP to identify its oxidation state. Many authors reported an increase of the OCP (moving to anodic direction) of steel coated with CP in comparison with bare steel (ennobling). Considering that the passivation potential of steel is expected to be between 0.5 and 1 V SCE, the observed ennobling can be an indication of passivation. However, it is important to keep in mind that the passivation potential is in general dependent on the local environment (pH, oxygen concentration, chlorides, etc.) normally unknown close to the corroding area. Ennobling is a necessary condition for anodic protection, but it is not sufficient, since the OCP of coated steel is often increased also for barrier coatings because of the different corrosion conditions (concentration polarization and ohmic drop). In addition, it has been proven that PANI can modify the steel surface conditions (electrochemical studies of bare steel and bare steel obtained after removal of the PANI layer exposed to the electrolyte). These results have been obtained using different techniques, as impedance measurements (charge transfer resistance), visual observation (change of color), XPS analysis (formation of Fe_2O_3, Fe_3O_4), mass spectroscopy, etc. It is important to remember that surface conditions depend on the PANI form, EB (emeraldine base) or ES (emeraldine salt).

One of the first mechanisms based on anodic protection has been proposed by Wessling et al. [85]. Using UV-VIS spectroscopy and elemental analysis following the reactions which occur between PANI and steel, it was possible to clarify the passivation

reaction responsible for the amazing corrosion protection performance of PAni*. A reaction scheme is presented in Fig. 2.44.
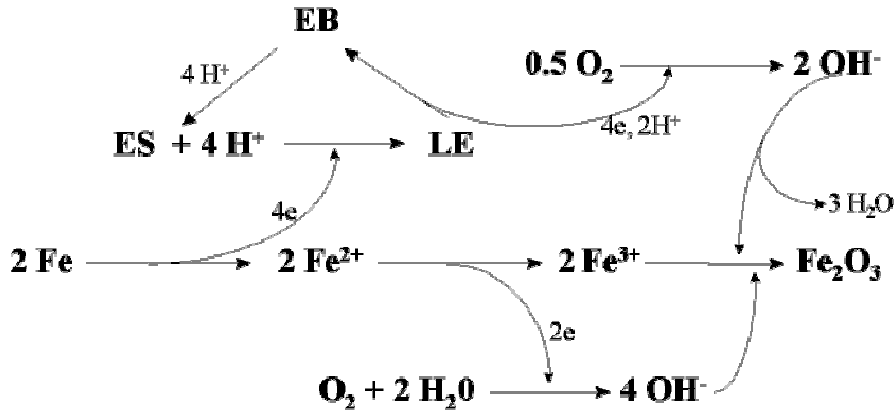
Fig. 2.44. A reaction mechanism proposed by Wessling et al. [85].

According to proposed scheme PANI is oxidizing iron to Fe^{2+} where it is itself reduced to leucoemeraldine. Further oxidation of the iron ions leads to Fe_2O_3, and oxygen is re-oxidizing the leuco form of PANI to the emeraldine salt. The full mechanism of the corrosion protection is consists of:

- potential shift due to the noble metal properties of PANI*, and
- the redox catalytic properties of PANI leading to the passivating oxide layer.

Similar mechanisms, given in Figs. 2.45 and 2.46, have been proposed by Dominis et al. [81] and Radhakrishnan et al. [76].
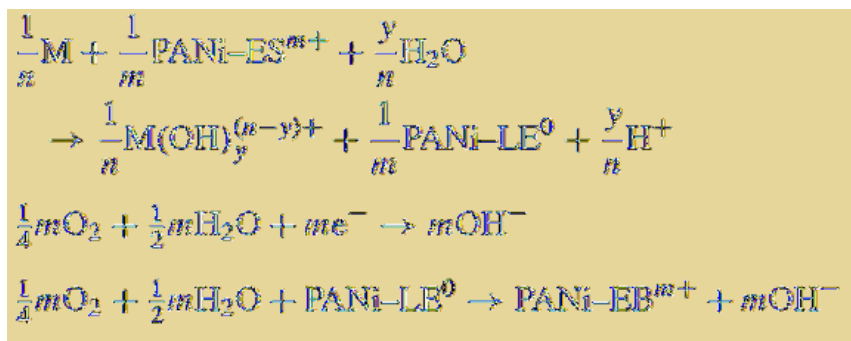
Fig. 2.45. A reaction mechanism proposed by Dominis et al. [81].
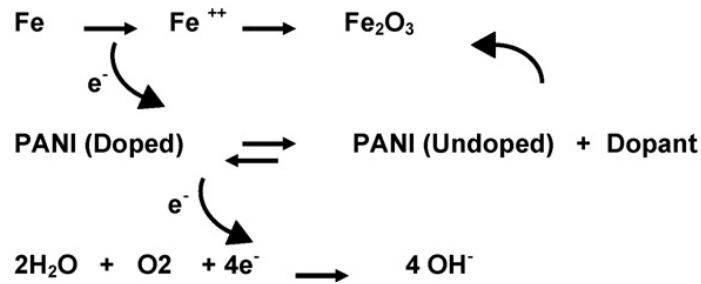
Fig. 2.46. A reaction mechanism proposed by Radhakrishnan et al. [76].

The mechanism of anodic protection of steel by PANI in acidic and neutral solutions has been proposed by Sathiyanarayanan et al [77], and is schematically shown in Fig. 2.47. Due to conducting nature of the coating, the oxygen reduction reaction takes place on the polyaniline coating while the oxidation of iron to passive oxides takes place on the exposed iron surface at pinhole areas and under the film in neutral media. However in acid media, the protection of pinholes takes place by the cathodic reaction PANI (ES)↔PANI (LS) where PANI (ES) is polyaniline emeraldine salt and PANI (LS) is polyaniline leuco salt. Similar type of mechanism of protection has been postulated by Kinlen et al. [86, 87].

Fig. 11. Schematic diagram of mechanism of iron passivation by PANI–phosphate coated steel.

Fig. 2.47. Schematic diagram of mechanism of iron passivation by PANI–phosphate coated steel [77].

The main complication in understanding the anodic protection mechanism of PANI, is the fact that there are the different possible equilibrium states of PANI, as shown in Fig. 2.48 [2].
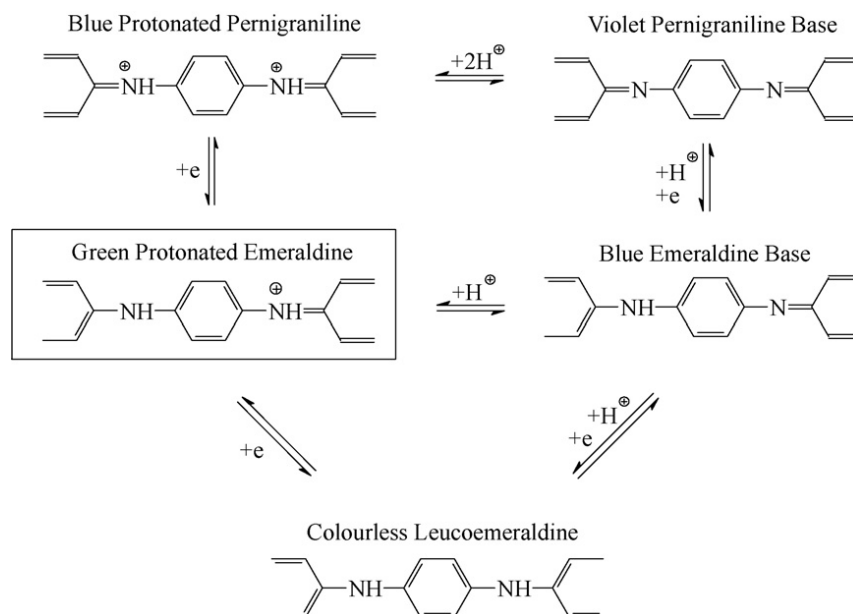
Fig.2.48. Possible PANI state Leucoemeraldine (LE), Emeraldine base (EB), Pernigraniline (PG) and the salty state Emeraldine salt (ES) [2].

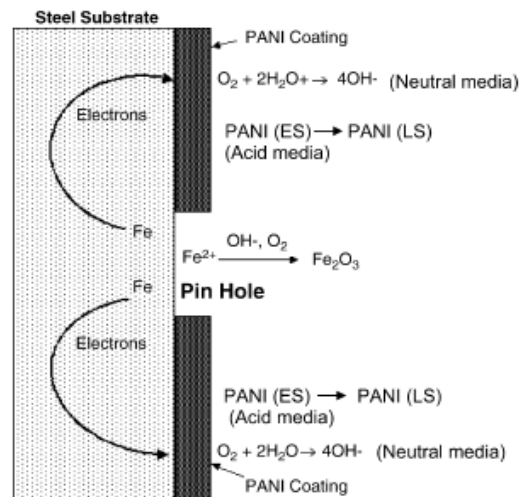The oxidation state increases from LE (completely reduced form) to EB, to PG (fully oxidized). However not all the possible PANI states are conductive, actually PANI ES is the only really conductive form. In the salty form, anions are necessary for balancing the charge of salts. Considering the salty and base states of emeraldine, the equilibrium reactions of PANI includes not only redox reactions (changing LE, EB, PG), but also proton exchange reactions, passing from EB to ES (and the opposite). It is clear that anions are necessary for balancing the charge of salts. Therefore the ES is often called doped PANI (while EB undoped PANI). XPS analysis proved the reduction of PANI from EB (or ES) to LE (with oxidation of steel as the coupled oxidation reaction). If the substrate is inert, this change is not measured.

Based on all these results and considerations, a conclusion can be drawn: **anodic protection is a possible corrosion protection mechanism for PANi on steel**, under

specific restrictive conditions, i.e., the presence of PANI in the ES form and the presence of balancing-counter anions.

A further critical issue in the PANI corrosion protection mechanisms is the role of counter ions [88]. It has already been established that we need the ES form (salty form) to have conductive PANI and in this case we need negative counter ions. The release of anions during redox processes could affect the corrosion rate, both promoting corrosion if the ions are aggressive (as chlorides) or reducing the corrosion rate by complexation with Fe ions and causing a precipitation of insoluble salts (pseudo-passivation). This possible mechanism is very important in the case of contemporary presence of other ions because of the formation of complex insoluble salts. Moreover some released ions could act as inorganic or organic corrosion inhibitors.

De Souza [89] observed that the protection depends on the formation of a passive film between the polymeric coating and the metallic substrate. Raman spectroscopy revealed that the degree of redox conversion of camphor sulphonate-doped polyaniline strongly depends on the reducing power of oxidizable metals, showing a galvanic coupling between the metal and polyaniline. After that, metallic cations form a passivating complex with the dopant anion (camphorsulphonate), which improved the barrier property of different metals modified polyaniline coating system. He proposed the mechanism schematically presented in Fig. 2.49.

E = emeraldine
L = leucoemeraldine
CSA$^-$ = camphorsulfonate anion

Polyaniline acrylic blend coating
Coating/metal interface
Metal
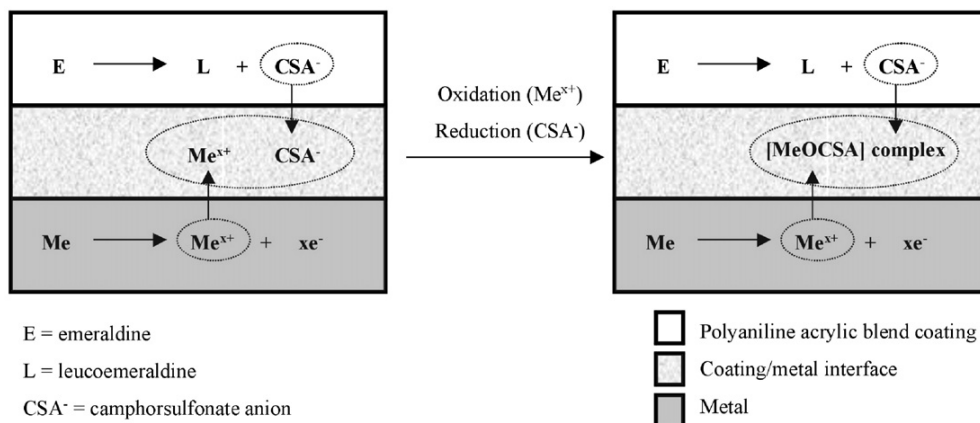
Fig. 2.49. Schematic diagram of the mechanism of metal passivation by polyaniline acrylic bend coating [89].

Considering the anions, Wang [90,91] proposed the anion exchange nature of emeraldine base (EB), which is totally unexpected from the conventional EB formula, at neutral pH as is shown in Fig 2.50 [90].
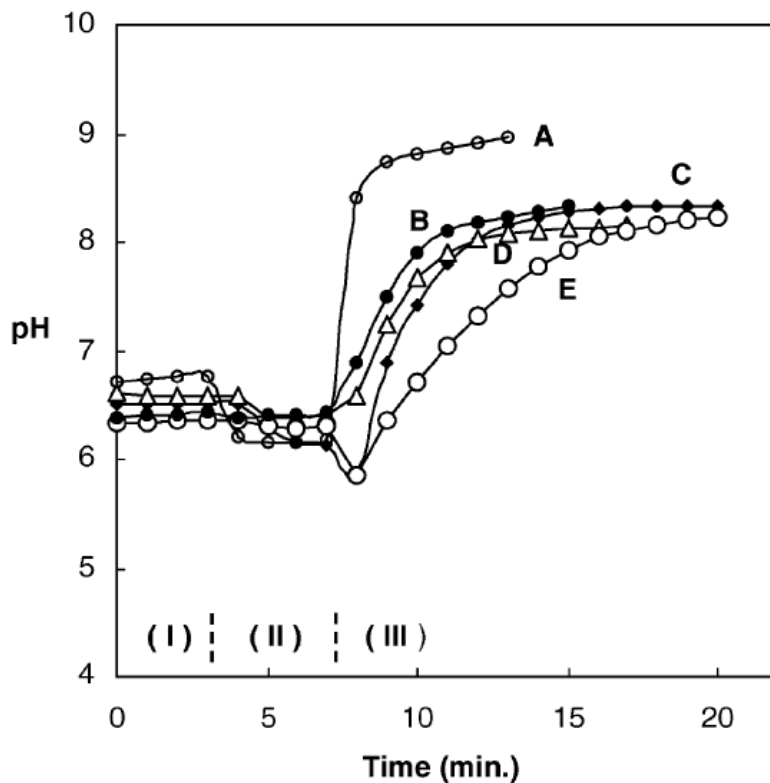
Fig. 2.50. The pH measurements of the H_2O–EB–NaCl system. Zone I: H_2O only. Zone II: EB added to the H_2O. Zone III: NaCl added to the H_2O–EB slurry. EB sources: (A) DuPont (C. Hsu); (B)Monsanto Co.; (C) Drexel Univ. (Y. Wei and S. Li); (D) Eeonyx Co.; and (E) Panipol Co. (Panipal PA) [90].

After EB was mixed with equimolar salt solutions of various anions, the pH values of the EB–salt slurries all increased as the result of anion exchanges, and then leveled off (Fig. 2.51). More OH^- could be exchanged into solution with anions having higher anion exchange selectivity. Therefore, the higher anion exchange selectivity leads to a higher plateau. Fig. 2.51 shows that the relative anion exchange selectivity decreased with the sequence: $I^- > SCN^- > NO_3^- > Br^- > Cl^- > F^-$.
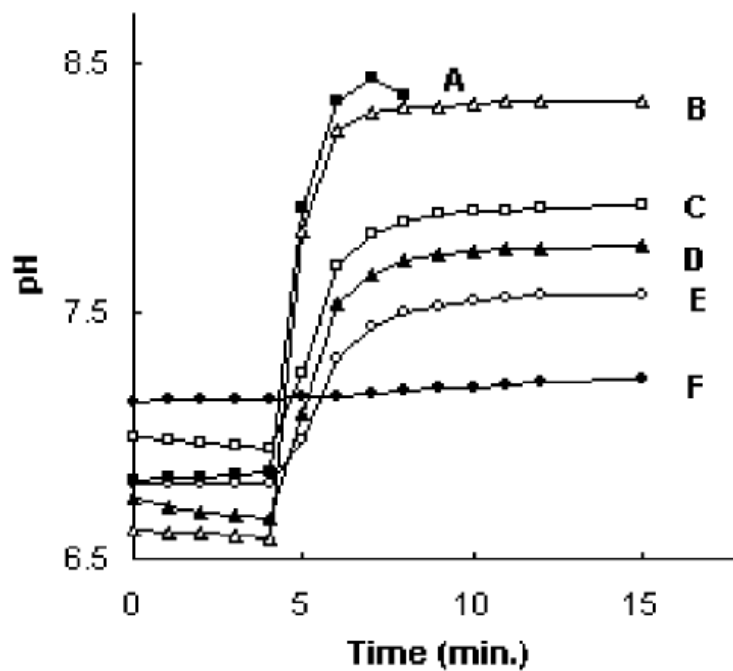
Fig. 2.51. The pH measurements of the salt solution–EB mixtures. EB added to salt solutions (2 M) at t = 4 min. (A) NaI; (B) NaSCN; (C) NaNO3; (D) NaBr; (E) NaCl; and (F) NaF.

Based on his ion exchange experiments EB is suggested to be a mixture of undoped emeraldine with doped emeraldine, in which the counter ion is hydroxide ion. This is in contrast to the commonly held concept that identifies EB as undoped emeraldine, as shown in Fig 2.52
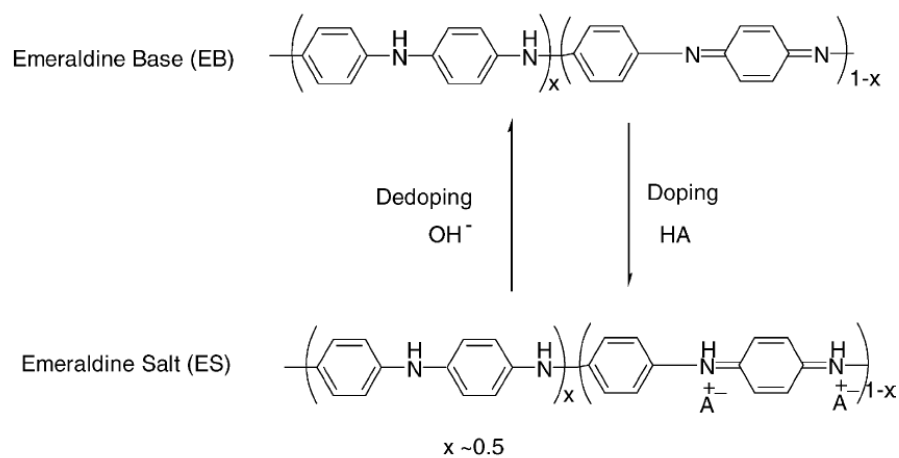
Fig. 2.52. The conventional doping–dedoping scheme of emeraldines

Accordingly, Wang proposed a modified EB formula, as shown in Fig. 2.53.
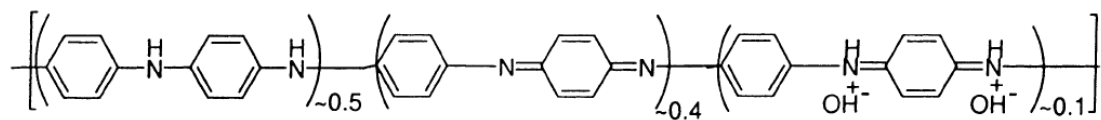
Fig. 2.53. A modified EB formula with OH$^-$ as a counter ion [90].

3. EXPERIMENTAL PART

3.1. MATERIALS AND CHEMICALS

For all experiments the mild steel (AISI 1212) with given chemical analysis in table 1, was used.

Table 3.1. Chemical analysis (AAS) of used mild steel (AISI 1212).

Element	Content (wt. %)
Iron, Fe	98.94
Manage, Mn	0.136
Zinc, Zn	0.003
Cadmium, Cd	0.0001
Lead, Pb	0.053
Nickel, Ni	0.022
Copper, Cu	0.038

All used chemicals was of p.a quality, and bi-distilled water (Miliporre 18 MΩ) was used for solution preparation.

- Sodium benzoate (p.a. Merck),
- Aniline (p.a. Aldrich). Prior to use aniline was distilled in argon atmosphere.
- HCl (36%) (p.a. Merck),
- Hexa-methylene-tetramine (p.a. Merck),
- Sodium chloride (p.a. Merck),
- Amonium persulfate (p.a. Merck),

- Sulfuric acid (98%) (p.a. Merck)

- Ammonium hydroxide (25%) (p.a. Zorka Pharma),

- Acetone (p.a. Zorka Pharma),

- Benzoic acid (p.a. Merck),

- N-methyl-2-pyrrolidone (NMP) (p.a. Aldrich),

- Chloroform (p.a. Lach. Ner).

3.2. METHODS

Electrochemical synthesis of PANI on the mild steel (AISI 1212) electrodes was performed at constant current density of 1.5 mA cm^{-2} from aqueous solution of 0.5 M Na-benzoate (p.a. Merck) and 0.25 M aniline (p.a. Aldrich). The mild steel electrodes, was mechanically polished with fine emery papers (2/0, 3/0 and 4/0, respectively), degreased in acetone and pickled in hydrochloric acid with addition of 0.5% urotropine (hexa-methylene-tetramine). All experiments were performed at ambient temperature (22-25^{0}C).

Ferroxyl indicator was prepared by dissolving the agar-agar in hot distilled water, and mixture of Phenolphthalein, sodium chloride, and potassium hexacyanoferrate(III). It produces a blue color with Fe^{2+} ions and a pink color with hydroxide ions (from oxygen reduction reaction).

Thin PANI film electrode was obtained galvanostatically (j = 2 mA cm^{-2}) on cylindrically shaped graphite electrode inserted in Teflon holder (S = 0.64 cm^2) from 0.5 M HCl with the addition of 0.3 M aniline monomer. After polymerization, electrode was discharged with 1 mA cm^{-2}, washed with bidistilled water, and transferred into the three-compartment electrochemical cell containing a pure 0.5 M HCl. Following the transfer, the electrode was conditioned at a potential of –0.6 V for 600 s to be completely discharged, and characterized using cyclic voltammetry.

PANI powder was synthesized electrochemically using galvanostatic mode with current, I of 0.2 A from the same solution, 0.5 M HCl with the addition of 0.3 M aniline monomer, on both side of the graphite electrode (5 × 10 cm, S = 100 cm^2), inserted

between two counter electrodes from stainless steel plates X5CrNi18-10 ($S = 50$ cm^2) in the polyethylene reactor with a volume of 0.8 dm^3.

Before experiments, both sides of the graphite electrodes were mechanically polished with fine emery papers (2/0, 3/0, and 4/0, respectively) and then with polishing alumina of 0.5 µm (Banner Scientific Ltd.) on the polishing cloths (Buehler Ltd.). After mechanical polishing, the traces of polishing alumina were removed from the electrode surface in an ultrasonic bath in water/ethanol mixture during 10 minutes.

After synthesis, electrode was removed from electrolyte, and polyaniline powder was collected by scratching with plastic knife. PANI powder was rinsed many times with distilled water to the negative reaction on chloride ions, and dried at 90^{0}C over night under vacuum condition. When the water insoluble PANI mass was determined, acetone soluble olygomers were removed in Soxhlet extractor during 3 h, than washed with distilled water and dried in the vacuum at 90°C. The same procedure was used for the water insoluble fraction from the electrolyte.

Beside electrochemically synthesized powder, chemical synthesis was also performed. Synthesis was conducted in 50 ml of 0.1 M H$_2$SO$_4$ in which 1.86 g aniline monomer was added. After vigorous steering, 50 ml of 0.1 M H$_2$SO$_4$ with 5.71 g of (NH$_4$)$_2$S$_2$O$_7$ was added drop by drop. After 4 h of steering green powder was filtrated, washed several times with distilled water and dried over night.

Chemically and electrochemically synthesized PANI powder was treated with 1 M NH$_4$OH for 4 hours to produce emeraldine base, and after drying part of the powder was treated with 0.1 M benzoic acid at 70°C for 10 hours, to produce polyaniline-benzoate doped emeraldine salt.

For all the electrochemical experiments, saturated calomel electrode (SCE) was used as a reference electrode. The electrochemical measurements (cyclic voltammetry polarization measurements, electrochemical impedance spectroscopy) were carried out using a PAR 273A potentiostat/galvanostat controlled by a computer via GPBI PC2A interface, and Biologic potenciostat SP-200. For the fitting of impedance data ZView 2.6 softer was used.

The ultraviolet-visible (UV-Vis) absorption spectra were recorded on a Schimadzu 1700 spectrophotometer.

Micrographs of the PANI powder were obtained with an optical microscope (Olympus CX41) connected to the computer.

Corrosion environments were: 3% NaCl, outdoor atmosphere in downtown Belgrade, and Sahara sand.

Composite coatings were prepared by mixing of the grounded polyaniline powders and using low corrosion resistant paint composed of nitrocellulose (20 wt.%) as a primary film former, toluene-sulfonamide-formaldehyde resin (10 wt.%) as secondary film former, dibutyl phthalate (5 wt.%) as plasticiser. All components was dissolved in the mixture of solvents (65 wt.%) composed of n-butyl acetate (40 wt.%), ethyl acetate (20 wt.%) and isopropyl alcohol (5 wt.%). The commercial TESSAROL-Helios primer for iron based on alkyd binder and red pigments in organic solvents was also used.

As a wet aerosol chamber Plexiglas box with volume of 5 dm^3, schematically present in Fig 3.1. was used.
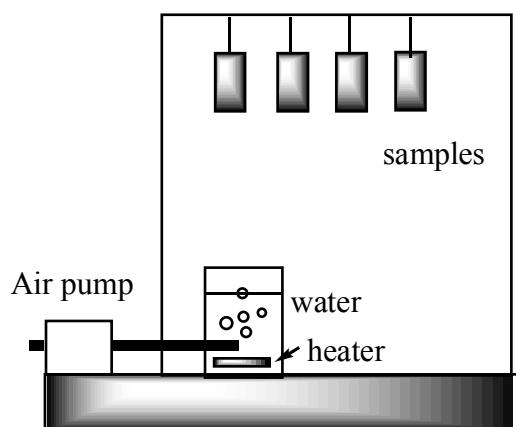
Fig. 3.1. Schematical presentation of a wet aerosol chamber.

4. RESULTS AND DISCUSION

4.1. ELECTROCHEMICAL SYNTHESIS OF THIN PANI FILM ON MILD STEEL

In Fig. 4.1, the anodic polarization curves of mild steel in 0.5 M Na benzoate solution and with 0.25 M aniline is shown. The corrosion potential of mild steel (E_{corr}) in pure 0.5 M Na benzoate solution was –0.67 V. The active dissolution of mild steel occurred until the potential reached –0.5 V with the maximum current density of 0.6 mA cm^{-2}. At the potentials more positive than –0.45 V, passivation of the electrode occurred with the mean passivation current density of ~5 μA cm^{-2}. Transpassive regions accompanied by oxygen evolution were observed at potentials more positive than 1.25 V.

Fig. 4.1. Anodic polarization curves (v = 1 mV s^{-1}) of mild steel in a 0.5 M sodium benzoate solution and with an addition of 0.25 M aniline monomer.

In the presence of aniline, the corrosion potential of the mild steel electrode was shifted positively, to the potential of –0.25 V. The electropolymerization of aniline on mild steel started at potentials more positive than 1 V, with a pronounced peak at 1.6 V.
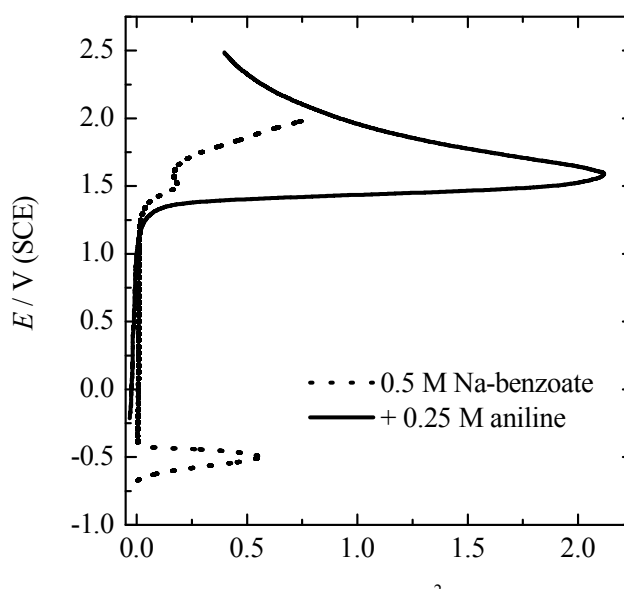
The galvanostatic transient of the mild steel electrodes in pure 0.5 M Na benzoate solution with the addition of 0.1 and 0.25 M aniline was given in Fig. 4.2.
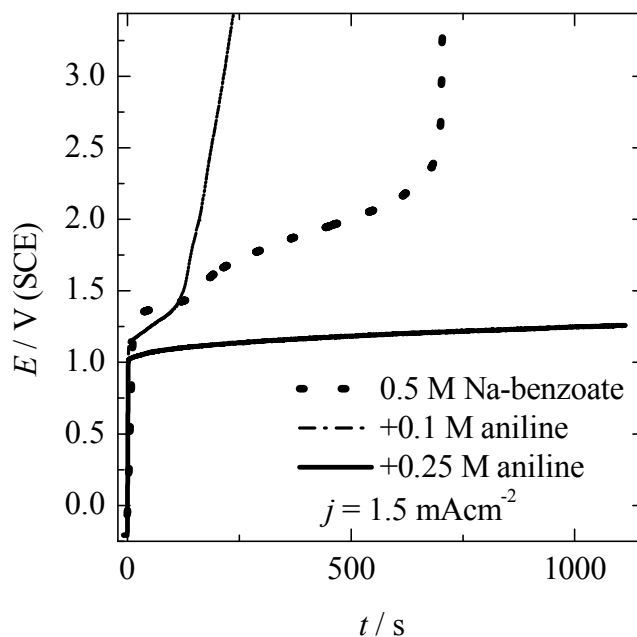
Fig. 4.2. Galvanostatic transient of the mild steel electrodes in pure 0.5 M Na benzoate solution with 0.1 and 0.25 M aniline.

Without aniline in the solution, the potential-time curves had a relatively stable potential plateau, while the induction period was not observed. Applying the current density of 1.5 mA cm^{-2}, the potential increased from 1.3 to 2.25 V during 700 s. After that period, a sharp increase of the potential could be related to the formation of a non-conducting precipitate (e.g. iron benzoate) onto the electrode surface. With aniline in the solution, the polymerization was dependent on the aniline monomer concentration. In a 0.1 M aniline solution, a sharp increase of the potential after 120 s could be brought into relationship with the diffusion limitation of the aniline monomer. In the solution with 0.25 M of aniline, diffusion limitations were not observed, while a slow increase of the potential, from 1 to 1.25 V, could be related to the polymerization of aniline. The

obtained film was black, with good adhesion, determined by cracking. Assuming that the density of benzoate-doped PANI is 1.4 g cm^{-3} [3], and using the equation [92]:

$$d = \frac{jt(M_m + yM_a)}{(2+y)\rho F}$$
(4.1)

where M_m and M_a are the molar mass of the aniline monomer and benzoate anions, and y the doping degree (the polymerization potential of 1.25 V suggests that PANI was in the pernigraniline form, $y = 1$), the thickness of the PANI film has been estimated to be 6 μm.

Figure 4.3 shows cyclic voltammogram of the mild steel (MS)-PANI electrode in a pure 0.5 M Na-benzoate solution. In the anodic scan, in the potential region from – 0.6 to 0.1 V, where doping with benzoate anions occurred, the current density was very small: ~ 1 μA cm^{-2}. The dedoping of benzoate anions occurred in the broad potential region, from 0.1 V to –0.7 V, and was probably overlapped with an oxygen reduction reaction. This means that the MS-PANI system is stable over a large potential range.
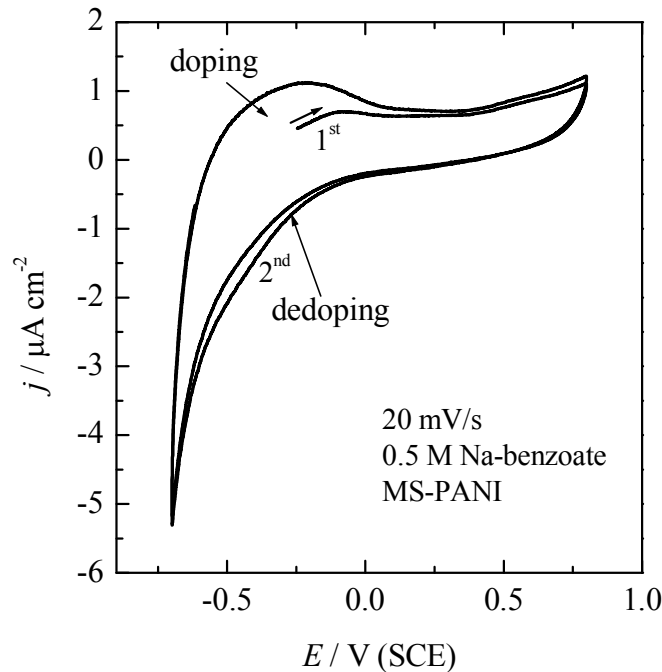
Fig. 4.3. Cyclic voltammogram of the mild steel – PANI-benzoate electrode in a 0.5 M Na-benzoate solution.

4.2. CORROSION OF MILD STEEL AND MILD STEEL WITH ELECTROCHEMICALLY DEPOSITED BENZOATE-DOPED PANI FILM

4.2.1 Corrosion in 3% NaCl

The corrosion of mild steel in sea water (simulated with 3% NaCl) is very important for practical applications of this material; therefore, this type of corrosion has been investigated in this section of the study.

Figure 4.4 shows the polarization curves for mild steel and mild steel with benzoate-doped PANI in 3% NaCl. The anodic polarization curve for the mild steel electrode is characterized by a single Tafel slope (0.114 V dec^{-1}), while the cathodic curve is diffusion-controlled.

Fig. 4.4. Potentiodynamic polarization curves ($v = 1$ mV s^{-1}) for mild steel and mild steel with a doped and de-doped PANI film in 3% NaCl.

The corrosion processes of mild steel is characterized by anodic dissolution of iron

$$Fe \rightarrow Fe^{2+} + 2e \qquad (4.2)$$

and the rate determining the mixed activation–diffusion-controlled cathodic oxygen reduction:

$$O_2 + 2H_2O + 4e \rightarrow 4OH^- \qquad (4.3)$$

The corrosion current density of 12 μA cm^{-2} for bare mild steel was obtained from the intercept of the anodic Tafel line with the corrosion potential ($E_{corr} = -0.466$ V).
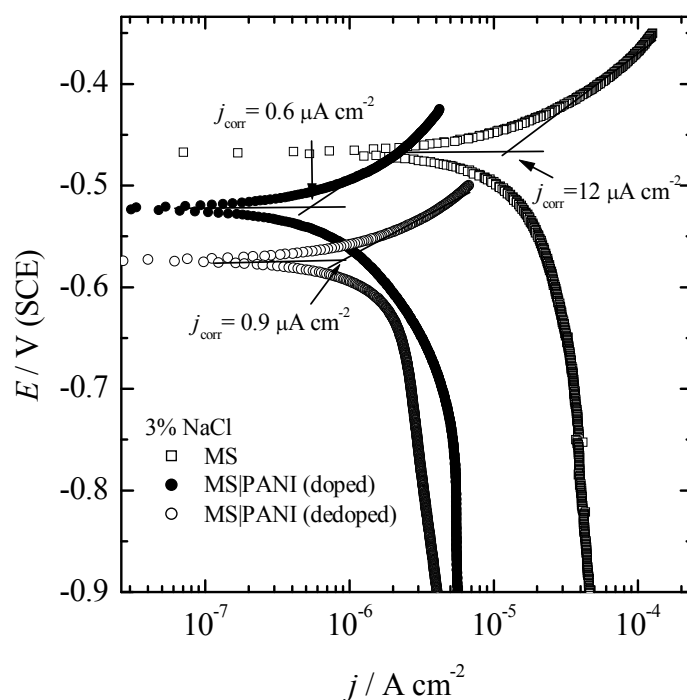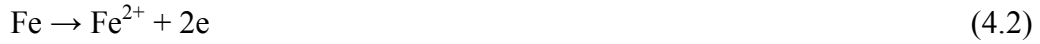
After an hour-long immersion in 3% NaCl, the mild steel electrode with PANI in the doped state had a corrosion potential of -0.527 V, which is by 70 mV more negative than the corresponding value for a bare mild steel electrode. During the first sweep, the anodic curve had the similar slope as bare mild steel, while the cathodic curve, related to the oxygen reduction reaction and de-doping of benzoate anions, was characterized by a broad peak in the potential range from ~-0.6 V to ~-0.9 V. After the cathodic polarization (dedoping), the broad peak disappeared, as observed from the polarization curve recorded after the first cathodic sweep. After the cathodic polarization (de-doping), the corrosion potential was shifted to more negative values, $E_{corr} = -0.573$ V, characteristic for the dedoped state of polyaniline. It is interesting to note that the values of the corrosion current density for mild steel with a doped and dedoped PANI film were almost identical: 0.6 and 0.9 μA cm^{-2}, respectively.

4.2.2. Influence of PANI on the cathodic protection of mild steel

The corrosion of mild steel in sea water is mainly connected to the reduction of dissolved oxygen. The cathodic reaction in nearly neutral solutions is a diffusion-controlled oxygen reduction reaction (Eq. 4.3) and the anodic reaction is the dissolution of iron (Eq. 4.2).

The theory of cathodic protection is based on the fact that the corrosion potential (E_{corr}) has to be shifted cathodically by applying the current from an external power source that can ensure the minimal polarization to the 'reversible' potential, $E_r(Fe^{2+}|Fe)$ of iron in the solution, defined by the equation:

$$E_r(Fe^{2+}|Fe) = -0.683 + 0.029 \log 10^{-6} \quad (vs \text{ SCE}) \tag{4.4}$$

This minimal polarization, ΔE_{min}^{P}, is usually ~0.2 V, as it can be seen in Fig. 6. Under such conditions, the dissolution of iron is practically eliminated, and only oxygen reduction occurs on the surface of mild steel. Since corrosion is more efficiently inhibited when polarization is higher, polarization should be as high as 0.45 V. After that, a hydrogen evolution reaction may occur at the potential of ~ -1.1 V vs SCE, E_{max}^{P}, which can provoke hydrogen penetration into the metal structure and cracking corrosion. Accordingly, the optimum current for mild steel protection should shift the potential of 0.2 V below the corrosion potential and to approximately -1.1 V vs SCE. In Fig. 4.5, the experimental polarization curve of mild steel in 3% NaCl and the theoretical curves of possible corrosion reactions are shown.
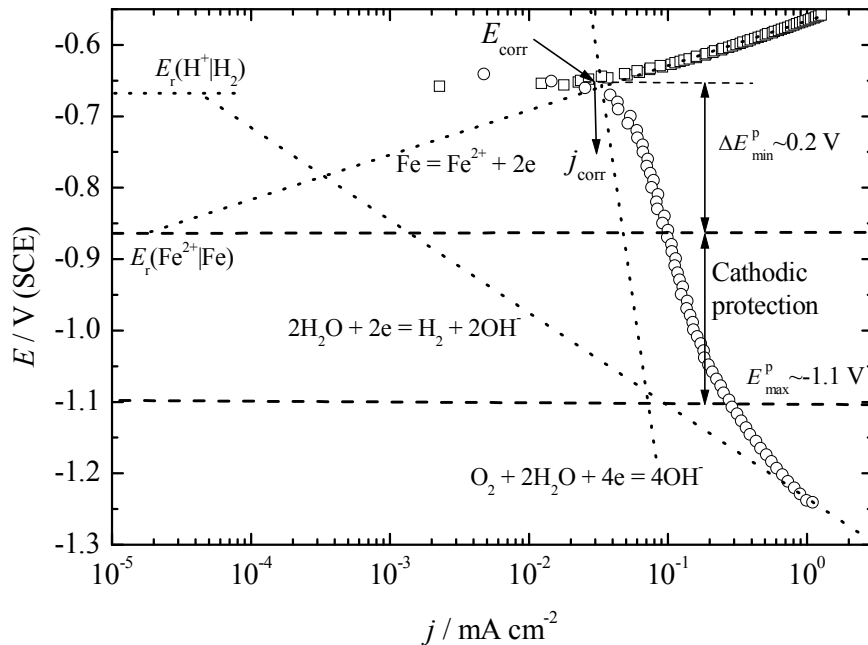
Fig. 4.5. Polarization curve of the mild steel electrode in a 3% NaCl solution, with the theoretical lines of possible corrosion reactions.

The main idea underlying the following experiments has been to investigate the influence of a benzoate-doped PANI film in cathodic protection and in the event of a failed cathodic protection.

The potential distribution along the mild steel sample during cathodic protection in 3% NaCl was investigated using the apparatuses shown on Fig. 4.6. The area of the exposed mild steel surface was 75 cm^2 (3 x 25 cm). The back side of the electrode was protected with a glued Plexiglas sheet. A titanium-coated ruthenium-oxide electrode with a surface of 1 cm^2 was used as an anode. The anode was placed near the mild steel sample, at the position denoted as $l = 0$.
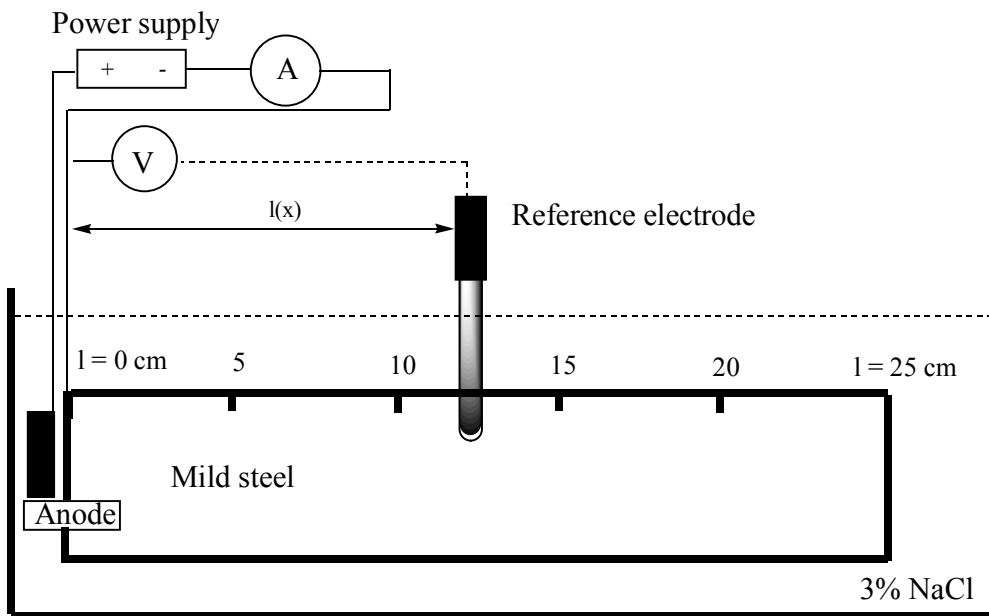
Fig. 4.6. Schematic presentation of the apparatuses used for cathodic protection experiments.

The mild steel sample was exposed to a 3% NaCl solution. After the stabilization of the corrosion potential, the distributions of the potential along the mild steel sample were measured, for different currents; the results are shown in Fig. 4.7.
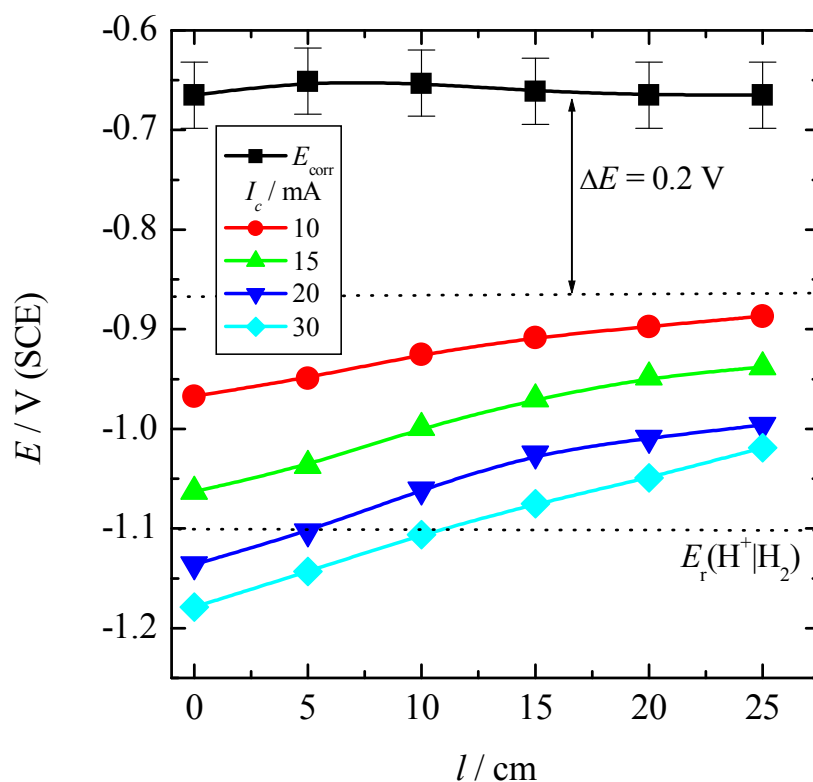
Fig. 4.7. Dependence of the potential along the mild steel electrode for different currents in a 3% NaCl solution.

As it can be seen in Fig. 4.7, for the current densities of 20 and 30 mA, at the position $l = 0$ and 5 cm, the potential is below the line where a hydrogen evolution reaction is likely to occur. For the current density of 10 mA, the potential at 25 cm is near ΔE_{min}^{p}. Therefore, an optimal current which meets the requirements for an efficient cathodic protection is ~15 mA ($j = 0.2$ mA cm^{-2}).

The experiment shown in Fig. 4.7 was repeated with a mild steel electrode partially covered with PANI and the results are shown in Fig 4.8.

It can be observed that the MS-PANI system requires a lower cathodic protection current, e.g. 10 mA (0.13 mA cm^{-2}) or even lower than a bare mild steel electrode. This means that the power consumption would be more than 30% lower than for a bare mild steel electrode.
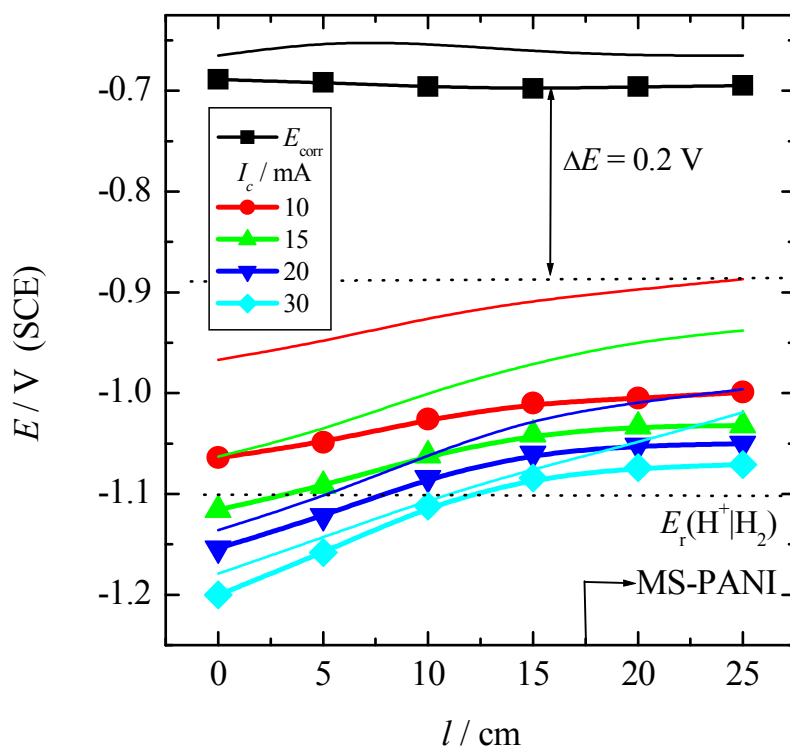
Fig. 4.8. Dependence of the potential along the mild steel electrode partially covered with PANI for different currents in 3% NaCl solution; the lines represent the data from Fig 4.7.

Figure 4.9 features the re-calculated currents, as the current density for $l = 0$ and 25 cm from Figs. 4.7 and 4.8, together with the polarization curve of bare mild steel.

It can be seen that for $l = 0$ cm practically identical current density-potential dependencies to polarization curve for bare mild steel were obtained. Hence, the optimal current density for the cathodic protection of bare mild steel under the investigated conditions was 0.2 mA cm^{-2}. For mild steel partially covered with PANI, the optimal current density for cathodic protection was ~0.1 mA cm^{-2} or 7.5 mA.
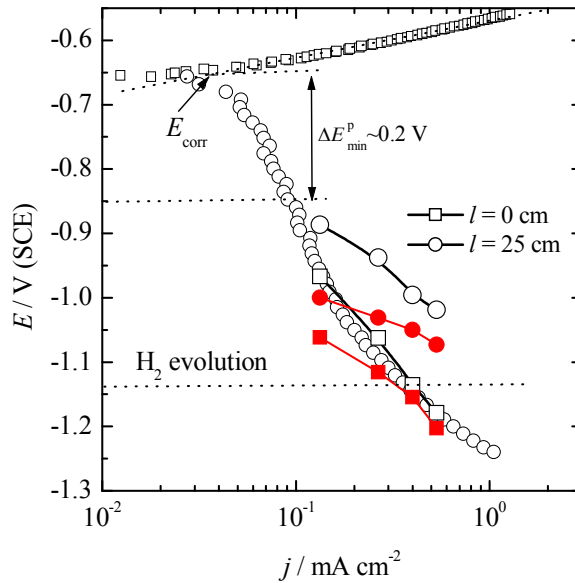
Fig. 4.9. Polarization curve of the mild steel electrode in a 3% NaCl solution with potentials at $l = 0$ and 25 cm for different applied currents (open symbols – mild steel; full symbols –MS/PANI).

Fig. 4.10 shows the dependence of the potential after the current of 10 mA was interrupted. It can be seen that the corrosion potential of ~–0.7 V was achieved within a few minutes. Accordingly, the corrosion of mild steel would occur rather rapidly. The experiment was also performed with partially covered mild steel and basically the same results were obtained. As it can be observed, after the current interruption, ~5 min were required for the potential to reach the value of the corrosion potential.
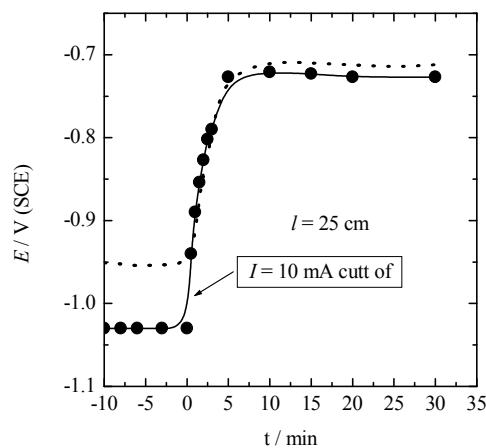
Fig. 4.10. Dependence of the potential at $l = 25$ cm after the current was interrupted for mild steel (----) and mild steel partially covered with polyaniline (-●-).

Figure 4.11 shows a comparison of the samples after a ten-hour immersion in 3% NaCl at the corrosion potential (simulating cathodic protection failure). It is obvious that mild steel partially covered with benzoate-doped PANI showed extraordinary protection of mild steel in the case of cathodic protection failure in a 3% NaCl solution.

Fig. 4.11. Comparison of the images of bare mild steel and mild steel with partial PANI-benzoate coatings after a ten-hour exposure to 3% NaCl at the corrosion potential.

4.2.3. Corrosion of mild steel and mild steel-PANI in the Sahara sand

The corrosion reactions of steel in the Sahara sand are practically the same as in the electrolyte. However, without moisture, corrosion of both samples was slowed down, as it can be seen in Fig. 4.12.

Fig. 4.12. Images of mild steel (left) and mild steel partially covered with polyaniline (right) after a 60-day exposure to dry Sahara sand..

In the presence of moisture corrosion is facilitated, as it can be seen in Fig. 13, probably due to the composition of the Sahara sand [93]. But even so, corrosion was less pronounced on the sample partially covered with benzoate-doped PANI coating than on bare mild steel.
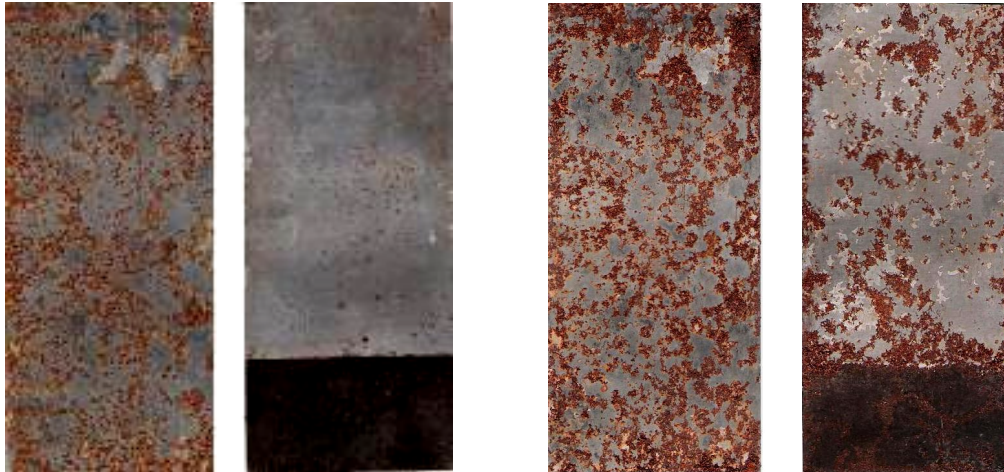
Fig. 4.13. Images of mild steel and mild steel partially covered with polyaniline after a five-day (left) and ten-day (right) exposure to wet (2.5%) Sahara sand.

4.2.4. Atmospheric corrosion of mild steel and mild steel-PANI

Atmospheric corrosion of the mild steel and mild steel partially covered with PANI samples were investigated in Belgrade downtown. As it can be seen in Fig. 4.14 partially covered mild steel sample shows much better corrosion resistance in comparison with unprotected mild steel. It should be noted that during the development of corrosion, exposed metal surfaces near the polymer coating was practically without visible corrosion products.

Fig. 4.14. Images of the mild steel samples after 1 (top), 15 (middle) and 45 (bottom) days exposed to atmospheric corrosion in Belgrade downtown. Left: bare mild steel, right: mild steel-PANI-benzoates.

During the atmospheric corrosion the increase of the samples mass was determined, and the results are shown in Fig. 4.15. It is obvious that partially PANI coated steel corroded less than uncoated. Corrosion protection efficiency, defined as:

$$CE = \frac{\Delta m_{Fe} - \Delta m_{Fe-PANI}}{\Delta m_{Fe}} 100\% \qquad (4.5)$$

was in the range of 50-60% during exposure.
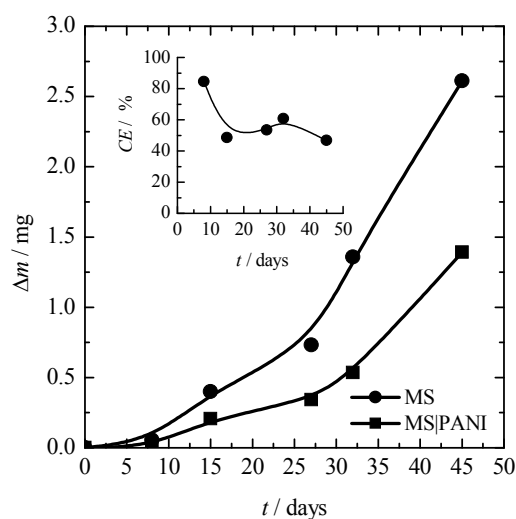
Fig. 4.15. Increase of the corrosion product mass during the atmospheric corrosion. Insert: corrosion protection efficiency.

4.3. POSSIBLE MECHANISM OF CORROSION PROTECTION

According to the presented results, the mechanism of the mild steel corrosion protection using the electrochemically deposited thin benzoate-doped PANI coatings in different environments could be proposed.

From the polarization experiments (Fig. 4.4) in 3% NaCl it is obvious that PANI is in doped states and that the corrosion potential shifts to negative values, compared to bare mild steel, suggesting the cathodic protection mechanism. It is reasonable to conclude that the corrosion potential of mild steel with a doped PANI film (initial period) is determined by slow cathodic reactions related to the dedoping of benzoate anions and the oxygen reduction reaction on the conducting PANI film:

$$[PANI^{y+}(C_6H_5COO^-)_y]_n + nye \rightarrow [PANI]_n + nyC_6H_5COO^- \qquad (4.6)$$

$$O_2 + 2H_2O + 4e \rightarrow 4OH^- \qquad (4.3)$$
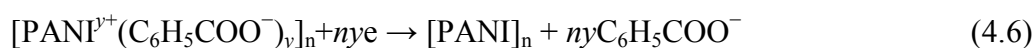
and the anodic iron dissolution reaction through the pores of PANI. The iron dissolution rate was small due to the slow reaction kinetics of oxygen reduction on the PANI

surface. There is also a possibility that the released anions react with Fe^{2+} in the pores, forming a poorly soluble precipitate.

After most of the anions were released, the corrosion potential of mild steel with a dedoped (low conducting) PANI film could be determined by oxygen reduction as a cathodic reaction at the surface of bare metal in to the bottom of the PANI pores, and the doping of a dedoped PANI film probably with chloride anions:

$$[PANI]_n + nyCl^- \rightarrow [PANI^{y+}(Cl^-)_y]_n + nye \qquad (4.7)$$
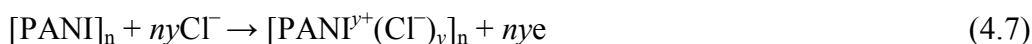
as an anodic reaction. The electrons released from the PANI films could be transferred through metal, as a cathodic site, where the oxygen reaction takes place. The negative charge of the metal surface induced by electron transfer from the PANI film could prevent anodic iron dissolution near corrosion potential due to the cathodic protection effect. After a partial doping of the film, the potential shifted to less negative potentials and the sequences from the initial period could be repeated. Accordingly, this mechanism could be designated as the 'switching zone mechanism'. This behavior is schematically presented in Fig. 4.16.
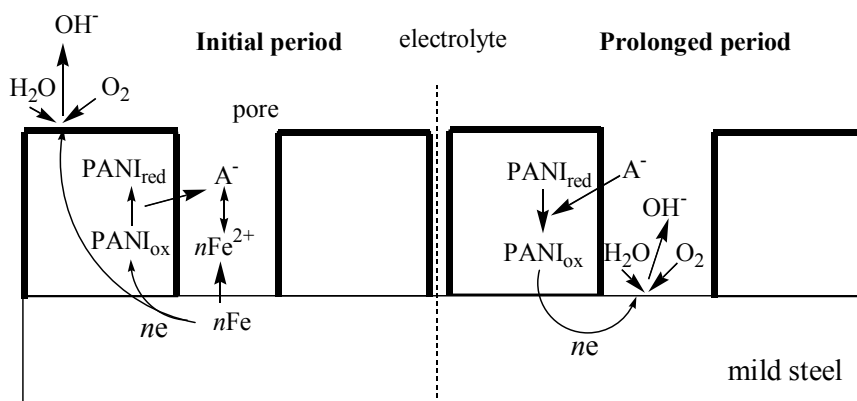
Fig. 4.16. Schematic presentation of proposed mechanism of the mild steel corrosion protection with PANI coatings.

From the experiments shown in Figs. 4.11, 4.13 and 4.14, it is obvious that the protection effect was not limited only to the metal under the PANI coatings. It is evident that the corrosion of mild steel partially covered with benzoate-doped PANI coating is practically prevented on the bare metal surface near the coating. To investigate this phenomenon, simple ferroxyl indicator test was applied on an unprotected and a PANI-

protected nail. From the images shown in Fig. 4.17, it can bee seen that anodic and cathodic zone on the unprotected nail are well separated. On the contrary, the cathodic zone on the PANI-protected nail is extended along the free metal surface.

Fig. 4.17. Ferroxyl indicator test of an unprotected (left) and a PANI-protected nail (right) after 10 h.

From these observations the following mechanism, shown in Fig. 4.18, could be suggested. Initially, the mechanism is probably similar to the above described one (Fig. 4.16). The differences is that Fe^{2+} probably reacts with OH^- or dissolved oxygen, producing a thin iron oxide film which has better catalytic properties for the oxygen reduction reaction than PANI and oxide-free iron surfaces. After the de-doping of PANI, a doping reaction may occur in a medium period, driven by an oxygen reduction reaction, but this time occurring on the thin iron oxide layer near PANI. The electrons released in the doping reaction are transferred along free metal surfaces but only to limited distances, due to the current distribution. As a consequence, at some distance after the protected zone, corrosion and rust formation may occur. The electrons formed during iron dissolution could be now involved in the oxygen reduction and the PANI doping reaction (with any kind of the present anions). Over time, the doping/de-doping properties of PANI decrease (due to degradation) and rust continues to grow along the protected metal surface, as it can bee seen in Fig. 4.14.
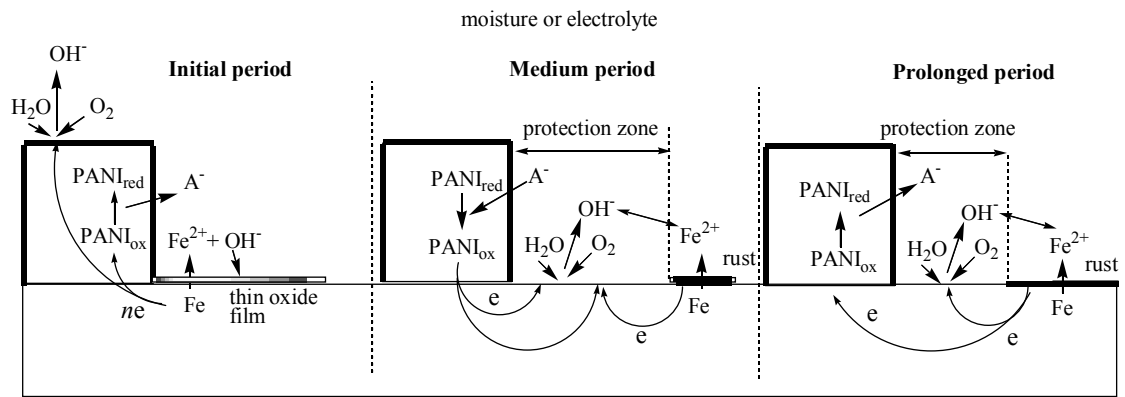
Fig. 4.18. Schematic presentation of proposed mechanism of the mild steel corrosion protection using a partial PANI coating.

It should be noted that anions in neutral pH region could be OH^-, as proposed by Wang [90]

4.4. THE INFLUENCE OF LIGHT ON CORROSION BEHAVIOR OF POLYANILINE COATED MILD STEEL

In the few papers, it has been suggested that polyaniline can produced photoelectric effect on inert electrodes [94-99]. But, up to now the influence of light on the corrosion of mild steel with the electroconducting polymer coatings has not been investigated.

Hence, in this part of the thesis the behavior of the mild steel and the mild steel with polyaniline polymer coatings (MS/PANI) based on the possibilities that polyaniline can generate photoelectrons has been investigated.

Figure 4.19 represents Nyquist plot of the mild steel electrode in 3% NaCl at corrosion potential ($E_{corr} = -0.642$ V) under dark and illumination conditions. As it can be seen illumination does not have any effect on the corrosion processes of the mild steel at the corrosion potential.

Fig. 4.19. Nyquist plot of the mild steel electrode in 3% NaCl under illumination (4 mW cm^{-2}) and in the dark conditions at corrosion potential.

Practically, the same results were obtained recording the polarization curves, as shown in Fig. 4.20. The determined corrosion current density under illumination and in the dark conditions was the same 20 μA cm^{-2}.

Fig. 4.20. Polarization curves ($v = 1$ mV s^{-1}) of the mild steel electrode in 3% NaCl under illumination (4 mW cm^{-2}) and in the dark conditions.

With polyaniline coated mild steel obtained for 800 s of deposition (Fig. 4.2), the above described corrosion experiments were repeated. Electrode was exposed to corrosion media for 3 hours, and impedance at the corrosion potential was determined. As it can be seen, from Fig. 4.21, were Nyquist plot of the MS/PANI electrode in 3% NaCl under illumination (4 mW cm^{-2}) and in the dark conditions at corrosion potential was shown, illumination has effect. In the dark conditions overall impedance was ~3000 Ω cm^2, while under illumination ~2550 Ω cm^2.
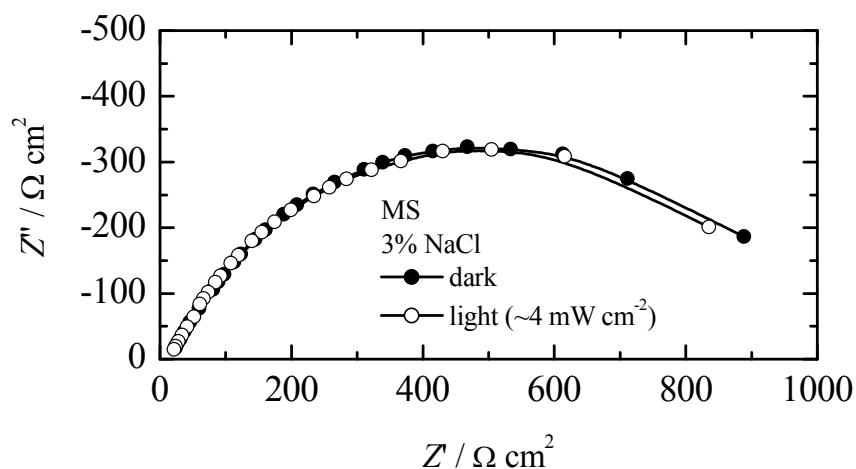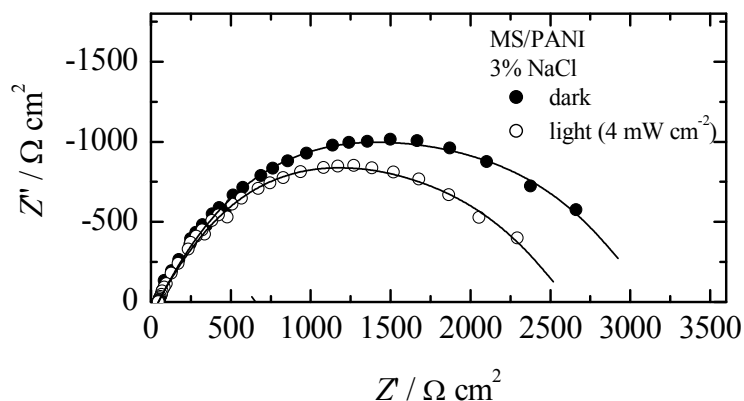
Fig. 4.21. Nyquist plot of the MS/PANI electrode in 3% NaCl under illumination (4 mW cm^{-2}) and in the dark conditions at corrosion potential.

Recording the polarization curves, the similar results were obtained. Determined corrosion current density under dark conditions was 5.7 μA cm^{-2} and under illumination 10 μA cm^{-2}. From the polarization curves it is obvious that illumination affects only anodic branch of the polarization curve. Cathodic branch remains practically unchanged. The insert in Fig. 4.22, shows the photocurrent density in the whole range of investigated potential. As it can be seen anodic photocurrent reaches few microampers near the corrosion potential.

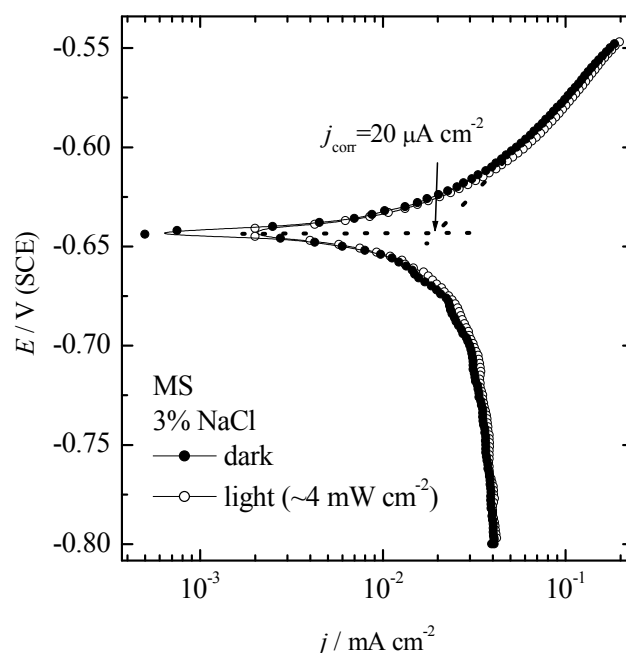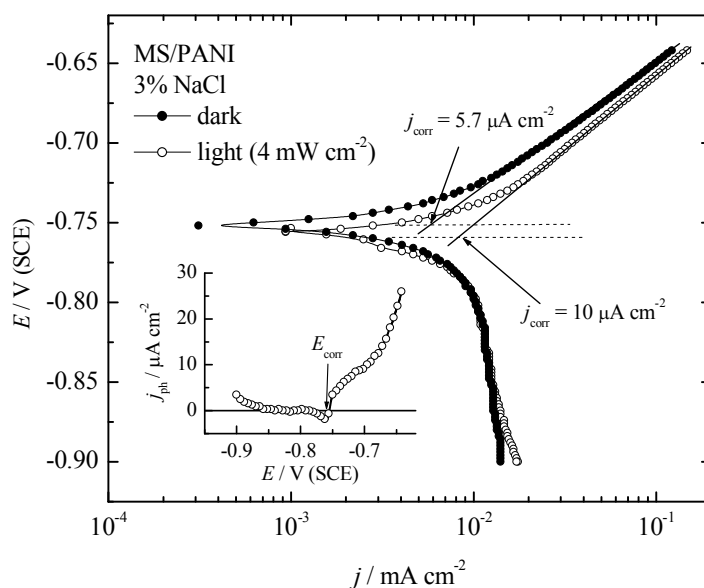**Fig. 4.22.** Polarization curve ($v = 1$ mV s^{-1}) of the MS/PANI electrode in 3% NaCl under illumination (4 mW cm^{-2}) and in the dark conditions.

This effect is steel under investigations, and the mechanism of the photoresponse of the present system can not be explained so far. It is questionable does the anodic photocurrent represents corrosion acceleration or suggests the presence of some chemical reaction such as photoelectrochemical polyaniline doping of the ions present in the solution.

4.5. ELECTROCHEMICAL SYNTHESIS AND CHARACTERIZATION OF THE POLYANILINE POWDER

The application of electrochemical synthesis of polyaniline in corrosion protection of mild steel is relativelly difficult. So, the some other method should be applied like polyaniline-paint composite.

In this part of the thesis was investigated the electrochemical synthesis of the PANI in the form of thin film and powder from dilute hydrochloric acid solution with addition of aniline monomer on the graphite electrode. The main goal of this part was to correlate characteristics of the PANI thin film with powder, and to determine the fraction of the electroactive polymers form (emeraldine salt) in the powder.

4.5.1. Synthesis and characterization of the PANI thin film electrode

Figure 4.23 shows synthesis and characterization of the PANI thin film electrode in 0.5 M HCl. Inset of Fig. 4.23 shows galvanostatic curve for the aniline polymerization in 0.5 M HCl and 0.3 M aniline monomer (ANI) at a constant current density of 2 mA cm^{-2} with a polymerization charge, q_{pol}, of 0.6 mA h cm^{-2} (1080 s). It is worth to mention that at higher polymerization current densities, due to the high polymerization potential more degradation products and lower current efficiency were obtained. As it can be seen from the inset of Fig. 4.23, aniline polymerization proceeds in the potential range between 0.7 and ~ 0.56 V according to the equation:

$$n(ANI) + nyCl^- \rightarrow [PANI^{y+} (Cl^-)_y]_n + nye \qquad (4.8)$$
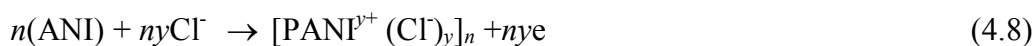
where y is doping degree.
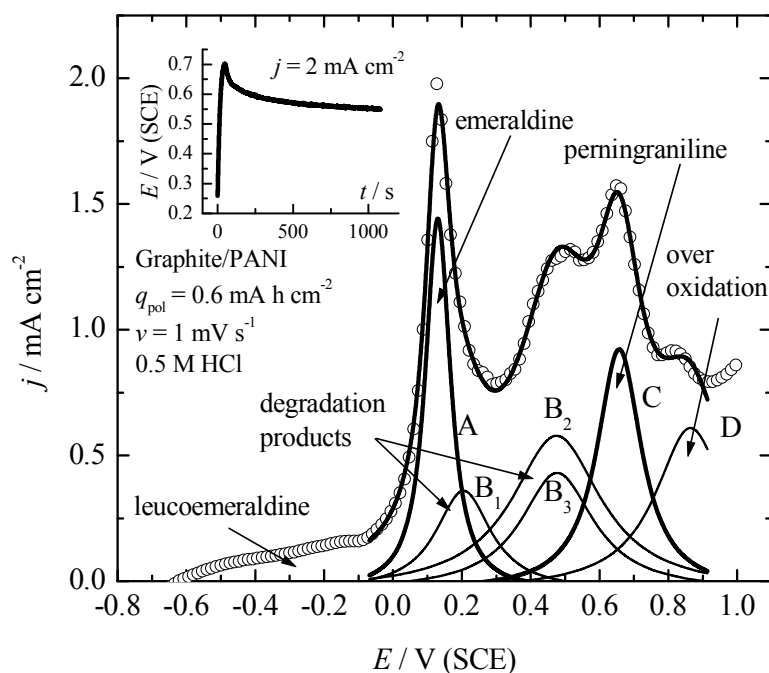
Fig. 4.23. Slow potendionamic anodic curve ($v = 1$ mV s^{-1}) of thin PANI film electrode in 0.5 M HCl (open symbols represent experimental data, while lines represent peak deconvolution using Lorentzian peak fit function).
Inset: Galvanostatic curve of the aniline polymerization from 0.5 M HCl + 0.3 M ANI at the current density of 2 mA cm^{-2}.

Figure 4.23 also shows the anodic part of cyclic voltammogram ($v = 1$ mV s^{-1}) of the thin dedoped PANI film electrode in pure 0.5 M HCl for the anodic potential limit of 1.0 V, and the main peak deconvolution. Open symbols represent experimental data, while lines represent peak deconvolution using Lorentzian peak fit function.

As it can be seen, doping of the PANI electrode with chloride anions starts at $\sim -$ 0.1 V and proceed up to the potential of 1 V through different oxidation states. The appearing of well defined peak (marked with A) at 0.1 V is followed by the change of color from deep green to almost black, and it could be attributed to the changes of the doping degree of emeraldine salt between $y > 0$ and 0.5. At low negative potentials ($E <$ -0.1 V), leucoemeraldine form ($y \approx 0$) could exist as well [100]. Further oxidation of emeraldine salt to pernigraniline salt (y between 0.5 and 1) can be attributed to the peak C at potential higher than 0.4 V. Between these two main oxidation states, few peaks

marked with B_1 to B_3 are observed and they correspond to the formation of the PANI degradation or hydrolysis products [2, 13-20]. The main degradation product appears to be soluble benzoquinone with the redox of the benzoquinone/hydroquinone couple. Other inactive insoluble degradation product has been suggested to remain on the electrode surface, including PANI strands containing quinoneimine end groups, and ortho-coupled polymers. Simultaneously with formation of perningraniline, over-oxidation reaction, marked with peak D, occurred producing the water insoluble, low conducting brown products [101].

4.5.2. Electrochemical synthesis and characterization of the PANI powder

Figure 4.24 shows the galvanostatic curve of the aniline polymerization from the solution containing 0.5 M HCl and 0.3 M aniline monomer on the graphite electrode ($S = 100$ cm^2) at a current of 0.2 A (2 mA cm^{-2}) during 22 h. Polymerization starts at a potential of ~0.7 V and proceeds in the potential range between 0.65 and 0.52 V (SCE). The inset of Fig. 4.24 shows the magnification of the initial polymerization curve.
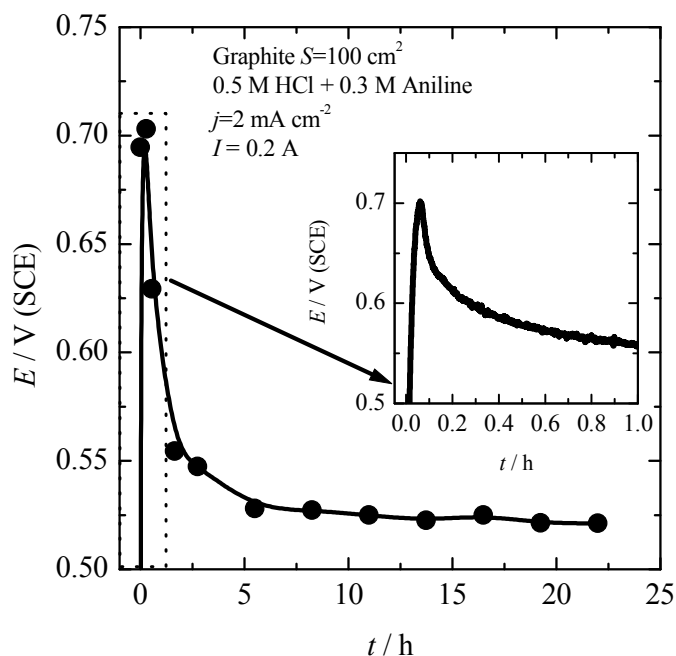
Fig. 4.24. Galvanostatic curve for the aniline polymerization in the solution containing 0.5 M HCl and 0.3 M aniline on graphite electrode. Inset: magnification of the initial polymerization curve during 1 h.

Applying the procedure explained in the experimental section, the water insoluble fractions of the PANI was determined, and the results are shown in Table 4.1.

Table 4.1. Mass of the water insoluble PANI fractions on the electrode and in the electrolyte during synthesis with a current of 0.2 A during 22 h.

Fraction	m / g water insoluble	%	Deposit color	Filtrate color
Electrode	7.35	91.8	bluish-green	purple
Electrolyte	0.660	8.2	brown	purple

As it can be seen from Table 4.1, the electrode deposit has the bluish-green color, suggesting that emeraldine salt was mainly produced. Brown color of the water insoluble fraction in the electrolyte could be connected with over-oxidized PANI form [101, 102].

The theoretical mass of the PANI for the given synthesis conditions can be calculated assuming the 100% current efficiency during polymerization of the aniline, taking into account average molar mass of one monomeric unit in the polymer, and using equation [92, 42]:

$$m_{th} = \frac{It(M_m + yM_a)}{(2+y)F} \qquad (4.9)$$

where m, g, is the mass of the PANI polymerized with current, I, A , over time, t, h, M_m and M_a, g mol^{-1}, are molecular mass of aniline monomer (93.13 g mol^{-1}) and an inserted chloride anion (35.5 g mol^{-1}), $F = 26.8$ A h mol^{-1} is Faraday constant, and y is doping degree (0 to 1).

Based on Eq. 4.9, Fig. 4.25 shows calculated theoretical mass of the PANI powder for different doping degrees.
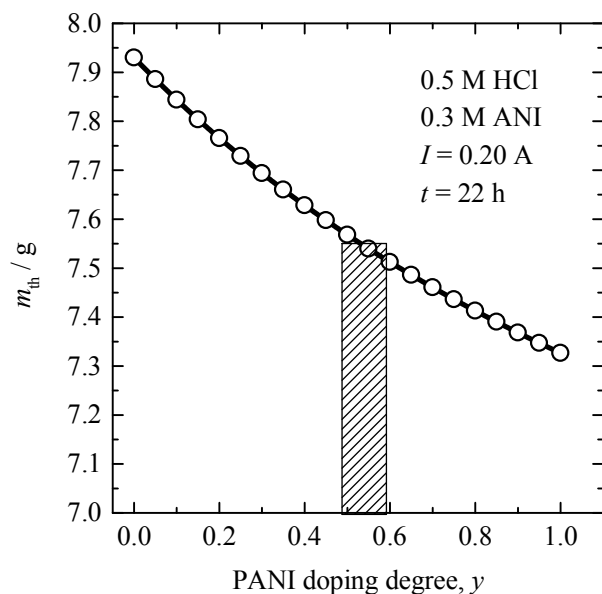
Fig. 4.25. Calculated theoretical mass of the PANI powder for different doping degrees under given synthesis condition.

Due to the polymerization potentials of ~ 0.52 V, considering the cyclic voltammogram, see Fig. 4.23, and color of the deposits, it should be suggested that after polymerization PANI powder on the electrode was mainly in the emeralidene salt form with y ~ 0.5 to 0.6. From Fig. 4.25, it could be estimated that for the applied polymerization current of 0.2 A over 22 h, and $y = 0.5$, theoretical mass of the PANI should be ~7.55 g. Since the experimentally obtained mass of the water insoluble PANI powder on the electrode was 7.35 g, and 0.66 g in the electrolyte, polymerization current efficiency seams to be over 100%. Unfortunately, during polymerization water insoluble inactive oligomers or other degradation products could be incorporated in the powder. From these reasons, powders were treated with pure acetone in Soxhlet extractor, and the obtained results are shown in Table 4.2.

As it can be seen from Table 4.2, the fractions of the acetone soluble products from the PANI powder on the electrode were 26%. Due to the dark green deposit color after acetone leaching, it is reasonable to conclude that practically only emeraldine salt remains. Hence, considering the Fig. 4.25 and obtained results, polymerization efficiency based on the pure PANI emeraldine salt ($y = 0.5$) are in the range of ~70%. The rest of 30% could be attributed to the formation of different, practically inactive PANI forms and degradation products.

Table 4.2. The fractions of the acetone soluble product
and in the water insoluble PANI powders.

PANI fraction	Mass before acetone leaching	Mass after acetone leaching	Acetone soluble products	Deposit Color	Filtrate color
Electrode	7.35 g	5.44 g	1.91 g (26%)	dark green	rubin red
Electrolyte	0.660 g	0.635 g	0.021 g (3.2%)	brown	dark red

The brown color of the water and acetone insoluble powder from the electrolyte suggests formation of over-oxidized polyaniline [101,102]. The conductivity of the PANI emeraldine salt is $\sim 10^{-3}$ S cm^{-1}, while for the over-oxidized product is 10^{-5} S cm^{-1}. So, former product cannot be considered as useful for any kind of application [101]. The different colors of the filtrates (purple, rubin red, or dark red) and their amounts were not important for this study, although it should be noted that such colors can produce perningraniline base or at the moment unknown water or acetone soluble degradation products which decrease polymerization efficiency. For the better undesigning of the nature of the degradation products, UV spectra of the filtrates should be investigated in the future.

4.5.3.. Morphology of the PANI deposits

Morphology of the PANI powder obtained on the electrode was investigated after acetone leaching as shown in Fig. 4.26 a) to d). From Fig. 4.26, it can be seen that PANI powder are mainly consisted of micrometers conglomerates and small dendritic particles which approached the nano-sized dimensions.
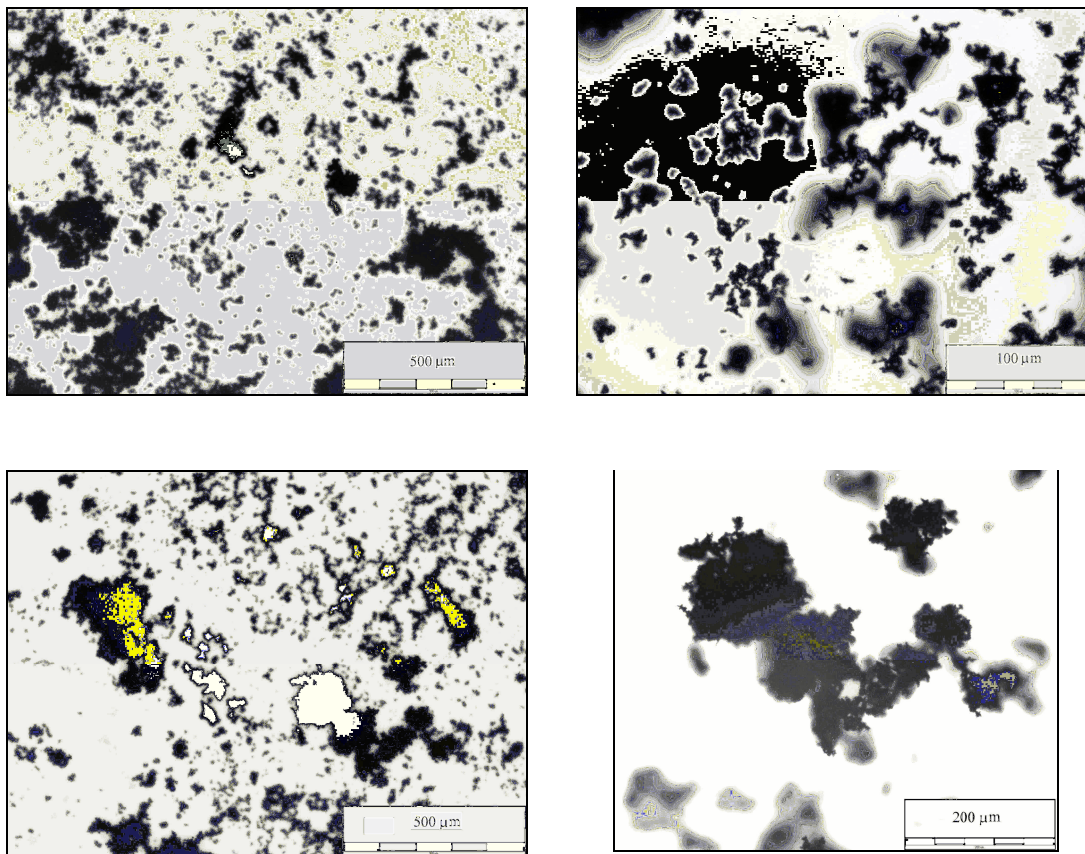
Fig. 4.26. Micrographs of the typical PANI powder with different magnification after acetone leaching.

Since, the main fraction of the PANI are consisted of relatively large micrometric conglomerates, the powder was ultrasonically treated in distilled water for 30 minutes. After drying, the micrograph was taken, and results are shown in Fig. 4.27. As it can be seen in Fig. 4.27 most of the conglomerates were beaked, and the size of the particles are mostly in nanometrics and some fraction in micrometrics dimensions remains.
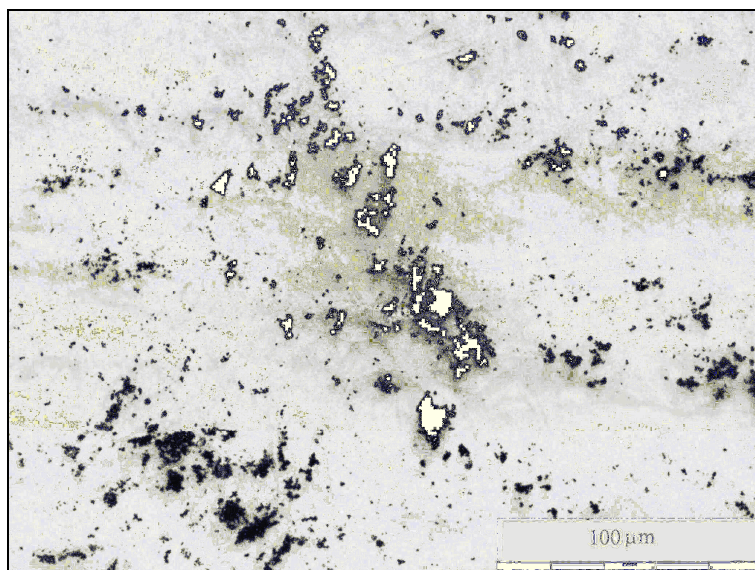
Fig. 4.27. Micrographs of the ultrasonically treated PANI powder in distilled water during 30 minutes.

4.6. CORROSION OF MILD STEEL WITH COMPOSITE POLYANILINE COATINGS

In order to investigate the influence of different oxidation states of polyaniline, different powder composition was prepared.

Beside electrochemically synthesized powder, chemical synthesis was also performed. Synthesis was conducted in 50 ml of 0.1 M H_2SO_4 in which 1.86 g aniline monomer was added. After vigorous steering, 50 ml of 0.1 M H_2SO_4 with 5.71 g of $(NH_4)_2S_2O_7$ was added drop by drop [103]. After 4 h of steering green powder was filtrated, washed several times with distilled water and dried over night. The mass of dry polyaniline-sulfate doped emeraldine was 2.553 g. Corresponding emeraldine base mass was 1.710 g, which gives 92% of the synthesis efficiency based to the used aniline monomer.

Chemically and electrochemically synthesized PANI powder was treated with 1 M NH_4OH for 4 hours to produce emeraldine base, and after drying part of the powder was treated with 0.1 M benzoic acid at 70°C for 5 hours, to produce polyaniline-benzoate doped emeraldine salt [104] as schematically presented in Fig. 4.28. Obtained dark green product was washed with hot distilled water and dried over night.

Fig. 4.29. Chemical conversion between emeraldine base and salt, $A^- = C_6H_5COO^-$ [104].

Since different anticorrosion coatings may have influence on corrosion measurements [105,106], the low corrosion resistant coating was used to eliminate possible interference. The low corrosion resistant coating was prepared from nitrocellulose (20 wt.%) as a primary film former, toluene-sulfonamide-formaldehyde resin (10 wt.%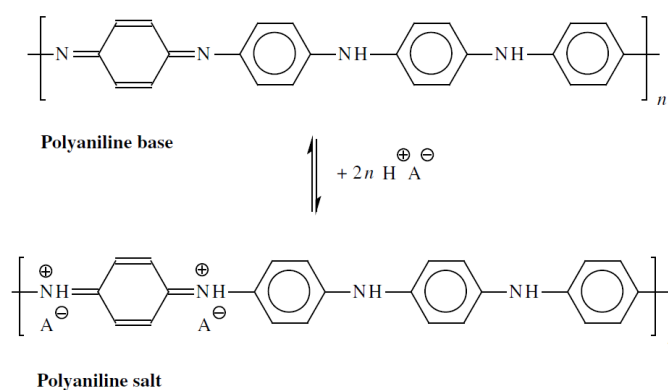) as secondary film former, dibutyl phthalate (5 wt.%) as plasticiser. All components was dissolved in the mixture of solvents (65 wt.%) composed of n-butyl acetate (40 wt.%), ethyl acetate (20 wt.%) and isopropyl alcohol (5 wt.%).

The same mass of low corrosion resistant coating was well mixed with 5 wt.% of grounded polyaniline powder prepared with different methods and inflicted by "doctor Blade" method on previously cleaned mild steel sample [107]. The used nomenclature of different composite coating which was used is given in table 4.3.

The thickness of the coatings after drying in all cases was 30±5 μm.

Table 4.3. The used nomenclature of different composite coating.

Label	Form / method of preparation
BS	Base coatings
ESC	Emeraldin salt chemical
EBC	Emeraldin base chemical
ESEC	Emeraldin salt electrochemical
EBEC	Emeraldin base electrochemical

The Nyquist plot of the mild steel with base coating for different time of immersion in 3% NaCl is shown in Fig. 4.30. Impedance is typical for the diffusion controlled reaction. It should be noted that practically complete degradation of the coatings occurred after 24 h. Hence, the fitting of the data with electrical equivalent circuit (EEC) shown in the Fig. 4.30 was performed for that time. EEC was consisted of solution resistance, R_Ω, coating capacitance, C_c, corrosion resistance R_{corr}, and constant phase elements, CPE,

Impedance of the constant phase element is given by [108, 109]:

$$Z(\text{CPE}) = Y_0^{-1} (j\omega)^{-n} \tag{4.10}$$

where Y_0 is the CPE constant, ω is the angular frequency (in rad s^{-1}), $j^2 = -1$ is the imaginary number and n is the CPE exponent.

Depending on n, CPE can represent resistance ($Z(CPE) = R$, $n = 0$), capacitance ($Z(CPE) = C$, $n = \sim0.80$ to 1), inductance ($Z(CPE) = L$, $n = -1$) or Warburg diffusion impedance for ($n \sim 0.5$).

The following equation can be used to convert Y_0 into C:

$$C = Y_0(\omega"_m)^{n-1} \tag{4.11}$$

where C is the capacitance and $\omega"_m$ is the angular frequency at which $Z"$ has a maximum.
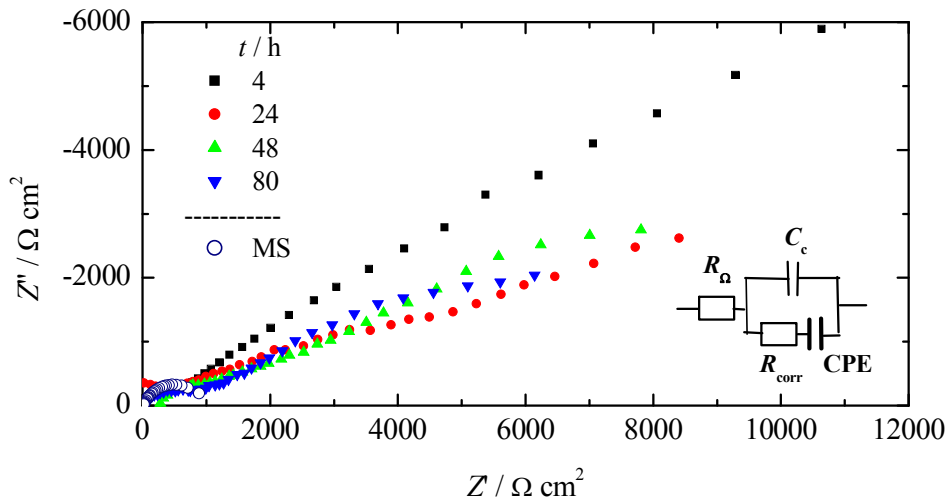
Fig. 4.30. Nyquist plot of the mild steel covered with base coating for different times of immersion in 3% NaCl.

Using the proposed EEC, the following values of the parameters of the mild steel covered with base coating was estimated:

$R_\Omega - 106\ \Omega\ \text{cm}^2$,

$C_c - 7 \times 10^{-7}\ \text{F cm}^{-2}$

$R_{corr} - 2310\ \Omega\ \text{cm}^2$

$\text{CPE} - Y_0 = 1.81 \times 10^{-4}\ \Omega^{-1}\ \text{s}^n\ \text{cm}^{-2}$, and $n = 0.36$.

Since CPE parameter n was 0.36, the impedance should be assigned to the Warburg diffusion impedance of the oxygen reduction reaction. From the other hand, the corrosion current density can be estimated from R_{corr} using modified Stern-Geary equation [110,111]:

$$j_{corr} = \frac{b_a \times b_c}{2.3 R_{corr}(b_a + b_c)}$$

(4.12)

where b_a and b_c are anodic and cathodic Tafel slopes. if one reaction is diffusion controlled, in this case cathodic, then $b_c \rightarrow \infty$, and modified Stern-Geary equation becomes [112]:

$$j_{corr} = \frac{b_a}{2.3 R_{corr}}$$

(4.13)

From Fig. 4.4 it can be seen that corrosion of bare mild steel is characterized with a single Tafel slope of $b_a = 0.114$ V dec^{-1}), while the cathodic curve is diffusion-controlled. Using Eq. 4.13 corrosion current density of 20 μA cm^{-2} was estimated, which is even higher than for bare mild steel probably due to the accelerations of the corrosion processes under delaminated coatings.

Nyquist plane plots of the mild steel covered with 30 μm of the different composite coatings for different immersion times in 3% NaCl are shown in Figs. 4.31-4.34. Since this part of the experiments has a goal only to determine the most corrosion resistant form of polyaniline the fitting procedure was not performed.
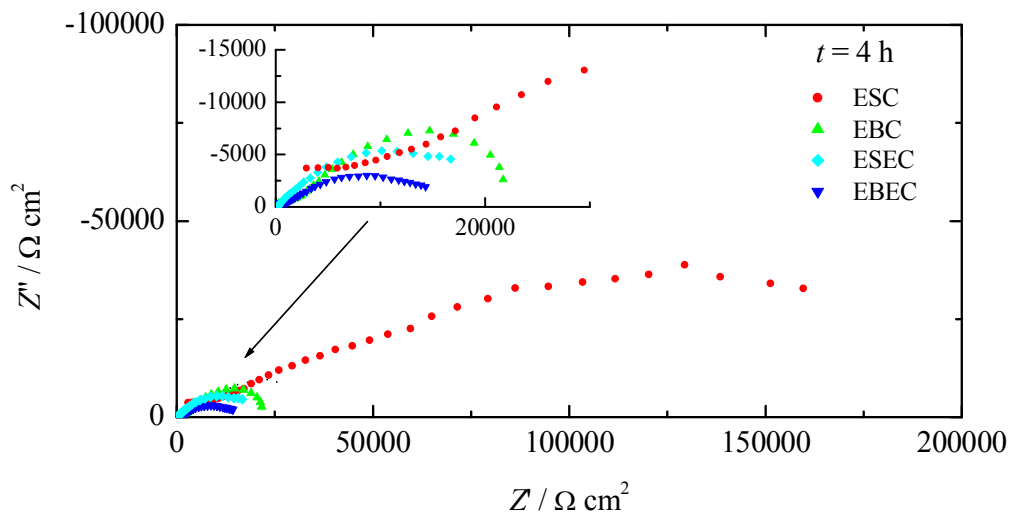
Fig. 4. 31. Nyquist plots of the mild steel covered with 30 μm of the composite coatings after 4 h of immersion in 3% NaCl.
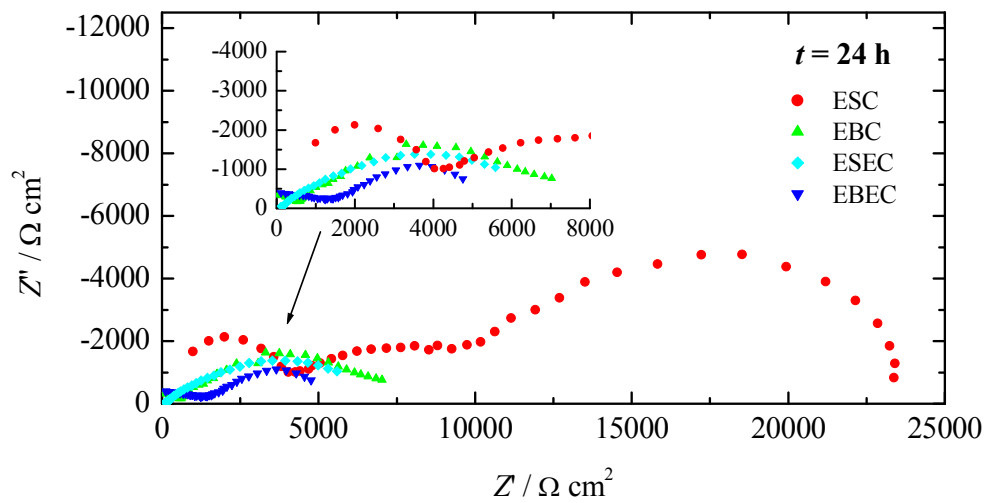
Fig. 4.32. Nyquist plots of the mild steel covered with 30 μm of the composite coatings after 24 h of immersion in 3% NaCl.
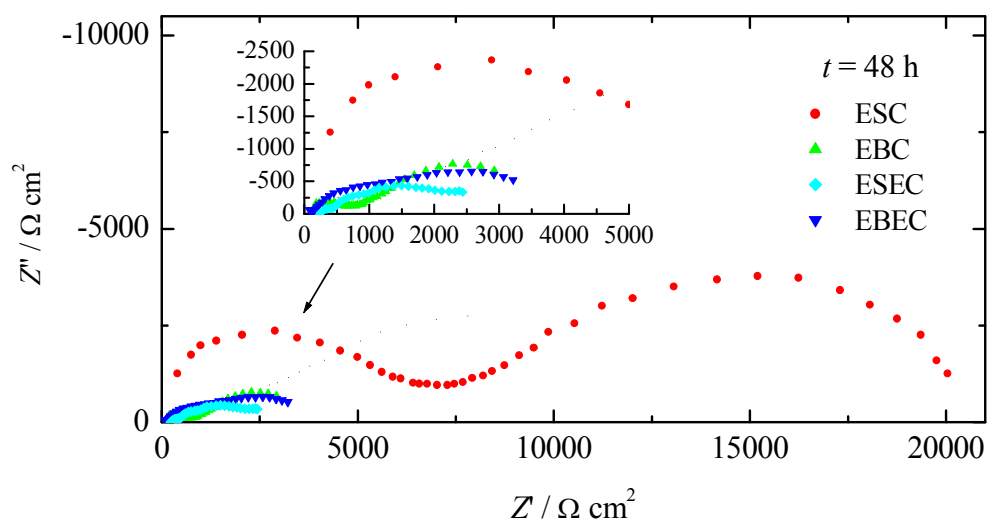
Fig. 4.33. Nyquist plots of the mild steel covered with 30 μm of the composite coatings after 48 h of immersion in 3% NaCl.
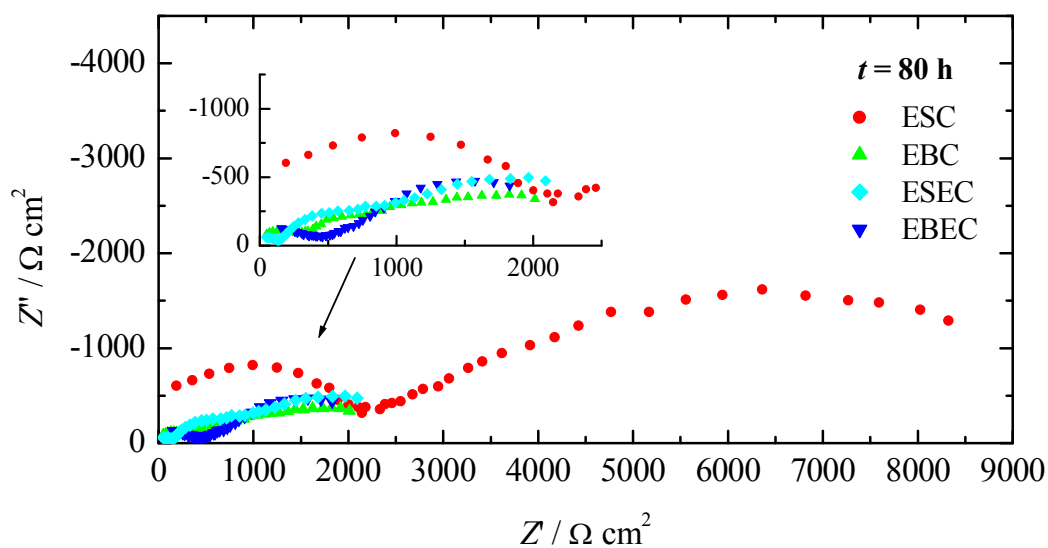
Fig. 4.34. Nyquist plots of the mild steel covered with 30 μm of the composite coatings after 80 h of immersion in 3% NaCl.

Even without fitting of the data, some qualitative observations could be driven from maximum impedance of real part (Z') at given frequency [112], in this case at 10 mHz, as shown in Fig. 4.35. It is obvious that coatings with 5 wt.% of chemically synthesized polyaniline in the emeraldine-salt form has superior characteristics then other investigated samples. The impedance of that sample was almost an order of the magnitude higher for all immersion times. It should be noted that vigorous corrosion was observed only on the samples covered with base coatings.
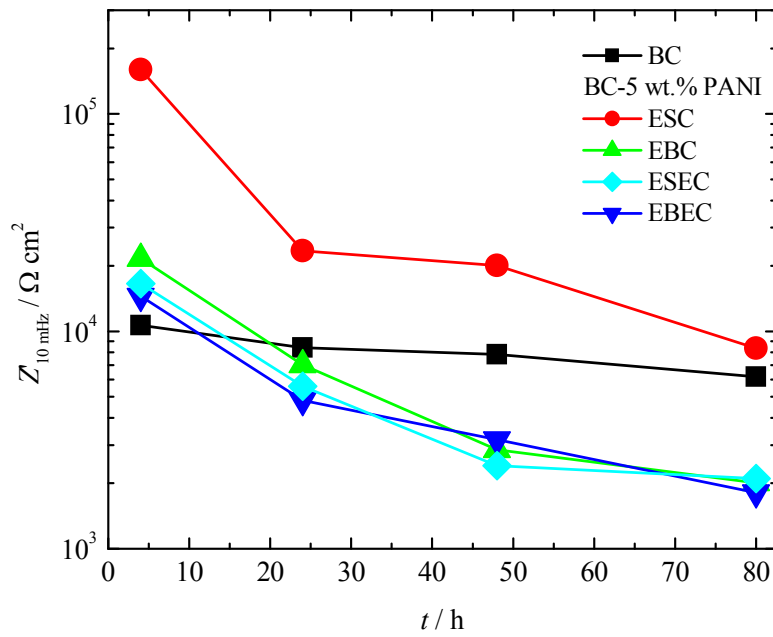
Fig. 4.35. Dependence of the maximum impedance of real part (Z') at frequency of 10 mHz for the mild steel covered with 30 μm of the composite coatings over time.

During the immersion the corrosion potential was also measured and results are presented in Fig. 4.36. It can be seen that in comparison with base coatings, some ennobling of ~70 mV was observed for ESC, EBC and ESEC composite coatings.
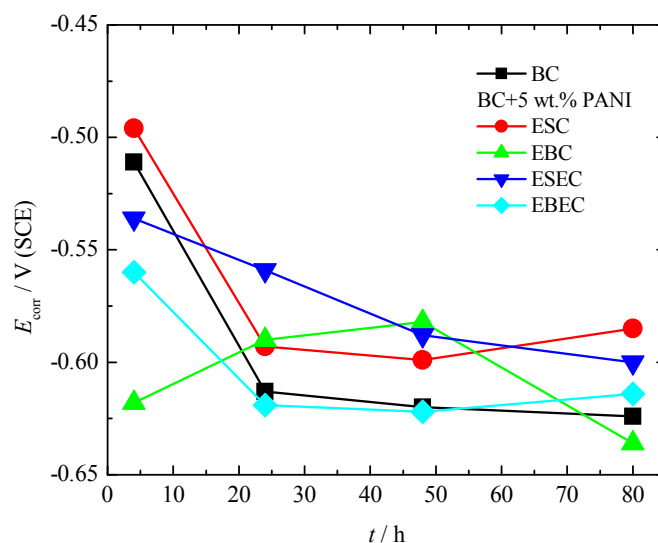
Fig. 4.36. Dependence of the corrosion potential of the mild steel covered with 30 μm of the composite coatings during immersion in 3% NaCl.

Hence, from the impedance measurements it could be concluded that formulation of base coatings with 5 wt.% of chemically synthesized emeraldine-benzoate salt provides the best corrosion protection of the mild steel. To ensure this observations the samples (6 x 4 cm) with the same coatings composition but deliberately scratched, was exposed to corrosion tests in the wet chamber during ten days. The images of initial samples and after exposition of ten days are shown in Figs. 4.37-4.41.

Fig. 4.37. Images of the mild steel samples with base coating before (left) and after 10 days (right) of exposition in wet chamber.
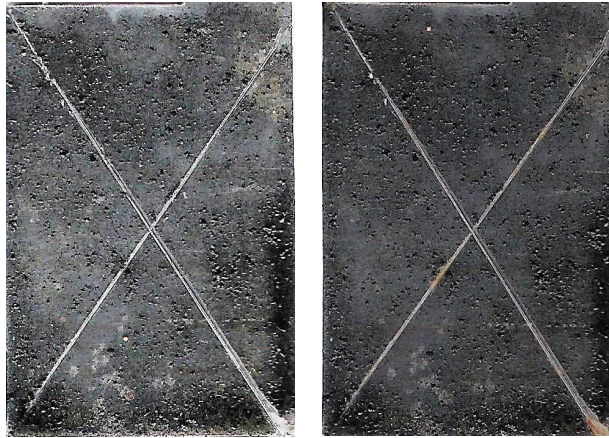
Fig. 4.38. Images of the mild steel samples with base coating + 5 wt.% ESC before (left) and after 10 days (right) of exposition in wet chamber.
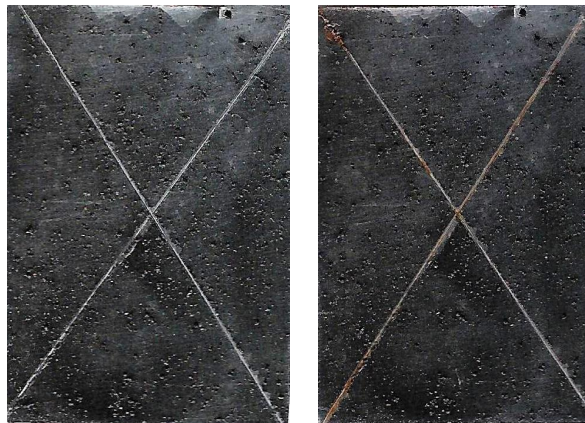
Fig. 4.39. Images of the mild steel samples with base coating + 5 wt.% EBC before (left) and after 10 days (right) of exposition in wet chamber.

Fig. 4.40. Images of the mild steel samples with base coating + 5 wt.% ESEC before (left) and after 10 days (right) of exposition in wet chamber.

Fig. 4.41. Images of the mild steel samples with base coating + 5 wt.% EBEC before (left) and after 10 days (right) of exposition in wet chamber.

From the visual observation and comparison given in Fig. 4.42, the resistance against corrosion are as follows:

$$\text{ESC} \gg \text{ESEC} \sim \text{EBC} > \text{EBEC} \gg \text{BC}$$

5 wt.% ESC   5 wt.% ESEC   5 wt.% EBC   5 wt.% EBEC   BC
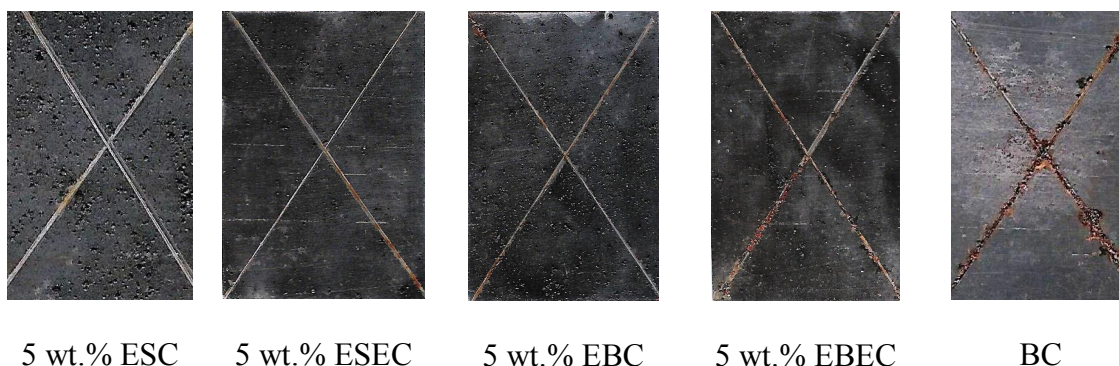
Fig. 4.42. Comparisons of the samples after exposition of ten days in wet chamber.

This difference in corrosion protection could be connected with existence of oligomers in used polyaniline prepared with different methods. Namely, the synthesis efficiency for the chemically prepared polyaniline was 92%, while for the electrochemically synthesized was ~70%. Further one contains oligomers and over-oxidized product which could influence quality of corrosion protection.

From that reasons the UV-visible studies were performed. A UV-visible spectrum in the range of wavelength from 325 to 800 nm of different PANI samples in NMP samples was shown in Fig. 4.43. The first absorption at ~325 nm is assigned for the π–π* transition within the benzenoid ring (B) while the peak at ~630 nm is attributed to the molecular excitation associated with the quinoid-imine (Q) structure [114]. In general, both these peaks represent the half oxidized emeraldine base form ($y = 0.5$) of polyaniline. Some variation in Q peak position and the ratio of quinoid units/benzenoid units (Q/B ratio) in the investigated samples are related to the changes of y ($0.4<y<0.6$), or with the molecular weight of polyaniline chains [115]. The obtained spectra are very similar to that of the pure emeraldine base, but even so the same spectra for partially doped emeraldine was obtained for the samples prepared in low concentration of different acids, for example 0.02 M HIO_3, H_2SO_4, $HClO_4$ [116] or in low concentrated (500 to 0.1 mM) sulfuric acid solutions which gives so called protically doped emeraldine with good anticorrosive properties [82].
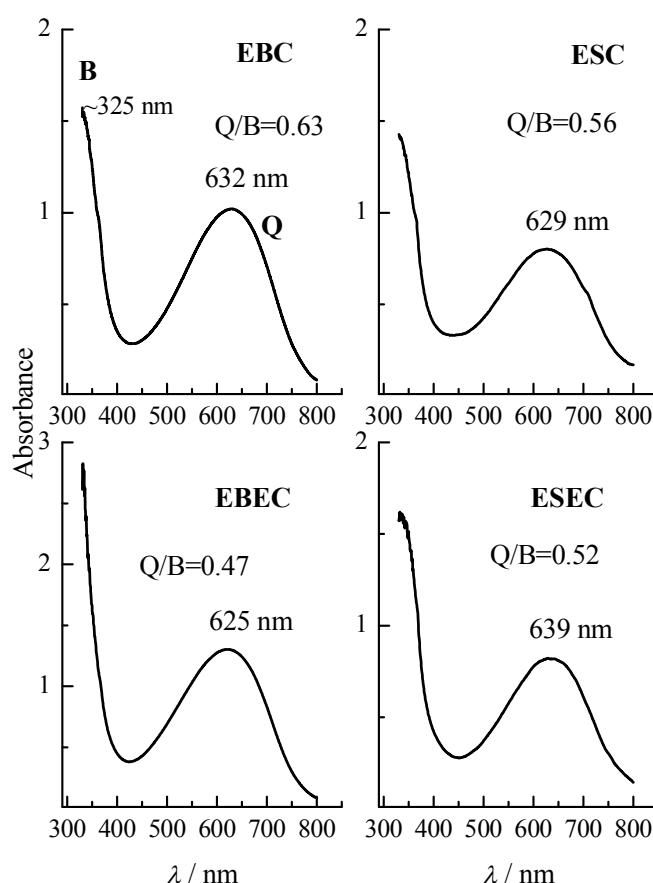
Fig. 4.43. UV-vis spectra of different PANI samples in NMP.

Unfortunately, UV-vis spectra in NMP practically did not give any information which can explain differences in the corrosion behavior of investigated samples. Since difference in corrosion protection was connected with existence of water insoluble oligomers in used polyaniline prepared with different methods [2, 3], in the following experiment UV-vis spectra was recorded in the saturated PANI solution in the chloroform after filtration, and results are shown in Fig. 4.44.
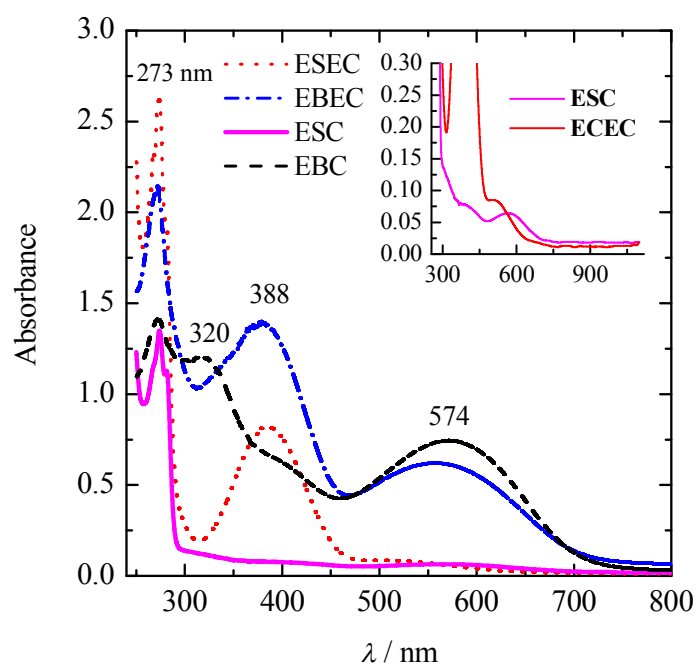
Fig. 4.44. UV-visible spectra of different PANI samples in chloroform. Insert: magnification of the spectra for ESC and ESEC.

Depending on the samples, few different peaks can be seen. The strong sharp peak at 273 nm is ascribed to the π–π* transition in the substituted phenazine. The band around 317-320 nm could be is assigned to the π–π* (band gap) electronic transition in the phenyl ring in the polymer backbone. The strong peak at 388 nm is generated from the π–π* transition in the PANI chains. However, this peak is 40–60 nm higher than that of conventional PANI samples, indicating the declined conjugated level of these synthesized PANI [117] The peak at 570 nm is due to inter band charge transfer

associated with excitation of the benzenoid to quinonoid moieties. [118, 119]. Peaks at 273 and 388 nm in chloroform lie in the same position as bands ascribed to substituted benzoquinones formed during aniline oxidation called **phenazine** and **azane** [120, 121].

Hence, the investigated samples were consisted of regular polyaniline chains (Fig. 4.45a), and some phenazine (Fig. 4.45b) and azane (Fig. 4.45c).

a)

b)

c)
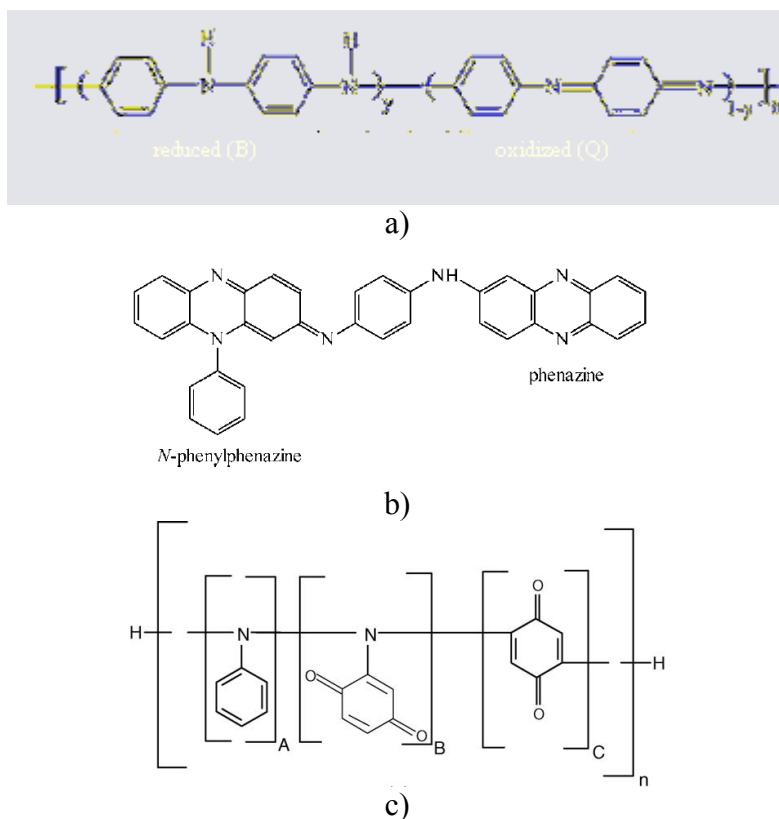
Fig. 4.45. Structures of the a) regular polyaniline emeraldine chains, b) phenazine [3] and of azane material (A=3-4; B=3-5; C=1) [120].

Assuming that content of phenazine and azane in the investigated samples are connected with corrosion protection ability, the spectra from Fig. 4.44 was integrated and the area under the peaks are compared: ESC(70 nm^{-1}) < ESEC(171 nm^{-1}) < EBC(329 nm^{-1}) < EBEC(374 nm^{-1}). This is in agreement with obtained corrosion resistivity using the impedance spectroscopy and wet chamber. From these results, it is obvious that better corrosion performances (ESC >> ESEC ~ EBC > EBEC) have material with lower phenazine and azane content.

In the above given experiments it has been concluded that chemically synthesized polyaniline in the form of emeraldine (benzoate) salt provide the best corrosion protection of the mild steel in the chlorine contained solution. In order to optimize composite coatings in this part of the thesis the influence of ESC content was investigated. Base coating was mixed with 1, 3, 5 and 10 wt.% of ESC and electrochemical impedance measurements was performed during the immersion in 3% NaCl corrosion solution.

Figures 4.46-4.48 shows development of the impedance spectra of the different composite coatings during the immersion in 3% NaCl solution. It can be seen that impedance spectra are very complex, consisted of tree overlapped semi-cycles. Overall impedance decreased with decrease of the ESC content in the composite coatings.
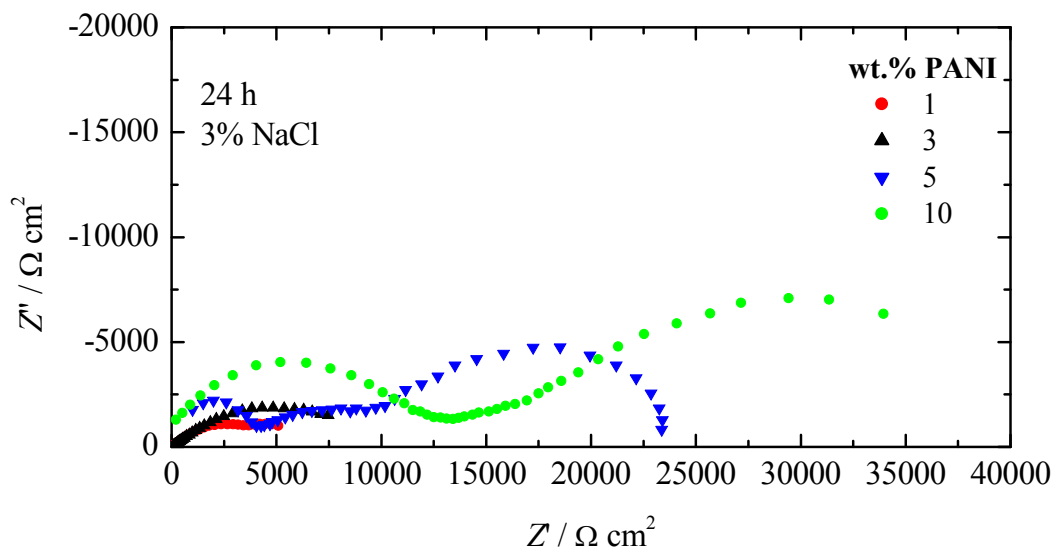
Fig. 4.46. Nyquist plots of the mild steel covered with 30 μm
of the composite coatings after 24 h of immersion in 3% NaCl.
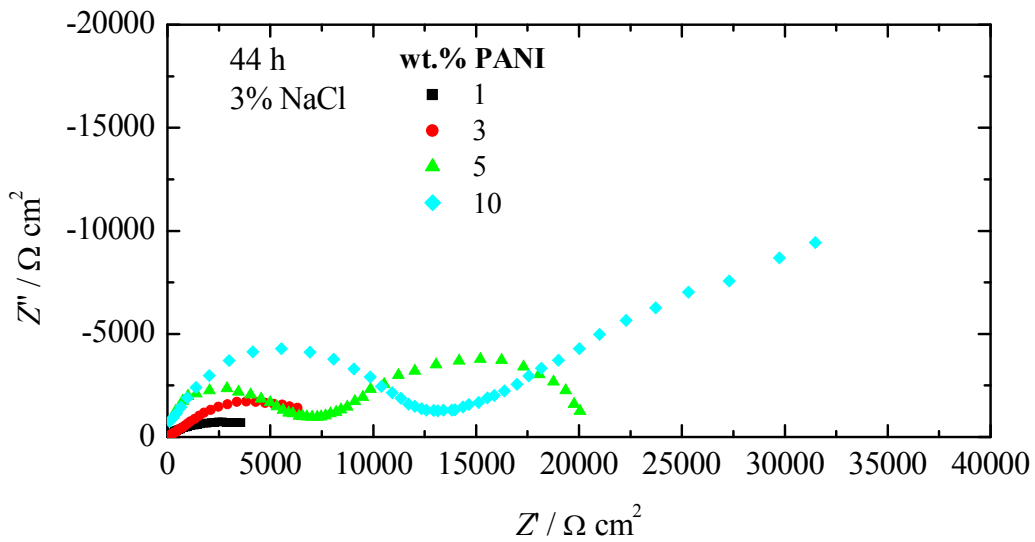
Fig. 4.47. Nyquist plots of the mild steel covered with 30 μm of the composite coatings after 48 h of immersion in 3% NaCl.
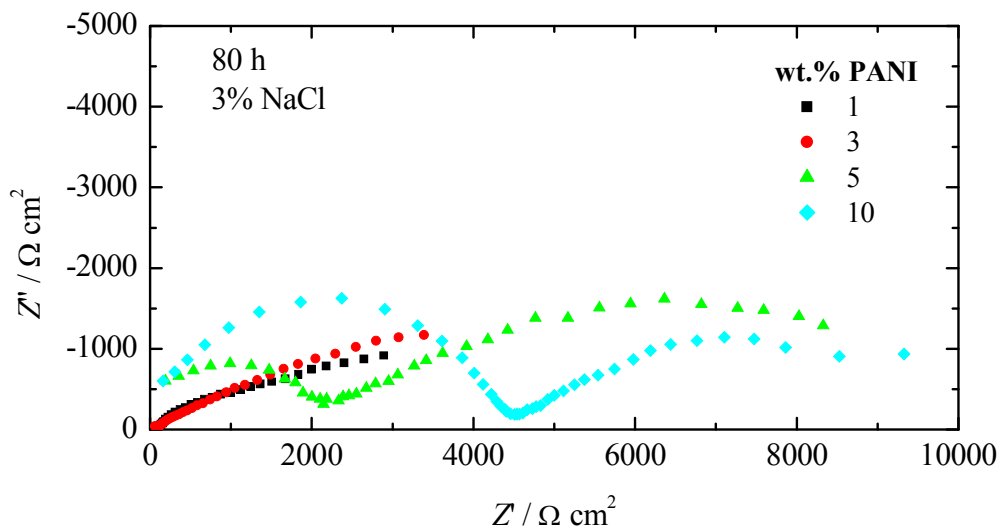
Fig. 4.48. Nyquist plots of the mild steel covered with 30 μm of the composite coatings after 80 h of immersion in 3% NaCl.

To obtain quantitative information about the corrosion protection proceses, the impedance data was fitted with electrical equivalent circuit shown in Fig. 4.49.
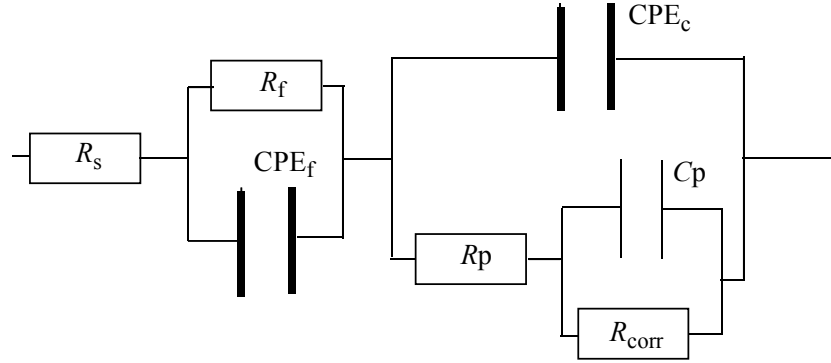
Fig. 4.49. Proposed electrical equivalent circuit for
corrosion processes of the composite coatings.

In the above given electrical equivalent circuit, the parameters represent:

R_s – solution resistance;

R_f – coatings film resistance;

CPE_f – coating constant phase element;

CPE_c – coating/solution interface constant phase element;

R_p – pore resistance;

C_p – capacity of the pores;

R_{corr} – corrosion resistance.

Corresponding physical model of the proposed electrical equivalent circuit for corrosion processes of the composite coatings is shown in Fig. 4.50. Namely, corrosion of the mild steel characterized with R_{corr} occurred into the bottom of coatings pores (represented with R_p and C_p). Coating/solution interface is characterized with constant phase element, CPE_c, and the coating properties are connected with film resistance, R_f and film capacitance represented with constant phase element, CPE_f.
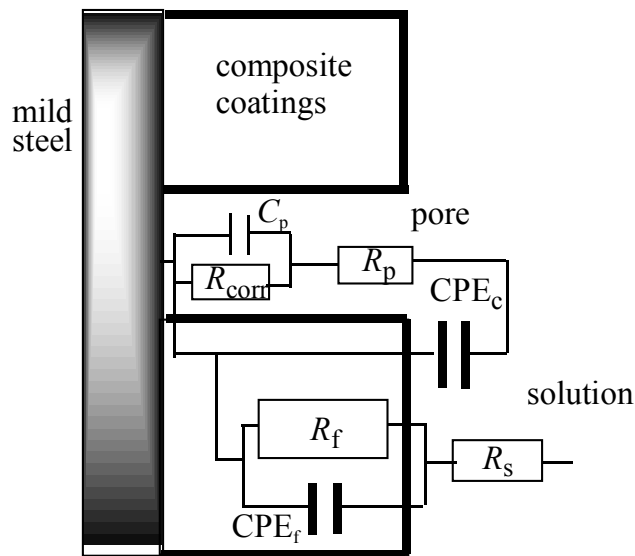
Fig. 4.50. Physical model of the proposed electrical equivalent circuit for corrosion processes of the composite coatings.

The very good quality of data fitting with proposed electrical equivalent circuit is shown as an example for the mild steel sample coated with coating containing 10 wt.% of ESC after 24 h of immersion in Fig. 4.51 as a Nyquist plot, and in Fig. 4.52 as a Bode plot.
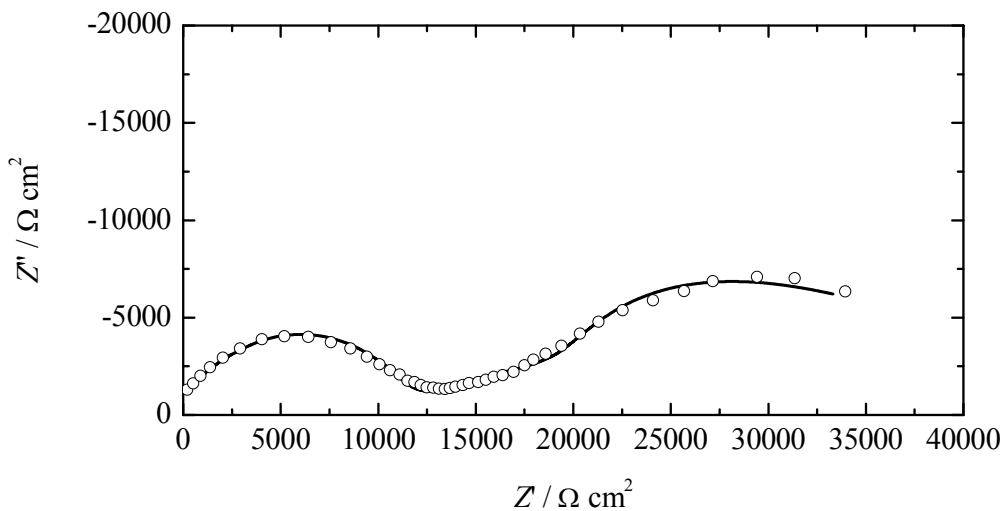
Fig. 4.51. Data fitting (Nyquist plot) with proposed electrical equivalent circuit (Fig. 4.46) for the mild steel sample coated with coating containing 10 wt.% of ESC after 24 h of immersion in 3% NaCl. Symbols - experimental data; lines - best fit.
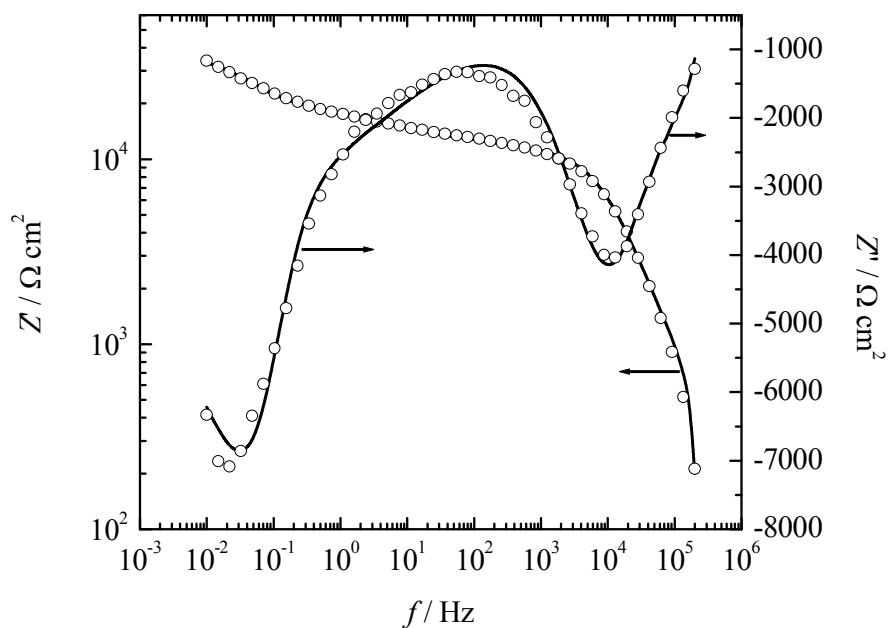
Fig. 4.52. Data fitting (Bode plot) with proposed electrical equivalent circuit (Fig. 4.49) for the mild steel sample coated with coating containing 10 wt.% of ESC after 24 h of immersion in 3% NaCl. Symbols - experimental data; lines - best fit.

The values of fitted parameters for the composite coatings with 5 and 10 wt.% of polyaniline-benzoate salt, which shows the best corrosion protection effect are shown in Tables 4.4 and 4.5.

Table 4.4. The values of fitted parameters for the composite coatings with 5 wt.% of polyaniline-benzoate salt.

t / h	R_f / Ω cm^2	$Y_{0,f}$ / S s^n cm^{-2}	n	$Y_{0,c}$ / S s^n cm^{-2}	n	R_p / Ω cm^2	C_p / F cm^{-2}	R_{corr} / Ω cm^2
4	4605	1.2×10^{-8}	0.80	3.9×10^{-6}	0.39	1.3×10^5	1.7×10^{-11}	1.3×10^5
24	2533	5.4×10^{-11}	0.99	8.9×10^{-6}	0.35	13511	8.2×10^{-6}	10479
48	5189	5.3×10^{-9}	0.84	2.1×10^{-5}	0.38	8238	7.2×10^{-6}	10070
80	1874	1.8×10^{-8}	0.87	8.6×10^{-5}	0.39	3083	9.8×10^{-9}	6636

Table 4.5. The values of fitted parameters for the composite coatings with 10 wt.% of polyaniline-benzoate salt.

t / h	R_f / Ω cm^2	$Y_{0,f}$ / S s^n cm^{-2}	n	$Y_{0,c}$ / S s^n cm^{-2}	n	R_p / Ω cm^2	C_p / F cm^{-2}	R_{corr} / Ω cm^2
24	10858	1.4×10^{-8}	0.79	4.7×10^{-5}	0.34	18839	1.3×10^{-4}	20778
48	11329	1.8×10^{-8}	0.81	6.5×10^{-5}	0.37	22020	2.0×10^{-4}	25655
80	4344	2.0×10^{-8}	0.81	2.5×10^{-4}	0.49	3335	8.0×10^{-4}	2335

From Tables 4.4 and 4.5 it can be seen that dye to the value of n coefficient of CPE$_f$ ($n \sim 0.8$) CPE$_f$ has a capacitive nature. On the contrary, the value of n coefficient of CPE$_c$ ($n \sim 0.4$-0.5) suggests diffusion Warburg element.

Dependence of the R_f, R_p and R_{corr} over time for composite coatings with 5 wt.% and 10 wt.% polyaniline are shown in Fig. 4.53. It can be seen that all R parameters is higher for coatings with 10 wt.% than for 5 wt.% of polyaniline during 48 h of immersion. After that 5 wt. % shows better characteristics (see discussion below).
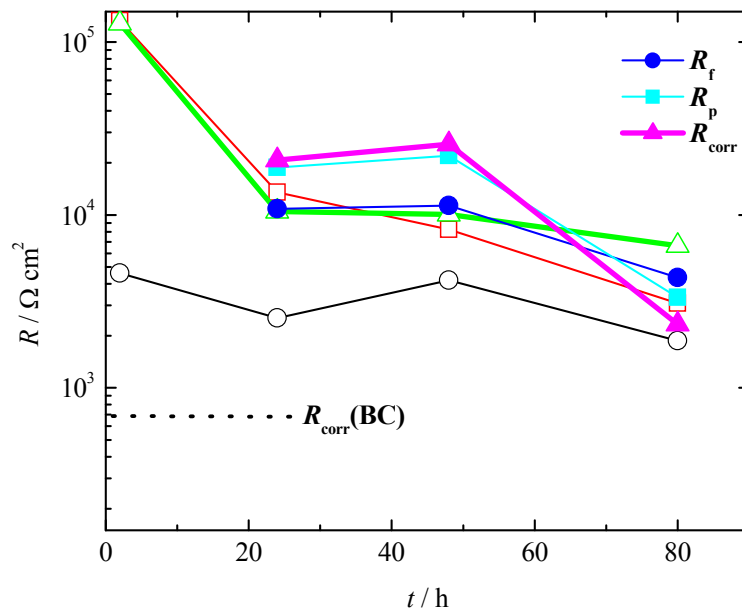
Fig. 4.53. Dependence of the R_f, R_p and R_{corr} over time for composite coatings with 5 wt.% (open symbols) and 10 wt.% (full symbols) of polyaniline.

For the samples with 1, 3, 5 and 10 wt.% of polyaniline immersed for 48 h in 3% NaCl solution the dependence of the R_p and R_{corr} parameters are shown in Fig. 4.54. It can be seen that practically linear dependence was obtained. In the insert of Fig. 4.54 the calculated corrosion current density according to Eq. 4.12, and with data taken from the Fig. 4.55. was shown.
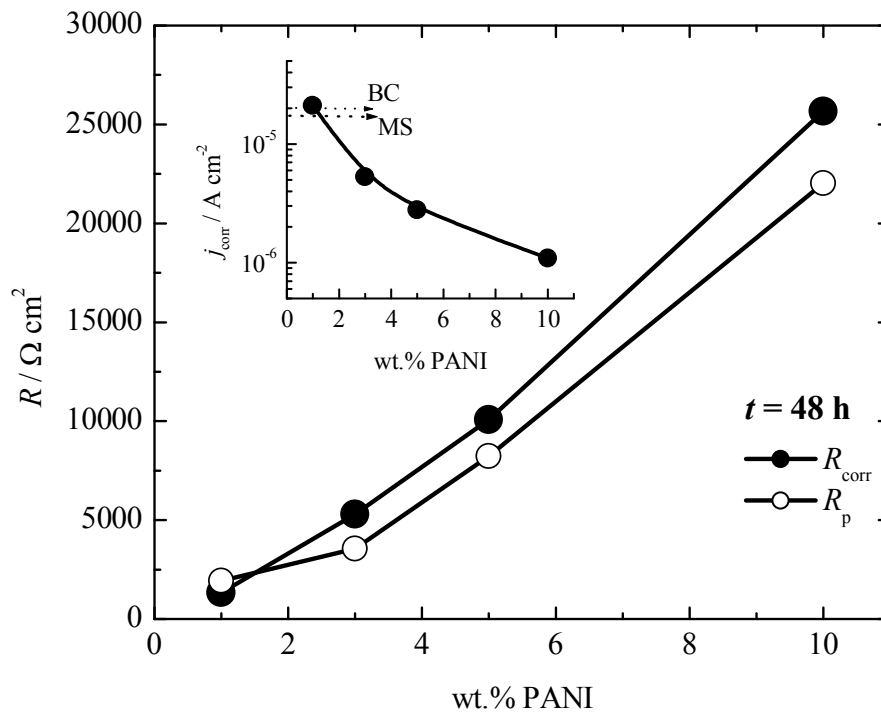
Fig. 4.54. Dependence of the R_p and R_{corr} for composite coatings with 1, 3, 5 and 10 wt.% of polyaniline after 48 h of immersion in 3% NaCl.
Insert: Dependence of calculated current density on PANI content.

Comparison of the polarization curve for mild steel and mild steel covered with composite coatings with 10 wt.% of polyaniline after 80 h of immersion was shown in Fig. 4.55. Corrosion current density of composite coatings with 10 wt.% of polyaniline of 0.6 μA cm^{-2} is in good agreement with that obtained from the impedance measurements, and was 25 times smaller than for bare mild steel.
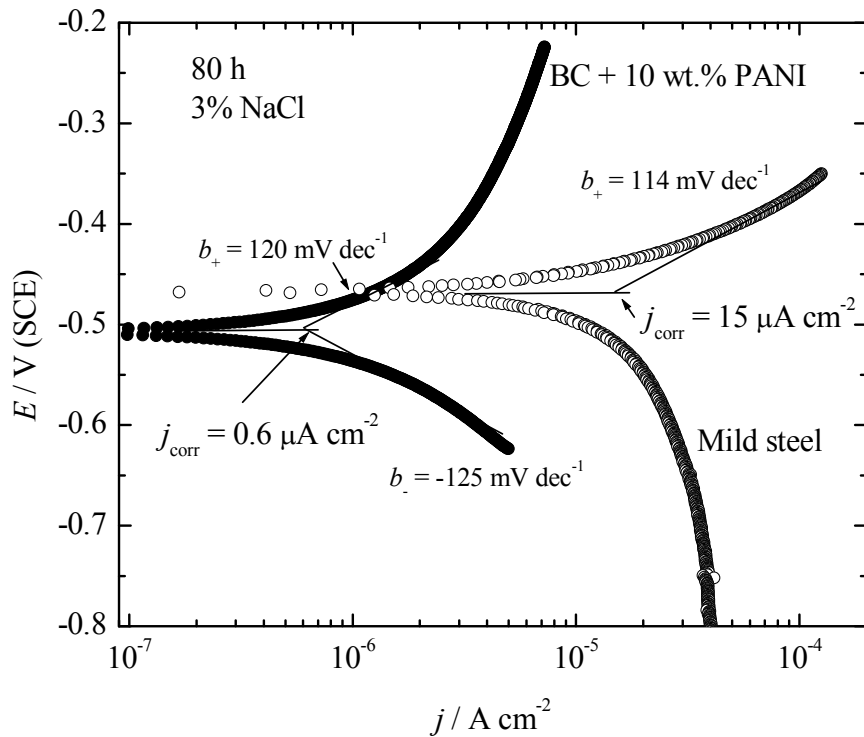
Fig. 4.55. Comparison of the polarization curve for mild steel and mild steel covered with composite coatings with 10 wt.% of polyaniline after 80 h of immersion in 3% NaCl.

Even the electrochemical measurements are useful tools to investigated corrosion processes, visual observations are much reliable.

From that reasons the corrosion behavior of the screeched samples (mild steel with base coating, 5 wt.% and 10 wt.% of polyaniline in the composite coatings) was investigated in 3% of NaCl solution.

Low corrosion resistive base coating, as shown in Fig. 4.56, was completely destroyed after 80 h of immersion in 3% NaCl. Composite coating with 10 wt.% of polyaniline, Fig. 4.57 shows much better corrosion resistivity than base coating. But even so, some small delamination process occurred with formation of the corrosion products.
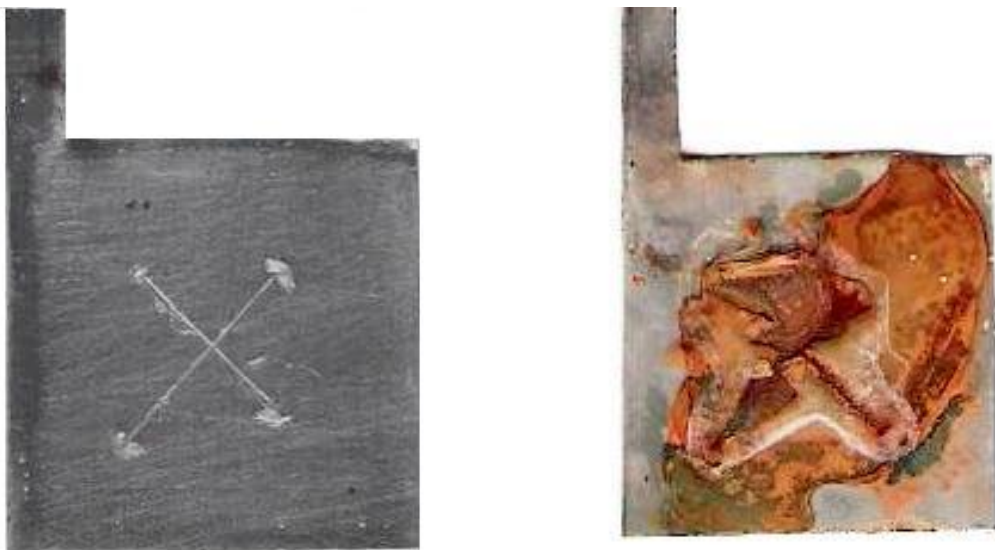
Fig. 4.56. Images of mild steel covered with 30 μm base coatings before immersion (left) and after immersion for 80 h (right) in 3% NaCl.
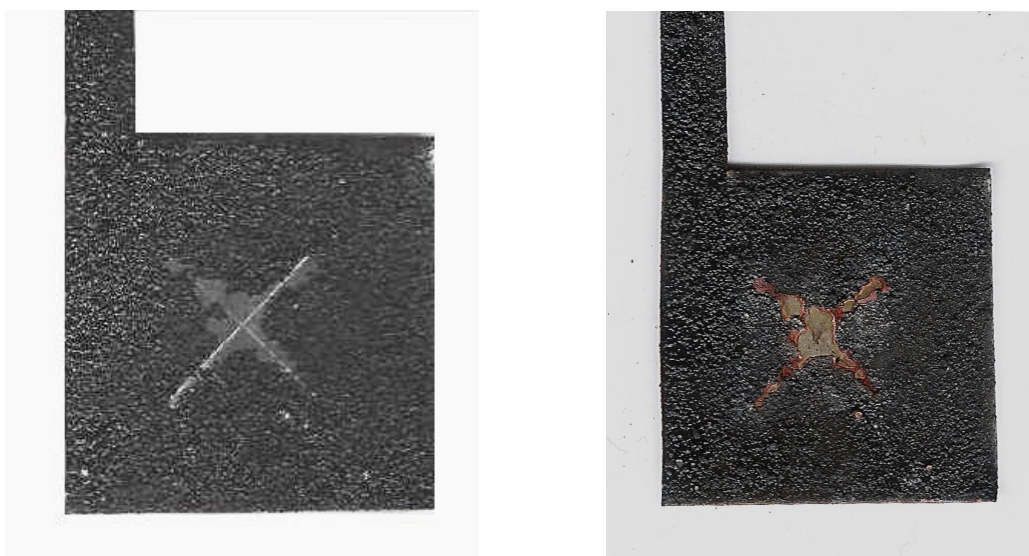
Fig. 4.57. Images of mild steel covered with 30 μm base coatings + 10 wt.% of polyaniline ESC before immersion (left), and after immersion for 80 h (right) in 3% NaCl.

On the contrary, mild steel covered with 30 μm base coatings + 5 wt.% of polyaniline shows significant improvements in corrosion protection. As it can be seen in Fig. 4.58, this coating after 24 h of immersion shows only a small appearance of corrosion products in the scratched surface. After 80 h of immersion visible corrosion

109

occurred into the bottom of the scratched surface, but no delamination was observed. Hence an optimum composition for the undercoat should be ~ 5 wt.% of chemically synthesized emeraldine salt as a active anticorrosion pigment.

Fig. 4.58. Images of mild steel covered with 30 μm base coatings + 5 wt.% of polyaniline ESC before immersion (left), after immersion for 24 h (middle) and 80 h (right) in 3% NaCl.

With such results composite coatings with 5 wt.% of ECS with commercial TESSAROL-Helios primer for iron paint was prepared and tested for 200 h in 3% NaCl solution. The image of the samples after corrosion test was shown in Figs. 4.59 and 4.60.

Fig 4.59. Images of the samples after 200 h of corrosion in 3% NaCl. left: TESSAROL-Helios primer for iron paint; right: TESSAROL-Helios primer for iron + 5 wt% ESC (based on dry paint).
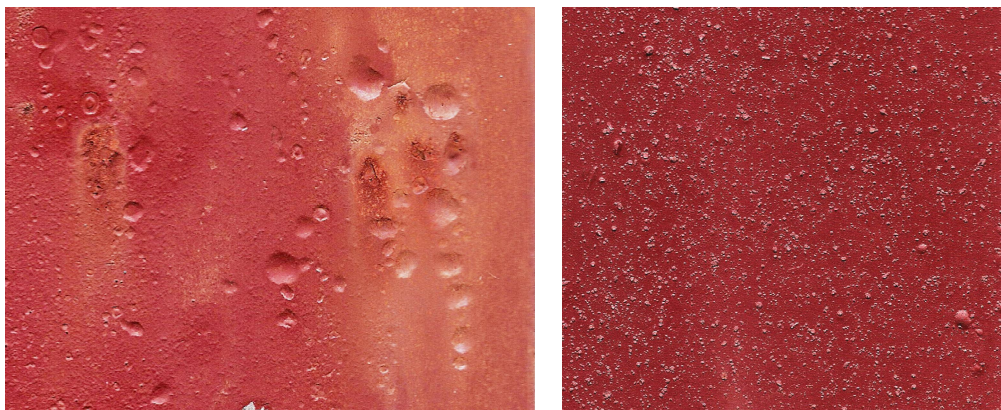
Fig 4.60. Magnification of the samples after 200 h of corrosion in 3% NaCl. left: TESSAROL-Helios primer for iron paint; right: TESSAROL-Helios primer for iron + 5 wt% ESC (based on dry paint).

From Figs. 4.59 and 4.60 it can be seen that primer paint corrodes with development of blisters and delamination of the coatings. On the contrary, primer paint with addition of 5 wt.% of ECS practically remains unchanged.

Based of presented experimental investigations the following mechanism can be proposed. The main problem with classical organic coatings is penetration of an corrosion agent (for example O_2 molecules) through the coating as illustrated in Fig. 4.61, which is followed with degradation and delamination of the coatings [105, 122,123].
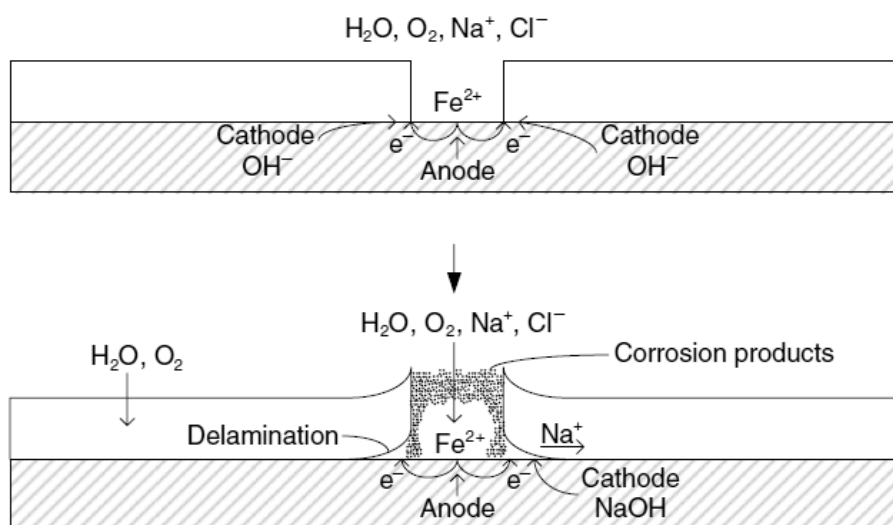
Fig. 4.61. Idealized sketch of corrosion followed with delamination [105, 122, 123].

If the poluaniline-salt is present in the screeched coating [124], in the contact with electrolyte initially anodic dissolution of iron occurs governed with dedoping of the benzoate anions:

$$Fe \rightarrow Fe^{2+} + 2e \qquad (4.2)$$

$$[PANI^{y+}(C_6H_5COO^-)_y]_n + nye \rightarrow [PANI]_n + nyC_6H_5COO^- \qquad (4.6)$$
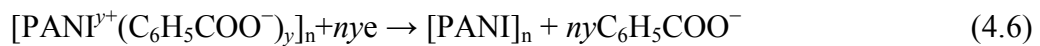
Released benzoate anions could form low soluble iron-benzoate which slows down the corrosion rate. Now, partially dedoped PANI could serve as a center for oxygen reduction reaction:

$$O_2 + 2H_2O + 4e \rightarrow 4OH^- \qquad (4.3)$$

as illustrated in Fig. 4.17. Liberated electrons can further be involved in dedoping of the benzoate anions and eliminate iron dissolution followed earlier proposed "switching zone mechanism". Schematic representation of this behavior is shown in Fig. 4.62. It should be noted that released OH⁻ ions could be chemically inserted in dedoped polyaniline, as well as to increase pH in to the pores which could additionally slow corrosion reactions.
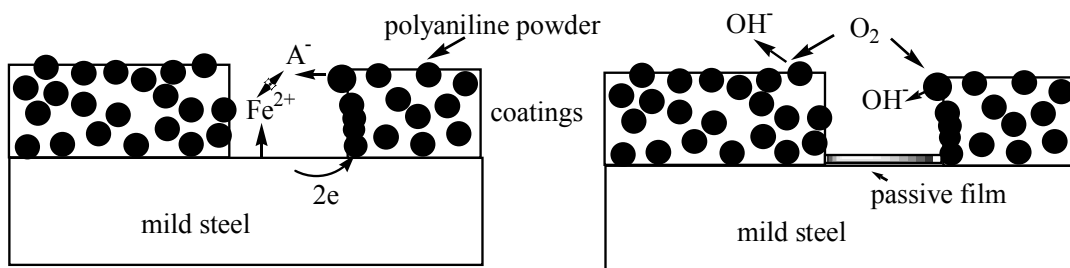
Fig. 4.62. Shematic representations of corrosion processes with polyaniline composite coatings.

5. CONCLUSIONS

- The corrosion of mild steel with partial PANI-benzoate coatings in tree different environments (3% NaCl, atmosphere and Sahara sand) was investigated. It was concluded that in all tree investigated environments PANI-benzoate coatings could protect mild steel even with partially applied coatings for limited period of time. It was also shown that partial PANI-benzoate coatings could protect mild steel under the case of cathodic protection failure. Based on the experimental evidences the "switching zone mechanism" was proposed and discussed.

- From the simple experiments it could be concluded that corrosion processes of mild steel covered with polyaniline is affected with light, even the mild illumination was applied (4 mW cm^{-2}) which is the usual light intensity in the laboratory conditions. Hence, any further works in application of electroconducting polymers in corrosion protection of metals should consider light intensity.

- Polyaniline powder was prepared by electrochemical and chemical methods. By the chemical dedoping and doping, polyaniline powder was prepared in the form of emeraldine (benzoate) salts or emeraldin base, since there is controversy in the literature which form gives better protection against corrosion of the mild steel. With such obtained and characterized powders the composite coatings with different content of PANI powder (1-10 wt%) was prepared, and applied on the mild steel samples, and the corrosion behavior was investigated using electrochemical impedance technique and the method of moist chamber for samples with artificially induced defects. It was found that chemically synthesized polyaniline in the form of emeraldin salts offers the best protection with the optimal concentration of polyaniline about 5 wt.%. The proposed mechanism of corrosion protection of mild

steel in a real system was also confirmed. This difference in corrosion protection could be connected with existence of oligomers in used polyaniline prepared with different methods. Namely, the synthesis efficiency for the chemically prepared polyaniline was 92%, while for the electrochemically synthesized was ~70%. Further one contains oligomers and over-oxidized product which could influence quality of corrosion protection. Using the UV-vis spectroscopy it was concluded that content of phenazine and azane structures in the investigated samples are connected with corrosion protection ability.

- Comparing the corrosion behavior of the real systems, TESSAROL-Helios primer for iron paint with and without addition of 5 wt% of ESC powder, it was concluded that addition of the polyaniline practically suppress corrosion of the mild steel.

REFERENCES

[1] J. Stejskal, R. G. Gilbert, Polyaniline. Preparation of a conducting polymer (IUPAC Technical Report), Pure and Applied Chemistry, 74 (2002) 857–867.

[2] J. Stejskal I. Sapurina, M. Trchová, Polyaniline nanostructures and the role of aniline oligomers in their formation, Progress in Polymer Science, 35 (2010) 1420–1481.

[3] J. Stejskal, I. Sapurina, M. Trchová, E. N. Konyushenko, Oxidation of aniline: Polyaniline granules, nanotubes, and oligoaniline microspheres, Macromolecules, 41 (2008) 3530-3536.

[4] J. Stejskal, M. Trchová, Aniline oligomers versus polyaniline, Polymer International, 61 (2012) 240–251.

[5] H. Letheby, On the production of a blue substance by the electrolysis of sulphate of aniline, J. Chem. Soc., 15 (1862) 161–163.

[6] M.M. Gvozdenović, B.Z. Jugović, T.Lj. Trišović, J.S. Stevanović, B.N. Grgur, Electrochemical characterization of polyaniline electrode in ammonium citrate containing electrolyte, Mat. Chem. Phys., 125 (3) (2011) 601-605.

[7] M. M. Gvozdenović, B. Z. Jugović, J. S. Stevanović, T. Lj. Trišović, B. N. Grgur,. Electropolymerization, Chapter 4: Electrochemical Polymerization of Aniline, Ewa Schab-Balcerzak (Ed.), InTech publication, 2011, pp 77-96.

[8] Y. Wei, G-W Jang, Ch-Ch. Chan, K.F. Hsuen, R. Hariharan, S,A, Patel, C.K. Whitecar, Polymerization of aniline and alkyl ring-substituted anilines in the presence of aromatic additives, J. Phys. Chem., 94 (1990) 7716–7721.

[9] Wei, Y., Tang, X., Sun, Y. and Focke, W. W., A study of the mechanism of aniline polymerization, J. Polym. Sci., 27 (1989) 2385–2396.

[10] N. Gospodinova, L. Terlemezyan, Conducting polymers prepared by oxidative polymerization: polyaniline, Prog. Polym. Sci., 23 (1998) 1443-1484.

[11] E. Smela, W. Lu, B.R. Mattes, Polyaniline actuators: Part 1. PANI(AMPS) in HCl, Synthetic Met. 151 (2005) 25–42.

[12] A.D. MacDiarmid, Nobel Prize 200 Lecture: "Synthetic metals" a novel role for organic polymers, Curr. Appl. Phys., 1 (2001) 269-279.

[13] H.N. Dinh, J. Ding, S.J. Xia, V. I. Birss, Multi-technique study of the anodic degradation of polyaniline films, J. Electroanal. Chem. 459 (1998) 45-56.

[14] D.E. Stilwell, S.-M. Park, Electrochemistry of conductive polymers III. Some physical and electrochemical properties observed from electrochemically grown Polyaniline, J. Electrochem. Soc., 135 (10) (1988) 2491-2496.

[15] D.E. Stilwell, S-M Park, Electrochemistry of conductive polymers, IV Electrochemical studies on polyaniline degradation - product identification and coulometric studies, J. Electrochem. Soc. 135 (10) (1988) 2497-2502.

[16] D.E. Stilwell, S.-M. Park, Electrochemistry of conductive polymers VI. Degradation Reaction Kinetics of Polyaniline Studied by Rotating Ring-Disk Electrode Techniques, J. Electrochem. Soc., 136 (3) (1989) 688-698.

[17] A.Q. Zhang, C.Q. Cui, J.Y. Lee, Electrochemical degradation of polyaniline in $HClO_4$ and H_2SO_4, Syntetic Met. 72 (1995) 217-223.

[18] J. López-Palacios, E. Muñoz, Á. Colina, A. Heras, V. Ruiz, Study of polyaniline films degradation by thin-layer bidimensional spectroelectrochemistry, Electrochim. Acta, 52 (2006) 234-239

[19] R. Mažeikienè, A. Malinauskas, Kinetic study of the electrochemical degradation of polyaniline, Synthetic. Met. 123(2) (2001) 349-354.

[20] R. Mažeikienè, A. Malinauskas, Electrochemical stability of polyaniline, European Polymer Journal, 38 (2002) 1947–1952.

[21] B. Jugović, M. Gvozdenović, J. Stevanović, T. Trišović, B. Grgur, Characterization of electrochemically synthesized PANI on graphite electrode for potential use in electrochemical power sources, Mat. Chem. Phys., 114 (2-3) (2009) 939-942.

[22] M. Gao, G. Zhang, G. Zhang, X. Wang, S. Wang, Y. Yang, The resistance to over-oxidation for polyaniline initiated by the resulting quinone-like molecules, Polym. Degrad. Stab., 96 (2011) 1799-1804.

[23] E. Dmitrieva, Y. Harima, L. Dunsch, Influence of phenazine structure on polaron formation in polyaniline: In situ electron spin resonance−ultraviolet/visible−near-infrared spectroelectrochemical study, J. Phys. Chem. B, 113 (50) (2009) 16131–16141.

[24] A.V. Nand, S.R., M. Gizdavic-Nikolaidis, J. Travas-Sejdic, P.A. Kilmartin, The effects of thermal treatment on the antioxidant activity of polyaniline, Polym. Degrad. Stab., 96 (2011) 2159-2166.

[25] S. Bhadra, D. Khastgir, Extrinsic and intrinsic structural change during heat treatment of polyaniline, Polym. Degrad. Stab., 93 (2008) 1094–1099.

[26] S. Sakkopoulos, E. Vitoratos, E. Dalas, Conductivity degradation due to thermal aging in conducting polyaniline and polypyrrole, Synthetic Met., 92 (1998) 63-67.

[27] Y. Kieffel, J. Pierre Travers, A. Ermolief, D. Rouchon, Thermal aging of undoped polyaniline: Effect of chemical degradation on electrical properties, J. Appl. Polym. Sci., 86 (2) (2002) 395-404.

[28] T. Chen, C. Dong, X. Li, J. Gao, Thermal degradation mechanism of dodecylbenzene sulfonic acid- hydrochloric acid co-doped polyaniline, Polym. Degrad. Stab., 94 (2009) 1788–1794.

[29] C. Heng Teo, F. Rahman, Degradation and protection of polyaniline from exposure to ultraviolet radiation, Appl. Phys. A., 99 (2010) 311–316.

[30] A.D. MacDiarmid, Nobel Prize 200 Lecture: "Synthetic metals" a novel role for organic polymers, Curr. Appl. Phys., 1 (2001) 269-279.

[31] K. Gurunathan, A. Vadivel Murugan, R. Marimuthu, U.P. Mulik, D.P. Amalnerkar Electrochemically synthesised conducting polymeric materials for applications towards technology in electronics, optoelectronics and energy storage devices, Mat. Chem. Phys., 61 (1999) 173-191.

[32] J.D. Stenger-Smith, Intrinsically electrically conducting polymers. Synthesis, characterization, and their applications, Prg. Polym. Sci., 23 (1998) 57-79.

[33] P. Novák, K. Müller, K. S. V. Santhanam, O. Haas, Electrochemically active polymers for rechargeable batteries, Chem. Rev., 97 (1997) 207-281.

[34] A. Malinauskas, J. Malinauskienė, A. Ramanavičius, Conducting polymer-based nanostructurized materials: electrochemical aspects, Nanotechnology, 16 (2005) R51-62.

[35] Z.W. Wicks, F.N. Jones, S. P. Pappas, D.A. Wicks, Organic Coatings: Science and Technology, Third Edition, John Wiley & Sons, Inc., NY, 2006

[36] S.P. Sitaram, J.O. Stoffer, T.J. O'Keefe, Application of conducting polymers in corrosion protection J. Coat. Technol. 69 (1997) 65-69.

[37] M. Kraljic, Z. Mandic, Lj. Duic, Inhibition of steel corrosion by polyaniline coatings, Corr. Sci. 45 (2003) 181-198.

[38] C.K. Tan, D.J. Blackwood, Corrosion protection by multilayered conducting polymer coatings, Corros. Sci. 45 (2003) 545-557.

[39] A.M. Fenelon, C.B. Breslin, Polyaniline-coated iron: Studies on the dissolution and electrochemical activity as a function of pH, Surf. Coat. Technol. 190 (2-3) (2005) 264-270.

[40] D.W. DeBerry, Modification of the Electrochemical and Corrosion Behavior of Stainless Steels with an Electroactive Coating, J. Electrochem. Soc. 132 (5) (1985) 1022-1026.

[41] N.M. Martyak, P.M. Andrew, J.E.M. Caskie, J. Dijon, Corrosion of polyaniline-coated steel in high pH electrolytes, Sci. Technol. Adv. Mater. 3 (2002) 345-352.

[42] M.M. Popović, B.N. Grgur, Electrochemical synthesis and corrosion behavior of thin polyaniline-benzoate film on mild steel, Synthetic Met. 143 (2004) 191-196.

[43] C.B. Breslin, A.M. Fenelon, K.G. Conroy, Surface engineering: corrosion protection using conducting polymers, Mater. Des. 26 (2005) 233-237.

[44] X.G. Li, M.R. Huang, J.F. Zeng, M.F. Zhu, The preparation of polyaniline waterborne latex nanoparticles and their films with anti-corrosivity and semi-conductivity, Colloids Surf. A: Physicochem. Eng. Aspects 248 (2004) 111-120.

[45] A.B. Samui, S.M. Phadnis, Polyaniline- dioctyl phosphate salt for corrosion protection of iron, Prog. Org. Coat., 54 (2005) 263-267.

[46] S. Sathiyanarayanan, S. Muthukrishnan, G. Venkatachari, Performance of polyaniline pigmented vinyl acrylic coating on steel in aqueous solutions, Prog. Org. Coat. 55 (2006) 5-10.

[47] M. Tiitu, A. Talo, O. Forsen, O. Ikkala, Aminic epoxy resin hardeners as reactive solvents for conjugated polymers: polyaniline base/epoxy composites for anticorrosion coatings, Polymer, 46 (2005) 6855-6861.

[48] S. Sathiyanarayanan, S. Muthukrishnan, G. Venkatachari, D.C. Trivedi, Corrosion Protection of Steel by Polyaniline (PANI) Pigmented Paint Coatings, Prog. Org. Coat. 53 (2005) 297-301.

[49] D. E. Tallman, G. Spinks, A. Dominis, G. G. Wallace, Electroactive conducting polymers for corrosion control: Part 1. General introduction and a review of non-ferrous metals, J. Solid State Electrochem. 6 (2002) 73-84.

[50] D. E. Tallman, G. Spinks, A. Dominis, G. G. Wallace, Electroactive conducting polymers for corrosion control. Part 2. Ferrous metals, J. Solid State Electrochem. 6 (2002) 85-100.

[51] F. Beck, R. Michaelis, F. Scholten, B. Zinger, Filmforming electropolymerization of pyrrole on iron in aqueous oxalic acid, Electrochim. Acta, 39 (2) (1994) 229-234.

[52] Grgur BN, Živković P, Gvozdenović MM. Kinetics of the mild steel corrosion protection by polypyrrole-oxalate coating in sulfuric acid solution. Prog. Org. Coat., 56(2-3) (2006) 240-247.

[53] J. L. Camalet, J. C. Lacroix, S. Aeiyach, K. Chane-Ching, P. C. Lacaze, Electrodeposition of protective polyaniline films on mild steel, J. Electroanal. Chem. 416 (1996) 179-182.

[54] Camalet, J.L., Lacroix, J.C., Aeiyach, S., Chane-Ching, K., Lacaze, P.C. Electrosynthesis of adherent polyaniline films on iron and mild steel in aqueous oxalic acid medium, Synthetic Met., 93 (2) (1998) 133-142.

[55] J. L. Camalet, J. C. Lacroix, S. Aeiyach, K., P. C. Lacaze, Characterization of polyaniline films electrodeposited on mild steel in aqueous p-toluenesulfonic acid solution, J. Electroanal. Chem. 445 (1998) 117-124.

[56] J.-C. Lacroix, J.-L. Camalet, S. Aeiyach, K.I. Chane-Ching, J. Petitjean, E. Chauveau, P.-C., Lacaze, Aniline electropolymerization on mild steel and zinc in a two-step process, J. Electroanal. Chem. 481 (2000) 76–81.

[57] J. L. Camalet, J. C. Lacroix, T. Dung Nguyen, S. Aeiyach, M. C. Pham, J. Petitjean, P. C. Lacaze, Aniline electropolymerization on platinum and mild steel from neutral aqueous media, J. Electroanal. Chem. 485 (2000) 13-20.

[58] M.M. Popović, N.V. Krstajić, B.N. Grgur, Ispitivanje anodnog ponašanja mekog čelika u različitim rastvorima u cilju izbora elektrolita za elektrohemijsku sintezu filmova elektroprovodnih polimera, Zaštita materijala, 43 (4) (2002) 9-14.

[59] G.G. Wallace, G.M. Spinks, L. P. Kane-Maguire, P.R. Teasdale, Conductive Electroactive Polymers, Intelligent Polymer Systems, Third edition, CRC Press, Taylor & Francis Group, NY, 2009.

[60] T. Ohtsuka, Corrosion Protection of Steels by Conducting Polymer Coating, International Journal of Corrosion, 1 (2012), 1- 7.

[61] M. I. Khan, A. Usman Chaudhry, S. Hashim, M. K. Zahoor, M. Z. Iqbal, Recent developments in intrinsically conductive polymer coatings for corrosion protection, Chemical Engineering Research Bulletin, 14 (2) (2010) 73-86

[62] B. Wessling, Passivation of metals by coating with polyaniline: Corrosion potential shift and morphological changes, Adv. Mater., 6 (1994) 226–228.

[63] Wei-Kang Lu, Ronald L. Elsenbaumer, Bernhard Wessling, Corrosion Protection of Mild Steel by Coatings Containing Polyaniline, Synthetic Met., 71 (1995) 2163-2166.

[64] B. Wessling, J. Posdorfer, Corrosion prevention with an organic metal (polyaniline): corrosion test results, Electrochim. Acta 44 (1999) 2139-2147.

[65] A. Mirmohseni, A. Oladegaragoze, Anti-corrosive properties of polyaniline coating on iron, Synthetic Met., 114 (2000) 105–108.

[66] S. Bhadra, D. Khastgir, N. K. Singha, J. H. Lee, Progress in preparation, processing and applications of polyaniline, Prog. Poly. Sci., 34 (8) (2009) 783–810.

[67] P. Pawar, A.B. Gaikawad, P.P. Patil, Electrochemical synthesis of corrosion protective polyaniline coatings on mild steel from aqueous salicylate medium, Science and Technology of Advanced Materials 7 (2006) 732–744.

[68] M. Fahlman, S. Jasty, A.J. Epstein, Corrosion protection of iron/steel by emeraldine base polyaniline: an X-ray photoelectron spectroscopy study, Synthetic Met., 85 (1997) 1323-1326.

[69] T. Schauer, A. Joos, L. Dulog, C.D. Eisenbach, Protection of iron against corrosion with polyaniline primers, Prog. Org. Coat., 33 (1998) 20–27.

[70] M.M. Popović, B.N. Grgur, V.B. Mišković-Stanković, Corrosion studies on electrochemically deposited PANI and PANI/epoxy coatings on mild steel in acid sulfate solution, Prog. Org. Coat. 52(4) (2005) 359-365.

[71] B.N. Grgur, M.M. Gvozdenović, V.B. Mišković-Stanković, Z. Kačarević-Popović, Corrosion behavior and thermal stability of electrodeposited PANI/epoxy coating system on mild steel in sodium chloride solution, Prog. Org. Coat. 56(2-3) (2006) 214-219.

[72] J. Anand, S. Palaniappan, D. N Sathyanarayana, Conducting polyaniline blends and composites, Prog. Polym. Sci., 23 (1998) 993–1018.

[73] A. Talo, P. Passiniemi, O. Forsen, S. Ylasaari, Polyaniline/epoxy coatings with good anti-corrosion properties, Synthetic Met., 85 (1997) 1333-1334.

[74] A.B. Samui, A.S. Patankar, J. Rangarajan, P.C. Deb, Prog. Org. Coatings 47 (2003) 1–7.

[75] Y. Chen, X.H. Wang, J. Li, J.L. Lu, F.S. Wang, Long-term anticorrosion behaviour of polyaniline on mild steel, Corr. Sci., 49 (2007) 3052–3063.

[76] S. Radhakrishnan, Narendra Sonawane, C.R. Siju, Epoxy powder coatings containing polyaniline for enhanced corrosion protection, Prog. Org. Coat. 64 (2009) 383–386.

[77] S. Sathiyanarayanan, S. Muthkrishnan, G. Venkatachari, Corrosion protection of steel by polyaniline blended coating, Electrochim. Acta, 51 (2006) 6313–6319.

[78] A.M. Fenelon, C.B. Breslin, Polyaniline-coated iron: studies on the dissolution and electrochemical activity as a function of pH, Surf. Coat. Technol. 190 (2005) 264-270.

[79] W.S. Araujo, I.C.P.Margarit, M. Ferreira, O.R. Mattos, P.L. Neto, Undoped polyaniline anticorrosive properties, Electrochim. Acta, 46 (9) (2001) 1307-1312.

[80] G.M. Spinks, A. Dominis, G.G. Wallace, Comparison of emeraldine salt, emeraldine base, and epoxy coatings for corrosion protection of steel during immersion in a saline solution, Corrosion, 59 (2003) 22-31.

[81] A.J. Dominis, G.M. Spinks, G.G.Wallace, Comparison of polyaniline primers prepared with different dopants for corrosion protection of steel, Prog. Org. Coat. 48 (2003) 43-49.

[82] R. Gasparac, C.R. Martin, The effect of protic doping level on the anticorrosion characteristics of polyaniline in sulfuric acid solutions, J. Electrochem. Soc. 149 (2002) B409-413.

[83] E. Armelin, R. Pla, F. Liesa, X. Ramis, J.I. Iribarren, C. Alemán, Corrosion protection with polyaniline and polypyrrole as anticorrosive additives for epoxy paint, Corr. Sci., 50 (2008) 721–728.

[84] E. Armelin, C. Alemán, J.I. Iribarren, Anticorrosion performances of epoxy coatings modified with polyaniline: A comparison between the emeraldine base and salt forms, Prog. Organ. Coat., 65 (2009) 88–93.

[85] B. Wessling, S. Schröder, S. Gleeson, H. Merkle, S. Schröder, F. Baron, Reaction scheme for the passivation of metals by polyaniline, Materials and Corrosion 47 (1996) 439-445.

[86] P.J. Kinlen, V. Menon, Y. Ding, A mechanistic investigation of polyaniline corrosion protection using the scanning reference electrode technique, J. Electrochem. Soc. 146 (1999) 3690-3695.

[87] P.J. Kinlen, J. Ding, D.C. Silverman, Corrosion protection of mild steel using sulfonic and phosphonic acid-doped polyanilines, Corrosion, 58 (2002) 490-497.

[88] A.A. Pud, G.S. Shapoval, P. Kamarchik, N.A. Ogurtsov, V.F. Gromovaya, I.E. Myronyuk, Yu.V. Kontsur, Electrochemical behavior of mild steel coated by polyaniline doped with organic sulfonic acids, Synthetic Met., 107 (1999) 111–115.

[89] S. de Souza, Smart coating based on polyaniline acrylic blend for corrosion protection of different metals, Surface & Coatings Technology, 201 (2007) 7574–7581.

[90] J. Wang, Anion exchange nature of emeraldine base (EB) polyaniline (PAn) and a revisit of the EB formula, Synthetic Met., 132 (2002) 49–52.

[91] J. Wang, Polyaniline coatings: anionic membrane nature and bipolar structures for anticorrosion, Synthetic Met., 132 (2002) 53–56.

[92] J. Kankare in: Electrical and Optical Polymer Systems: Fundamentals, Methods, and Applications, Chapter 6, D. Wise, G.E. Wnek, D.J. Trantolo, T.M. Cooper, J.D. Gresser (Eds.), Marcel Dekker, New York, 1998.

[93] C. Varlikli, V. Bekiari, M. Kus, N. Boduroglu, I. Oner, P. Lianos, G. Lyberatos, S. Icli, Adsorption of dyes on Sahara desert sand, J. Haz. Mat. 170 (2009) 27–34.

[94] M. Kaneko, Hideki Nakamura, Photoresponse of a liquid junction polyaniline film, J. Chem. Soc., Chem. Commun., 6 (1985) 346-34.

[95] X. Wang, M. Shao, G. Shao, Z. Wu, S. Wang, A facile route to ultra-long polyaniline nanowires and the fabrication of photoswitch, J. Colloid Interface Sci., 332 (2009) 74-77.

[96] P. A. Kilmartin, G. A. Wright, Photoeffects at a polyaniline film electrode, Electrochim. Acta, 41 (10) (1996) 1677-1687.

[97] P. A. Kilmartin, G. A. Wright, Anion insertion and expulsion in polyaniline electrodes studied by photocurrent transients, Electrochim. Acta, 43 (21-22) (1998) 3091-3103.

[98] I.M. Arafa, H.M. El-Ghanem, A.L. Ahmad, Photoconductivity and photovoltaic properties of polyaniline immobilized onto metallurgical porous silicon powder, Polym. Int., 2012, doi: 10.1002/pi.4418.

[99] K. Inoue, T. Akiyama, A. Suzuki, T. Oku, Organic solar cells based on electrodeposited polyaniline films, Jpn. J. Appl. Phys. 51 (2012) 4-8.

[100] S.-B. Yoon, E.-H. Yoon, K.-B. Kim, Electrochemical properties of leucoemeraldine, emeraldine, and pernigraniline forms of polyaniline/multi-wall carbon nanotube nanocomposites for supercapacitor applications, J. Power Sources, 196 (2011) 10791– 10797.

[101] J-Y. Wang, C.-Mu Yu, S-C. Hwang, K-C. Hoa, L-C. Chen, Influence of coloring voltage on the optical performance and cycling stability of a polyaniline–indium hexacyanoferrate electrochromic system, Solar Energy Materials & Solar Cells, 92 (2008) 112–119.

[102] S. Murugesan, G. S. Sur, G. Beaucage, J.E. Mark, In situ generation of polyaniline in poly(dimethylsiloxane) networks, Silicon Chem., 2 (2005) 217-221.

[103] I. Yu. Sapurina, J. Stejskal, Oxidation of aniline with strong and weak oxidants, Russ. J. Gen. Chem., 82 (2) (2012) 256–275.

[104] J. Stejskal, J. Prokeš, M. Trchová, Reprotonation of polyaniline: A route to various conducting polymer materials, Reactive & Functional Polymers 68 (2008) 1355–1361.

[105]   P.A. Sørensen, S. Kiil, K. Dam-Johansen, C. E. Weinell, Anticorrosive coatings: a review, J. Coat. Technol. Res., 6 (2) (2009) 135–176.

[106]   G.W. Walter, A critical review of the protection of metals by paints, Corros. Sci., 26 (1) (1986) 27-38.

[107]   H. Yang, P. Jiang, Large-scale colloidal self-assembly by doctor blade coating, Langmuir, 26 (16) (2010) 13173–13182.

[108]   E. Akbarinezhad, F. Rezaei, J. Neshati, Evaluation of a high resistance paint coating with EIS measurements: Effect of high AC perturbations, Prog. Org. Coat., 61 (2008) 45–52.

[109]   M. Musiani, M. E. Orazem, N. Pebere, B. Tribollet, V. Vivierd, Constant-phase-element behavior caused by coupled resistivity and permittivity distributions in films, Journal of The Electrochemical Society, 158 (12) (2011) C424-C428.

[110]   M. Stern, A. L. Geary, Electrochemical polarization: I. A theoretical analysis of the shape of polarization curves, J. Electrochem. Soc. 104 (1) (1957) 56-63.

[111]   M. Stern, A method for determining corrosion rates from linear polarization data, Corrosion, 14 (9) (1958) 440-444.

[112]   E. McCafferty, Introduction to Corrosion Science, Springer, Alexandria VA, 2010, p. 199.

[113]   S. Feliu, Jr., M. Morcillo, S. Feliu, The reproducibility of impedance parameters obtained for painted specimens, Prog. Org. Coat., 25 (1995) 365-377.

[114]   J.E. de Albuquerquea, L.H.C. Mattoso, R.M. Faria, J.G. Masters, A.G. MacDiarmid, Study of the interconversion of polyaniline oxidation states by optical absorption spectroscopy, Synthetic Met., 146 (2004) 1–10.

[115]   D. Yang,W. Lu, R. Goering, B. R. Mattes, Investigation of polyaniline processibility using GPC/UV–vis analysis, Synthetic Met., 159 (2009) 666–674.

[116]   D.B. Dupare, M.D. Shirsat, A.S. Aswar, Inorganic acids doped PANI-PVA composites films as a gas sensor, The Pacific Journal of Science and Technology, 10 (1) (2009) 417-422.

[117]   E. Jin, N. Liu, X. Lu,W. Zhang, Novel micro/nanostructures of polyaniline in the presence of different amino acids via a self-assembly process, Chem. Lett. 36 (2007) 1288-1289.

[118] Y. Lia, B. Wang, W. Feng, Chiral polyaniline with flaky, spherical and urchin-like morphologies synthesized in the l-phenylalanine saturated solutions, Synthetic Met., 159 (15-16) (2009) 1597-1602.

[119] A. Saraswat, L. K. Sharma, S. Singh, R.K.P. Singh, Electrochemical assisted synthesis and characterization of perchloric acid-doped aniline-functionalized copolymers, Synthetic Met., 167 (2013) 31– 36.

[120] E. C. Venancio, P-C. Wang, A.G. MacDiarmid, The azanes: A class of material incorporating nano/micro self-assembled hollow spheres obtained by aqueous oxidative polymerization of aniline, Synthetic Met., 156 (2006) 357–369.

[121] L. Zhang, H. Peng, Z. D. Zujovic, P. A. Kilmartin, J. Travas-Sejdic, Characterization of polyaniline nanotubes formed in the presence of amino acids, Macromol. Chem. Phys., 208 (2007) 1210–1217.

[122] T. Nguyen, T.B. Hubbard, J.M. Pommersheim, Unified model for the degradation of organic coatings on steel in a neutral electrolyte, J. Coat. Technol., 68 (1996) 45-52.

[123] F. Deflorian, S. Rossi, The role of ions diffusion in the cathodic delamination rate of polyester coated phosphatized steel.'' J. Adhes. Sci. Technol., 17 (2003) 291-299.

[124] M. Rohwerder, A. Michalik, Conducting polymers for corrosion protection: What makes the difference between failure and success? Electrochim. Acta, 53 (2007) 1300–1313.

BIOGRAFY

Ali Ramadan Elkais was born 07.10.1970, in Khoms, Libya. In 1994 he graduated at the Department of Chemical Engineering at Al-Fath University, Tripoli, Libya. From 1997 to 2004. was employed at the Central DP4 oil platform in Libya, ENI Oil. Co - The Libyan branch. Master Degree majoring in corrosion control ended in 2004 at the University UMIST, Manchester, UK, with the master thesis "Effect of copper ions on chromate conversion coatings on aluminum".

School year 2010/11 he enrolled in doctoral studies at the Faculty of Technology and Metallurgy, Chemistry study program, under the guidance of mentor Professor Branimir Grgur, Ph.D. In the framework of doctoral studies passed the 11/11 exam of study program with average grade 9.73 and 21 Feb 2011. He defended the Final exam - access work for his doctoral dissertation.

Ali Ramadan Elkais is the Author of tree papers published in international journals.

He is married and has three children.

Прилог 1.

<div align="center">

Изјава о ауторству

</div>

Потписани: <u>Али Р. Елкаис</u>
број индекса: <u>   4084/10   </u>

<div align="center">

Изјављујем

</div>

да је докторска дисертација под насловом:

The influence of the polyaniline coatings on corrosion protection of mild steel in different environments

- резултат сопственог истраживачког рада,
- да предложена дисертација у целини ни у деловима није била предложена за добијање било које дипломе према студијским програмима других високошколских установа,
- да су резултати коректно наведени и
- да нисам кршио/ла ауторска права и користио интелектуалну својину других лица.

<div align="right">

Потпис докторанда

</div>

У Београду, 08.04.2013 год.

Прилог 2.

Изјава о истоветности штампане и електронске верзије докторског рада

Име и презиме аутора: Али Р. Елкаис

Број индекса: 4084/10

Студијски програм: ХЕМИЈА

Наслов рада: **The influence of the polyaniline coatings on corrosion protection of mild steel in different environments**

Ментор: Др Бранимир Гргур, ред. проф. Технолошко-металуршког факултета,

Потписани   Али Р. Елкаис

Изјављујем да је штампана верзија мог докторског рада истоветна електронској верзији коју сам предао/ла за објављивање на порталу **Дигиталног репозиторијума Универзитета у Београду.**

Дозвољавам да се објаве моји лични подаци везани за добијање академског звања доктора наука, као што су име и презиме, година и место рођења и датум одбране рада.

Ови лични подаци могу се објавити на мрежним страницама дигиталне библиотеке, у електронском каталогу и у публикацијама Универзитета у Београду.

Потпис докторанда

У Београду, 08.04.2013 год.

Прилог 3.

Изјава о коришћењу

Овлашћујем Универзитетску библиотеку „Светозар Марковић“ да у Дигитални репозиторијум Универзитета у Београду унесе моју докторску дисертацију под насловом: <u>The influence of the polyaniline coatings on corrosion protection of mild steel in different environments</u> која је моје ауторско дело.

Дисертацију са свим прилозима предао/ла сам у електронском формату погодном за трајно архивирање.

Моју докторску дисертацију похрањену у Дигитални репозиторијум Универзитета у Београду могу да користе сви који поштују одредбе садржане у одабраном типу лиценце Креативне заједнице (Creative Commons) за коју сам се одлучио/ла.

1. Ауторство

2. Ауторство - некомерцијално

3. Ауторство – некомерцијално – без прераде

4. Ауторство – некомерцијално – делити под истим условима

5. Ауторство – без прераде

6. Ауторство – делити под истим условима

Потпис докторанда

У Београду, 08.04.2013 год.

_____

Прилог 1.

Изјава о ауторству

Потписани: Али Р. Елкаис
број индекса: 4084/10

Изјављујем

да је докторска дисертација под насловом:

The influence of the polyaniline coatings on corrosion protection of mild steel in different environments

- резултат сопственог истраживачког рада,
- да предложена дисертација у целини ни у деловима није била предложена за добијање било које дипломе према студијским програмима других високошколских установа,
- да су резултати коректно наведени и
- да нисам кршио/ла ауторска права и користио интелектуалну својину других лица.

Потпис докторанда

У Београду, 08.04.2013 год.

_____

Прилог 2.

Изјава о истоветности штампане и електронске верзије докторског рада

Име и презиме аутора: Али Р. Елкаис

Број индекса: 4084/10

Студијски програм: ХЕМИЈА

Наслов рада: **The influence of the polyaniline coatings on corrosion protection of mild steel in different environments**

Ментор: Др Бранимир Гргур, ред. проф. Технолошко-металуршког факултета,

Потписани   Али Р. Елкаис

Изјављујем да је штампана верзија мог докторског рада истоветна електронској верзији коју сам предао/ла за објављивање на порталу **Дигиталног репозиторијума Универзитета у Београду.**

Дозвољавам да се објаве моји лични подаци везани за добијање академског звања доктора наука, као што су име и презиме, година и место рођења и датум одбране рада.

Ови лични подаци могу се објавити на мрежним страницама дигиталне библиотеке, у електронском каталогу и у публикацијама Универзитета у Београду.

Потпис докторанда

У Београду, 08.04.2013 год.

Прилог 3.

Изјава о коришћењу

Овлашћујем Универзитетску библиотеку „Светозар Марковић" да у Дигитални репозиторијум Универзитета у Београду унесе моју докторску дисертацију под насловом: <u>The influence of the polyaniline coatings on corrosion protection of mild steel in different environments</u> која је моје ауторско дело.

Дисертацију са свим прилозима предао/ла сам у електронском формату погодном за трајно архивирање.

Моју докторску дисертацију похрањену у Дигитални репозиторијум Универзитета у Београду могу да користе сви који поштују одредбе садржане у одабраном типу лиценце Креативне заједнице (Creative Commons) за коју сам се одлучио/ла.

1. Ауторство

2. Ауторство - некомерцијално

3. Ауторство – некомерцијално – без прераде

4. Ауторство – некомерцијално – делити под истим условима

5. Ауторство – без прераде

6. Ауторство – делити под истим условима

Потпис докторанда

У Београду, 08.04.2013 год.

_____